Title/Titre

Biophysical and Pharmacological Characterization of Stretch-Activated K^+ Channels

Name/Nom

Daniel Leroy Small

Thesis submitted to
School of Graduate Studies and Research
in partial fulfillment of the requirements for the Ph.D.
degree in Biology

ISBN 0-612-15762-8

UNIVERSITÉ D'OTTAWA
UNIVERSITY OF OTTAWA

This thesis is dedicated to Sigo.

Acknowledgements

This work would have not been possible without the love and understanding of my wife, Cathy-Jo, and for that I wish to thank her. For their generous support and encouragement, I would like to thank my parents and parents-in-law. Cathy Morris has been a super mentor and teacher whose motivation and guidance is greatly appreciated. The exhilaration with which she approaches science is both infectious and invigorating. I will continue to admire and respect her for this. Special thanks go out to Dave Vandorpe for his helping me obtain my first giga-seal and for the contibutions he made to the work presented in Chapter 3. I am indebted to Peter Juranka for the common sense way in which he introduced me to molecular biology and the patience he displayed while working with such a novice molecular biologist. For her friendship and willingness to listen to lamentation of experiments failed, I thank Christine Murray. Thanks to all those who attended the infamous Rideau Canal Club meetings or were charitable enough to allow themselves to be stopped in the hall to share in my enthusiasm for discussing ion channels; Zhigang Xiong, Xiaodong Wan, Vladamir Senotrov, Dave Spanswick, Micheal Hermes, Christophe Reuzeau, Leo Renaud, Bin Hu, Peter Stys and Alastair Buchan. Moe' s help taming the fax machine, sending off important packages, and greeting me with a smile every morning will be sorrily missed. The considerate suggestions and criticisms made by my advisory committee members were greatly appreciated.

Abstract

Mechanosensitive ion channels were studied in various preparations (*Lymnaea stagnalis* cultured neurons, and ventricular heart cells, *Aplysia californica* mechanosensitive neurons, and *Xenopus* oocytes) using cell-attached and excised inside-out patch-clamp techniques to characterize their biophysical and pharmacological properties. Whole-cell patch-clamp techniques were not enlisted due to the fact that stretch-activated (SA) channels do not elicit macroscopic currents. Despite the fact that SA channel mechanosensitivity can be artifactually high in the patch-configuration, they occur in almost all cell types in most species. In most cases it is unclear what role the channels play but it is unlikely that most are mechanotransducers.

It has been demonstated that a well studied K-selective channel which plays an important role in "cellular learning" in *Aplysia* mechanosensory neurons, is stretch-activated. Using multi-channel patch analysis I have provided further evidence that this channel is indeed a SA K^+ channel similar to those found in virtually all molluscan neurons. I demonstrated that the number of SA K^+ channels in a patch is finite and the response saturable. Kinetic stationarity was tested. In patches which passed the stationarity tests and in which channels were found to be independent and identical, the kinetics were determined. The kinetic analysis yielded results consistent with the hypothesis that S-channels (those which responded to FMRF-amide and to 5-HT) were identical to SA K^+ channels (those which were stretch-activatable).

I then tested the hypothesis that all molluscan SA K^+ channels were S-like in that

they were modulated by neurotransmitters via second messengers. I found that the inherent variability of normal channel activity prohibited adequate testing of this hypothesis even when a homogeneous population of cells containing similar SA K^+ channels was examined. Attempts were made also to study the regulation of the channel by phosphorylation and dephosphorylation but the difficulty in obtaining appropriate dephosphosphorylating agents was a hindrance.

Given that this path of questioning had not been as fruitful as anticipated, I set out to further characterize SA K^+ channel dynamics. I also studied pharmacology and permeation properties of the channel in the hopes that a cloning strategy might be developed through a better understanding of the channel and through comparisons with other already cloned channels whose structure/function relationships were known.

Dynamics

When care was taken to obtain gigaseals in a gentle fashion (< 10 mmHg suction) and disruption to the patch integrity was minimized, SA K^+ channels in *Lymnaea* neurons exhibited dynamic characteristics. These characteristics included a delayed response to rapid suction steps. The delay lessened with suction steps of increasing magnitude. The delay phenomenon was fragile in nature in that the delay was lost with repeated suction stimuli of the same magnitude or by non-gentle seal formation. The delay was voltage independent. Cells left in culture longer (4, 5, and 6 days as opposed to 1 and 2 days), responded to similar stimuli with longer delays. Given the increased delay in older cells and the loss of delay with mechanical manipulation it was hypothesized that the delay was

dependent on the underlying membrane cytoskeleton. When the cells were treated with an actin-disrupting agent, cytochalasin D, SA K^+ channels responded with greater sensitivity and a markedly decreased delay. It, therefore, seems unlikely that SA K^+ channels normally have the ability to sense discrete changes in membrane tension. In fact, it would seem that SA K^+ channels are protected from membrane tension by load bearing membrane cytoskeletal elements.

Pharmacology

In keeping with a characterization which would facilitate the cloning of SA K^+ channels, I focused on SA K^+ channel pharmacology. Although there has not been a single agent which has proven specific for SA channels in exclusion, I set out to sketch a pharmacological profile or fingerprint of the SA K^+ channels. I found SA K^+ channels to be blocked by extracellular TEA (IC_{50}= ~50 mM), but not by intracellular TEA, extracellular diltiazem or Gd^{3+}. Extracellular amiloride and quinidine blocked SA K^+ channels with IC_{50}s of ~2.15 mM and ~0.75 mM respectively. Ethanol (3%) had no apparent effect on SA K^+ channels yet reduced the efficacy of quinidine block.

Permeation

Given that *Lymnaea* SA K^+ channels seem to be K-selective channels which are specialized to **avoid** sensing membrane tension under normal conditions, I characterized the pore properties with the intent to make comparisons to other SA channels and K^+ channels whose structure/function relations are fairly well understood. I found that the

pore of SA K^+ channels has an affinity for inward and outward moving K^+ currents of 28.1 ± 5.0 mM and 91.9 ± 6.7 mM. SA K^+ channels exhibited an anomalous mole fraction effect with mixtures of Rb^+ indicative of a multi-ion pore. The selectivity sequence established using reversal potentials under biionic conditions was $Cs^+ > K^+ > Rb^+ > NH_4^+ > Na^+ > Li^+$ and using relative conductances in symmetrical solutions was $Tl^+ = K^+ > Rb^+ > NH_4^+ >> Na^+ = Li^+ = Cs^+$. Extreme variations in external pH had no effect on single SA K^+ channel conductance. External Mg^{2+} (2 mM) blocked inward SA K channel currents. Ba^{2+} enters the pore only from the inside resulting in a voltage-dependent, open channel block.

This body of work, as a whole, creates a picture of SA K^+ channels in *Lymnaea* neurons which, it is hoped, will both facilitate ongoing efforts to clone SA channels and once cloning is well underway, help identify a clone expressed in a heterologous environment. The work should add to the catalog of descriptions of wildtype SA K^+ channels which will be used to classify clones and newly discovered related channels.

TABLE OF CONTENTS

CHAPTER V Dynamic Behaviour of MS Channels

CHAPTER VI

Pharmacology of Stretch-Activated K Channels in *Lymnaea* Neurons

CHAPTER VII

Pore Properties of SA K Channels in *Lymnaea* Neurons

Figure List

List of Tables

Abbreviations

AA; arachidonic acid

AC; adenylate cyclase

4-AP; 4-aminopyridine

ACM; *Aplysia* culture medium

ARS; *Aplysia* recording solution

ATP; adenosine-5'-triphosphate

cAMP; cyclic adenosine monophosphate

Cat; cation

dbcAMP; dibutryl cAMP

FMRF-amide; PHE-MET-ARG-PHE-amide

FNS; frog normal saline

G-protein; guanine nucleotide binding protein

GTP; guanine triphosphate

H5 or P or SS1-SS2; pore region of K^+ channel

HPETE; hydroperoxy-5,8,10,14-icosatrienoic acid

5-HT; 5-hydroxytryptamine

hKv1.5; voltage-activated K channel

HYPER; stripping solution

I_{MS}; macroscopic MS currents

IP_3; inositol triphosphate

I-V; current-voltage relation

K_{ATP}; ATP-sensitive potassium channel

K_{Ca}; calcium-activated potassium channel

KF; potassium fluoride

LCM; *Lymnaea* culture medium

LNS; *Lymnaea* normal saline

LPM; *Lymnaea* plating medium

MS; mechanosensitive

MR; mechanoreceptor

ND96; frog medium

OR2; Ca^{2+}-free frog medium

PCP; phencyclidine

PK; protein kinase

PKA; protein kinase A

PL; phospholipids

PLA_2; phospholipase A_2

P_{open}; open probability

PrP; protein phosphatase

PTX; pertussis toxin

RVD; regulated volume decrease

S4; voltage sensing region of channel

SA; stretch-activated

TEA; tetraethylammonium

VSM; vascular smooth muscle

ZNS; zebra-fish normal saline

CHAPTER I General Introduction

Long before it was first possible to study the activity of a single ion channel, (Neher and Sakmann, 1976), mechanosensitive (MS) ion channels that would transduce mechanical stimuli into electrical signals were postulated. They were proposed in order to account for the mechanoelectrical transduction of specialized mechanoreceptors such as muscle spindles (Matthews, 1981), crustacean stretch-receptors (Nakajima and Onodera, 1969), and Pacinian corpuscles (Loewenstein, 1971). Based on microelectrode studies of *Paramecium*, (Naitoh, 1984), calcium (Ca^{2+})-selective and potassium (K^+)-selective mechanosensitive (MS) ion channels were thought to underlie the organism's *avoiding reaction* (Jennings, 1906) and *escape reaction* (Naitoh, 1974), respectively. The patch-clamp giga-seal technique (Hamill *et al.*,1981), facilitated single channel studies but *paramecia* have cilia which make gigaseal formation difficult, (Naitoh, 1984). Later in 1984, however, Guharay and Sachs (1984) used the giga-seal technique to describe SA channels in vertebrate skeletal muscle which were non-selective cation (SACat) channels. These channels, unlike most channel types, responded to membrane tension induced by suction during single-channel recording. Two years after the discovery of SACat channels, SA K^+ channels were described in molluscan heart (Brezden *et al.*, 1986). Because these channels were K^+-selective rather than non-selective, they constituted a second type of SA channel. SA K^+ channels were found to be uniformly distributed at a relatively high density ~ 1 μm^{-2}. This, and the fact that molluscan heart is both mechanically active and stretch sensitive (Jones, 1983), made it tempting to think that these channels, too, were MS channels with a mechanotransducing function as proposed

earlier.

Shortly after SA K^+ channels were decribed in molluscan heart, nearly identical SA K^+ channels were found to be ubiquitous in neurons of gastropods (Morris and Sigurdson, 1989; Sigurdson and Morris, 1989). Similar SA K^+ channels have also been described in insect somatic muscle (Gorczyca and Wu, 1991; Zagotta *et al.*, 1988), and in various vertebrate cell types including rat heart, (Kim, 1992), (for review see Morris, 1990). Other types of SA channels have been described in most cell types from protozoa to humans.

SA channels are integral membrane components of a plethora of non-specialized cells and are not restricted to specialized mechanotransducing cells. One postulate has been that these channels are found in all cells in order to accomodate changes in the colloidal osmotic stress that all cells experience (Kullberg, 1987).

A probing question was whether the microscopic behaviour of MS channels, described using single channel patch-clamp techniques, reflected the macroscopic behaviour of these channels. Morris and Horn (1991) were unable to obtain any significant macroscopic MS currents from cells in which they had already characterized microscopic MS currents. To the chagrin of all who had hoped that these MS channels were mechano-transducers, it seemed as though the stretch-sensitivity of SA K^+ channels in molluscan neurons might be experimentally induced (Morris and Horn, 1991). The controversy persists, however (Gustin *et al.*, 1991). A decade has passed since the first SA channel was described, yet evidence that these channels are responsible for mechanotransduction is meagre. The pursuit of evidence is hindered by the lack of pharmacological tools and by the problem of stretching a membrane of intact cells in a calibrated, reproducible manner.

Recent studies of genes (mec-4, 6 and 10 and deg-1) coding for proteins essential to normal mechanosensory behaviour in nematodes, *C. elegans* (Huang and Chalfie, 1994; Hong and Driscoll, 1994) together with cloned renal epithelial sodium channel subunits (α, ß, and gamma rENa) (Canessa et al., 1994) have yielded promising results to suggest that this class of channel underlies mechanosensitivity. Although the mec genes of *C. elegans* are clearly involved in mechanosensitivity, (mutants lacking these genes do not exhibit mechanosensitive behaviour and mec-4 and mec-10 are found only in touch cells), and the sequence of these genes is very similar to the genes which code for the renal epithelial sodium channel subunits, it has not yet been established that these mec genes actually produce channel proteins similar to the rENa channels.

The most convincing evidence to date, that some ion channels may function as cellular mechanotransducers, comes from the non-selective cationic stretch-inactivated (SI Cat) channels in the neurons of the supra-optic nucleus of rats which function as osmo-mechanical transducers (Oliet and Bourque, 1993).

Since they are most mechanosensitive in mechanically-disrupted membrane (Morris and Horn, 1991; Small and Morris, 1994a), SA K^+ channels may act to signal incipient cell trauma but they show little promise of serving as physiological transducers. If these channels are not mechanotransducers in vivo, and their mechanosensitivity is a trait conferred by disruptions in the patch environment, then what are they? What physiological role do they play in the cell? Until these channels are cloned or until a specific blocker is available, the true physiological function of these channels will remain unclear.

In an effort to facilitate the eventual cloning of this channel, biophysical and

pharmacological characterizations of SA K^+ channels have been carried out. These studies will enable structural predictions of SA K^+ channels based on comparisons with other already cloned channels whose structure/function relations have been described. Furthermore, these studies should provide a means of identification of SA K^+ channels when they are cloned and expressed in an heterologous environment.

1. Mechanotransduction

i) Mechanoreceptors

Mechanotransduction -- the transferral of some mechanical energy, usually a physical deformation of cell membrane, into an electrical signal -- is the primary task of cellular mechanoreceptors (MRs) (French, 1992). Quite often MRs are specialized nerve endings like Pacinian corpuscles or Merkel's disks. Although the physiological behaviour of MRs is well understood in a number of preparations such as the crustacean stretch receptor and the mammalian muscle spindle (for extensive review see Kuffler *et al.*,1984), the mechanisms at the cellular level are not. This is due in part to the fact that most MRs have a complex structure which makes the transduction sites inaccessible for experimentation (i.e. single-channel patch-clamp recordings).

Regardless of the scarcity of supporting evidence from non-specialized cells, MS ion channels continue to be implicated in the process of mechanotransduction in MRs. The initial motivation for this thinking comes primarily from microelectrode studies of unicellular forms (protozoa) and some MRs like crayfish stretch receptors. In protozoa,

divalent-selective and K^+-selective MS currents were recorded using microelectrodes (Naitoh, 1988). In crustaceans, a generator potential, or depolarizing receptor potential is produced in the dendrites of the sensory neuron and can lead to an action potential (AP) upon mechanical deformation of the dendrites (Brown *et al.*, 1978). This generator potential is carried predominantly by Na^+ but the channels underlying this potential are somewhat permeable to Ca^{2+}, as well as Mg^{2+}, Sr^{2+} and Ba^{2+} (Edwards *et al.*, 1981). Single channel recordings of the cell body and primary afferents (the dendritic tips are inaccessible to patch electrodes) have revealed the presence of SA ion channels with a similar selectivity profile (Erxleben, 1989). Unfortunately, function-by-association (i.e. presence in a mechanoreceptor cell) is necessary but not sufficient evidence.

ii) Hair Cells

The mechanosensory system which is understood better than any other is the vertebrate hair cells responsible for hearing and balance (Fig. 1.1; Hudspeth, 1989). A cluster of 20-300 cylindrical processes, stereocilia, project from the flattened apical surface of a hair cell (Jacobs and Hudspeth, 1990). Each stereocilium consists of an actin cytoskeleton ensheathed in a tube of plasma membrane. The cluster is organized in a bundle that, in profile, appears like the bevelled tip of a hypodermic needle. At the highest point of the bundle is a single, axonemal cilium, the kinocilium,

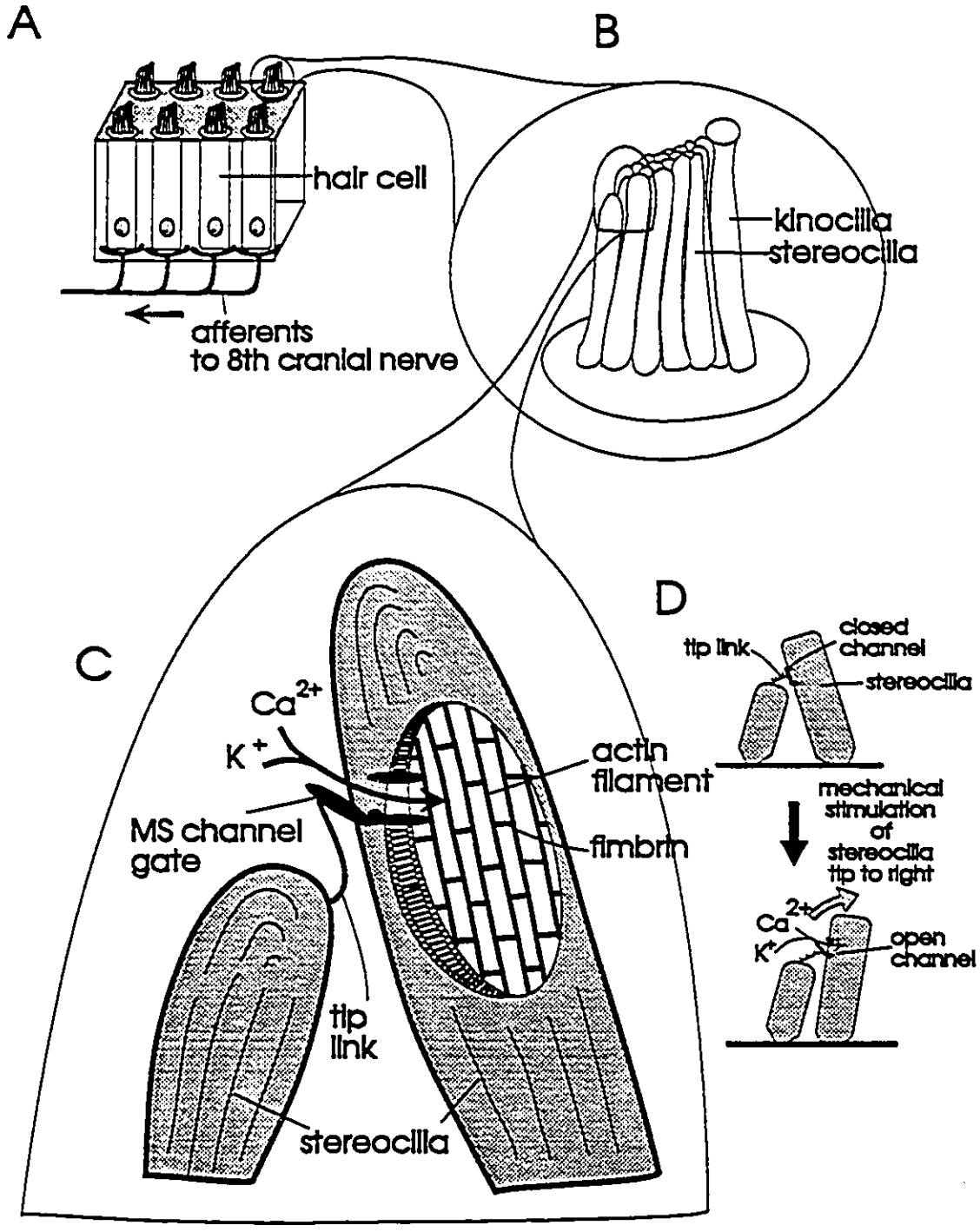

Figure 1.1. Mechanosensory system of hair cell. The hair cell (A), has a hair bundle (B), on top which is exposed to a viscous, K^+-rich fluid. This fluid "sloshes" around creating a mechanical force on the stereocilia, resulting in an influx of K^+ and Ca^{2+}, (C) and (D) (Hudspeth, 1989).

whose role in mechanotransduction remains unclear as its removal leaves the process intact (Hudspeth and Jacobs, 1979).

Within each stereocilium, actin filaments are held in longitudinal register by fimbrin so that the stereocilium is very rigid along its longitudinal axis (Flock *et al.*, 1977). Towards its base, the stereociliary diameter decreases from several hundred nm to less than 100 nm and the actin filaments number decreases from ~3000 to ~20 (Jacobs and Hudspeth, 1990). These 20 anchor the entire stereocilium to the thick mesh of interlinked actin filaments of the cuticular plate. Consequently, the stereocilium does not bend in response to a mechanical stimulus at its tip but instead, pivots at its attenuated base.

Each stereocilium is linked to a neighbour by a tip link, a fine filamentous tether connecting the distal end of one stereocilium to the side of the longest adjacent process (Pickles *et al.*, 1984). When the stereocilia pivot in the direction of the longest process, the tip link pulls a proposed "gating spring" for a single MS channel, as pictured in Fig. 1.1 D (Hudspeth, 1982; Ohmori, 1985; Hudspeth, 1989; Assad *et al.*, 1991). The channel is a non-selective cationic channel and its opening results in the depolarization of the process (Shotwell *et al.*, 1987). There is controversy as to how many MS channels there are on each stereocilium and where on the stereocilium these channels are found (French, 1992) but is it agreed that there are ~1 to 3 channels per cilium.

Though this system is so well decribed (Hudspeth, 1989), the MS ion channels, integral to the hair cell's mechanotransduction have not been studied using single channel patch-clamp techniques. Since the stereocilia are too small to be patched and since the complex architecture of the tip link is required, this will almost certainly continue to be an impossible

pursuit.

2. Mechanosensitive Channels

i) Introduction

Mechanical senses are found in organisms throughout the plant and animal kingdom. Roots go down and stems go up. The *Paramecium* backs away from barriers and escapes from predators. A gymnist on a balance beam, or a child on a bicycle will make use of their sense of gravity. Someone in a dark alley will be acutely aware of a light tap on the shoulder. Mechanical senses are responsible for all of these phenomena yet we still do not fully understand the basic mechanism of mechanical sensitivity. It is at the level of mechanoelectrical transduction that the questions arise. MS channels may contribute to these processes despite the dearth of supporting evidence. Regardless of whether all MS channels are physiological transducers or as it seems more likely, only some of them serve in this capacity, they sense membrane tensions induced by suction to the back end of a recording pipette in the single channel patch-clamp configuration. This mechanosensitivity is special to an ill-defined subset of a cell's channels; most, such as those gated by voltage or neurotransmitters, do not exhibit this characteristic.

ii) Classification

MS channels fall into categories based on the type of stimulation to which each responds. There are stretch-activated (SA) channels, stretch-inactivated (SI) channels (Morris and Sigurdson, 1989), putative shear-sensitive channels (Olesen *et al.*, 1988), and putative transduction channels of hair cells (Howard *et al.*, 1988), described earlier. SA

channels constitute by far the largest number (for reviews see Sachs, 1990 and Morris, 1990). In addition to the type of stimulus to which the channel responds, MS channels can be classified according to ion selectivity. The most common is the SA non-selective cationic (SA Cat) channel. It is permeable to Ca^{2+}, Na^{+} and K^{+}. There are also SA K^{+} channels which are selective for K^{+}, a Na^{+}-selective channel (Gardner and Brezden, 1990), and anion-selective channels which preferentially allow the passage of Cl^{-} ions. One group, (Schwiebert et al., 1994; Mills et al., 1994), has shown SA Cl^{-} channels that appear to be associated with osmoregulation and a regulated volume decrease (RVD) during cell swelling in response to a hypoosmotic shock. Not all SA Cl^{-} channels, however, can be assumed to serve such functions. SA Cl^{-} channels are evident in excised patches, but their characteristics suggest they are as likely to be malfunctioning carriers as physiological mechanotransducing channels, (Bedard and Morris, 1992).

iii) Distribution

MS channels have been found in all major taxa that have been tested from prokaryotes to vertebrates. They are also found in all cell types; those which demonstrate a specialized ability to sense mechanical stimuli as well as more pedestrian cells with no obvious need for a mechanotransducer. In most cells, MS channel density is uniform and on the order of 1 μm^{-2} (Morris, 1990).

iv) Patch-Clamp Studies

MS channels are predominantly studied using patch-clamp techniques (Hamil *et al.*, 1981).

The patch clamp records picoampere currents across a micron-sized patch of membrane. The patch is formed when, after pressing a saline-filled pipette tightly against the surface of the cell, a bleb of membrane is slowly sucked up so that it forms a bond with the glass of the pipette. This bond is so tight that it has an electrical resistance of more than one gigaohm (GΩ). The membrane of the cell itself will tear before the seal is broken. This high-resistance seal permits the recording of current flowing through a single ion channel. The opening and closing of the channel is observed in real time so that direct record of the history of conformation changes in an individual channel is possible.

v) Transduction Models

Insofar as the geometry of a patch resembles a section of a sphere (Sokabe and Sachs, 1990; Sokabe *et al.*, 1991), membrane tension in response to applied pressure can be determined using the law of Laplace: tension (T) is proportional to the pressure difference across the membrane (P) and the radius of curvature (r), thus

$$T=Pr/2.$$

It is membrane tension created by pressure and not pressure itself that affects the channel as evidenced by the fact that SA K^+ channels open in response to positive and negative pressure whereas SI K^+ channels close in response to pressure of either polarity (Morris and Sigurdson, 1989). What kind of molecular machinery is required by the channel to enable it to sense membrane tension? A number of models exist, (Sachs, 1990; Howard et al., 1988; Sachs and Lecar, 1991) which describe mechanotransduction. In all of these models the free energy barrier of the two-state channel is one dimensional: This

is satisfactory for a tip-link type gating spring, but unrealistic for a channel with a radially disposed tension sensor. Another treatment (Morris and Lecar, 1993), of the Sachs and Lecar model, (1991), that is less restricting allows for a second degree of freedom in the energy barrier to accomodate other possibilities other than merely a change in the size of the channel when it undergoes a conformation state change.

It was proposed that MS channels are achored to one another via the cell's cytoskeletal meshwork (Guharay and Sachs, 1984). The idea that MS channels are "protected" by virtue of their association with the cytoskeleton is consistent with the fact that MS channels could only be recorded in the single channel patch-clamp configuration (Morris and Horn, 1991), a configuration normally associated with the disruption of cytoskeletal elements. The involvement of actin in mechanosensitivity is complex. Cytochalasins, agents which promote actin depolymerization, augment the stretch-sensitivity of SA channels (Guharay and Sachs, 1984) suggesting that the elastic elements of SA channels are actin based but the membrane elasticity constant did not change in patches following overnight incubation of cells in 10 μM cytochalasin B (Sokabe et al., 1991). It was therefore proposed that the submembrane spectrin network might constitute the elastic elements of SA channels (Sokabe et al., 1991). However, cytochalasin D increased the sensitivity of SA K^+ channels in snail neurons (Small and Morris, 1994a) and both cytochalasin B and D increase the open probability of SA Cl^- channels in a renal cortical collecting duct cell line (Schwiebert, et al., 1994). It is likely that cortical cytoskeletal proteins play some role in the behaviour of MS channels. They may provide mechanical protection for these channels acting to buffer membrane tension, (i.e. SA K^+ channels) or they may act as dashpots allowing MS channels

to adapt to prolonged mechanical stimuli as would seem to be the case for SA Cat channels (McBride and Hamill, 1992; McBride and Hamill, 1993, Hamill and McBride, 1992). These functional cytoskeleton-channel associations have as yet only been demonstrated in single channel patch-clamp studies and need to be confirmed using whole-cell techniques where the patch geometry is less artificial.

vi) Whole-Cell Studies

The patch recording configuration is more disruptive to the cytoarchitecture than the whole-cell recording configuration (Sokabe, et al., 1991; Sokabe and Sachs, 1990). Therefore it should be possible to assess whether disruption of cytoarchitecture is necessary for stretch-activation of channels or not using whole-cell recording configuration. Also, given that the whole-cell recording configuration is less disruptive, (i.e. more representative of the normal physiological environment), it is desirable to obtain whole-cell recordings of SA channels which correspond to single channel records as a way of implicating these channels in a physiological mechanosensitive process. There are only a few examples of whole-cell recordings of MS channels, (Davis et al., 1992; Gustin et al., 1988; Zhou et al., 1991; Morris and Horn, 1991; Oliet and Bourque, 1993a; Oliet and Bourque, 1993b; Wan et al., 1994; Doroshenko and Neher, 1992). One reason for this is that it is difficult to prove that the whole-cell currents are, indeed, from MS channels. The need for a pharmacological tool identifying the channel is great. Another difficulty lies in introducing an appropriate physiological stimulus to the channel. Any cell might experience an environmental osmotic perturbation (i.e. hypo- or hyper- tonic challenge). Experimentally, this particular type of

physiological stimulus has been mimicked by exposing cells to 1) hypotonic media (Bear, 1990; Ubl *et al*., 1988; Sackin, 1989), 2) a solution of amino acids to accelerate the amino acid/Na^+-coupled transport (Hudson and Schultz, 1988), and 3) application of positive pressure to the recording pipette while in the whole-cell configuration, (Morris and Horn, 1991; Doroshenko and Neher, 1992).

vii) Criteria

What is necessary before we can safely say that these MS channels are physiological mechanotransducers? Morris, (1992), suggests five criteria that should be satisfied.

1) Demonstrate and characterize the MS channel at the single-channel level.

2) Find a specific blocker of the channel, or a mutant organism with which a wild-type comparison can be made.

3) Show that some physiological aspect of the cell's behaviour or development is mechanosensitive.

4) Show that the mechanosensitivity of (3) is impaired with the selective blocker or mutant of (2).

5) Using physiological stimuli (not something that will irreparably damage the cell), obtain macroscopic recordings (preferably using perforated patch as well as whole-cell configurations) which correspond to single channel recordings: selectivity, pharmacology, noise characteristics consistent with single channel kinetics and amplitude, saturation indicative of a finite number of discrete channels, expected mechanosensitive current densities based on single channel data, and stretch sensitivity.

viii) Attempts to Satisfy Criteria

Several studies have put forth evidence suggesting that MS channels are physiological mechanotransducers. Many reports of single channel MS channels exist (for review see Morris, 1990). A difficult criterion to satisfy has been #4 but one study has partially met it by cloning one type of MS channel from *E. coli*. Unfortunately, its sequence, as might have been anticipated, bears no relation to other cloned ion channels. Another criterion which has historically been difficult to satisfy is #5. One of the earlier ones, (Gustin *et al.*, 1988), was carried out on spheroplasts of the yeast *Saccharomyces cerevisiae*. It demonstrated that macroscopic MS (I_{MS}) currents which were the result of MS channel activity. It showed that I_{MS} saturates and is gadolinium (Gd^{3+})-sensitive as are single MS channels. It does not, however, demonstrate that I_{MS} was a response to physiological stimuli nor does it prove that the MS channels are physiological transducers. The spheroplasts were seriously disrupted mechanically and should perhaps be seen as large patches rather than "intact whole-cell prepartions".

Another study (Davis *et al.*, 1992), demonstrated whole cell MS currents in vascular smooth muscle (VSM) cells. The cells were stimulated by rapidly stretching the cells lengthwise between two GΩ-sealed pipettes. Although they demonstrate that the I_{MS} are reversible and repeatable, they do not show any saturating responses. The dose response they show has three data points representing 12, 15 and 25% length increases, through which a curve is constructed which does not look to be part of a saturating Boltzmann curve. They could not demonstrate Gd^{3+}-sensitivity of the MS current because Ca^{2+} channels are blocked by Gd^{3+} in VSM.

I_{MS} currents corresponding to single channel currents have been recorded from germlings of the phytopathogen *Uromyces appendiculatus*, a germ tube protoplast (Zhou *et al.*, 1991). The growth of this fungus is guided, topographically, along the surface of the bean leaf to an appropriate site of entry. When a stomatum is sensed by the fungus it ceases polarized growth and develops appressoria which are necessary for infecting the host. The *Uromyces* I_{MS} saturate and show Gd^{3+}-sensitivity as do the single channel currents. Gd^{3+} also inhibits germ tube growth and differentiation. Although calculations of tensions that might be experienced during growth suggest that the tensions would be large enough in magnitude to activate the channel, it is unclear how the non-selective MS channels with a conductance of such enormity (600 pS) would be used by the growing tip. In addition, the germlings are so small, that even in whole cell, the total membrane area is 55 μm^{-2} (not that much larger than a patch). The cell wall is removed and it is conceivable that the cytoskeleton of the entire cell is disrupted in the same way as a patch is, consequently rendering all of the MS channels hypersensitive to membrane tension as suggested by Morris and Horn (1991).

In another study cultured chick heart cells were monitored with a Ca^{2+}-sensitive dye as well as single channel patch techniques (Sigurdson *et al.*, 1992). The cells were stimulated by proding with a blunt probe which could very well have damaged the cells or at least altered the cytoskeletal environment of the channels by the shearing motion that was used. To address this point a cell which was coupled to several others was "pulled" and resulted in adjacent cells fluorescencing indicating a rise in intracellular Ca^{2+} concentration. It is not clear how the cell was secured in order to "pull" it. If the process damaged the cell, and it was electrically coupled to the other heart cells, an influx of Ca^{2+} would cause a spread in

fluorescence. They were also unable to demonstrate that the fluorescence was the result of calcium influx through MS channels. Nevertheless this study provides circumstantial evidence that MS channels in chick heart cells act as mechanotransducers but as the authors point out, the possibility that the Ca^{2+} response is caused by some other transducer system was not eliminated.

Recent studies, (Oliet and Bourque, 1993a; Oliet and Bourque, 1993b), provide convincing evidence suggesting that MS channels in neurons of the supraoptic nucleus are physiological mechanotransducers. They demonstrate that physiological variations in fluid osmolality accompany changes in cell volume and that these modulate the activity of mechanosensitive cation (SI Cat) channels in a way that is consistent with the macroscopic regulation of membrane voltage and action potential discharge (Oliet and Bourque, 1993a). While whole-cell current clamping, hyperosmolality depolarized and hypoosmolality hyperpolarized isolated supraoptic neurons through the activation of non-selective cation channels (Oliet and Bourque, 1993b) suggesting that these neurons express a depolarizing current that is active under steady-state conditions and that the increase or decrease of this current contributes to the excitation or inhibition of these cells upon acute exposure to hypo- or hyper- osmolar conditions.

3. SA K^+ Channels

It is not clear yet what role MS channels play. They have been studied most extensively in molluscs but have been described in vertebrate embryo and insect somatic muscle.

i) Role in Neuronal Growth?

In the mollusc, it was postulated that SA K^+ channels could play a role in cellular growth given that both SA K^+ channels and SI K^+ channels occur in the growth cone of cultured neurons (Sigurdson and Morris 1989). The pressure response curves of these channels were mirror-image sigmoids with some overlap in the foot of the sigmoids, (Morris and Sigurdson, 1989). An intermediate membrane tension would minimize K^+ permeability making it easier to excite voltage-dependent Ca^{2+} influx. Cytoskeletal machinery is modulated by Ca^{2+} and growth cone elongation is highly sensitive to levels of internal Ca^{2+} (Rehderr and Kater, 1992). Probing filapodia anchor themselves, then pull the rest of the cone towards the anchor site (Lamoureux *et al.*, 1989). Therefore, as the growth cone is being pulled, it was thought that SI K^+ channels would inactivate, but if tension got dangerously high, SA K channels would be recruited. Thus, if the growth cone were pulled too strenuously or too gently, SA K^+ or SI K^+ channels respectively would activate decreasing membrane excitability and intracellular Ca^{2+}.

However, these single channel currents were not representative of any macroscopic currents elicited with mechanical stimuli (Morris and Horn, 1991). The MS macroscopic currents recorded were minute even at near lytic membrane tensions. These SA K^+ channels, however, are found in many cell types of the mollusc and are homogeneously distributed at high densities in these cells. What are these channels doing? Since they are essentially insensitive to Ca^{2+}_{int} and membrane potential, (Bedard and Morris, 1992; Sigurdson *et al.*, 1987), what are they sensing? Are they sensitive to second messengers or ligands?

ii) Role in Embryology/Development?

In another attempt to establish a physiological role for SA K^+ channels, vertebrate developing embryos were studied (Medina and Bregestovski, 1988; Medina and Bregestovski, 1991). Single channel recordings of isolated loach blastomeres containing 3-10 cells revealed a stretch-sensitive channel which was modulated by cAMP-dependent protein kinase (PK). Whole cell currents of this channel have not yet been described. Gadolinium effectively blocks SA channels in *Xenopus* oocytes, (Yang and Sachs, 1990), that are abundant in this preparation. However, when gadolinium, at concentrations 100 times the single channel IC_{50}, was included in the growth medium used to rear the Xenopus oocytes, embryogenesis was unaffected and healthy tadpoles developed (Steffensen, *et al.*, 1991). If the SA channels have a role in controlling the morphogenetic movements, it is evidently not an essential one.

iii) S-like?

The S-channel is named for the fact that serotonin regulates its activity. It's behaviour has been implicated in synaptic modulation and learning in *Aplysia* (for review see Kandel and Hawkins, 1992). A mechanosensory neuron, which forms an excitatory synaptic connection with a motorneuron, is under the control of interneurons which release serotonin and FMRF-amide. The sensory-motor synapse represents a very simple neural circuit mediating a defensive reflex in *Aplysia*, the gill and siphon withdrawal reflex. This reflex can be strengthened or weakened by inputs from interneurons. This dual modulation is due to the facilitory and inhibitory interneurons which synapse on presnaptic terminals of the sensory neurons. 5-HT is responsible for facilitation and FMRF-amide is responsible for inhibition.

The S-channel's behaviour is regulated by different ligand-mediated, cascading second messengers. These second messenger pathways have been described in great detail (Fig. 1.2). 5-HT binds to a receptor that is probably a type $1_{A,B,D}$ or 4 (Maricq *et al.*, 1991; Mercer *et al.*, 1991; Peroutka, 1990). The receptor ligand complex couples to a G_s-type G-protein which activates adenylate cyclase (AC) resulting in an increase in cAMP production (Shuster *et al.*, 1985). The cAMP activates cAMP-dependent PK (PKA) which phosphorylates the channel. The channel is inactivated when phosphorylated by PKA. A decrease in K^+ conductance results in a more excitable membrane. This is the underlying mechanism of

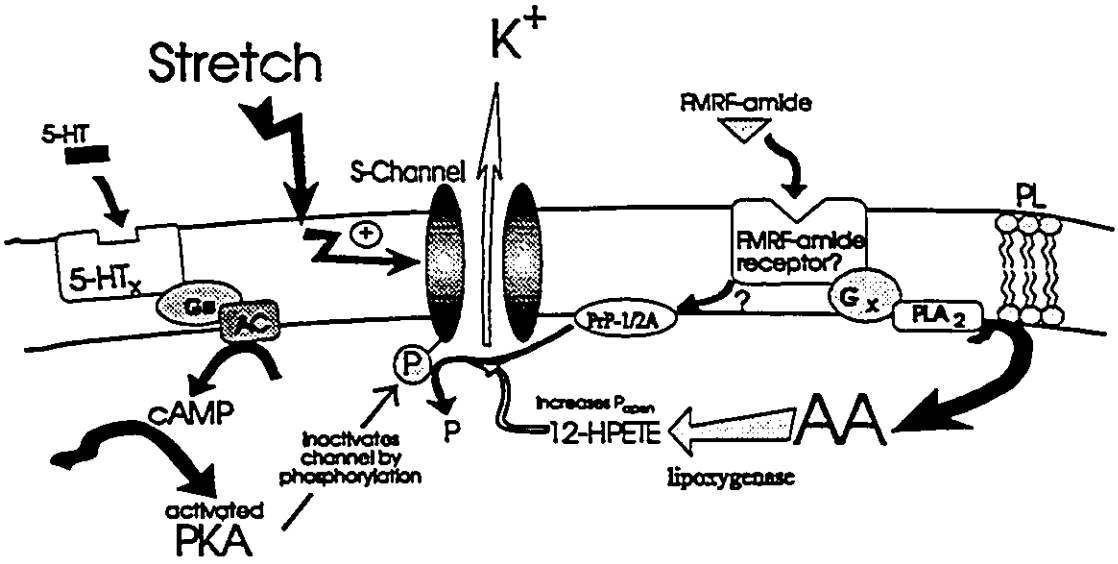

Figure 1.2. Schematic representation of modulation of S-Channel in *Aplysia* mechanosensory neurons. (see text for details)

presynaptic facilitation of the sensory neuron. Desensitization and inhibition is mediated through the same channel via FMRF-amide. FMRF-amide binds to its receptor, activating a PTX-sensitive G-protein which is not G_i, and activates phospholipase A_2 (PLA_2) (Volterra

and Siegelbaum, 1988; Sweatt *et al.*, 1989). The PLA_2 metabolizes membrane phospholipids resulting in the production of arachidonic acid which is further metabolized into 12-HPETE (Piomelli *et al.*, 1987a). 12-HPETE and some of its metabolic by-products act on the S-channel resulting in an increase in open probability and relief of 5-HT mediated inactivation (Piomelli *et al.*, 1989; Piomelli, 1989; Piomelli *et al.*, 1987b; Piomelli *et al.*, 1988; Belardetti *et al.*, 1989). This 12-HPETE effect is thought to be due, in part, to the action of protein phosphatase-1 (PrP-1) dephosphorylating the channels (Ichinose and Byrne, 1991; Endo *et al.*, 1991).

Because of the similarities of the S-channel in *Aplysia* which has been studied in great depth (for review see Volterra and Siegelbaum, 1989), and SA K^+ channels in *Lymnaea* and *Cepaea* (Sigurdson *et al.*, 1987; Bedard and Morris, 1992), the S-channel in *Aplysia* was tested to determine whether it was also stretch-sensitive (Vandorpe and Morris, 1992). If so, this would be the first channel with a known function which had been shown to be sensitive to stretch. This would provide significant direction for further studies of SA K^+ channels in other preparations. The results were positive; the S-channel of identified mechanosensory neurons was activated by stretch, and moreover, as in other molluscs (Sigurdson and Morris, 1989), SA K^+ channels were found in all *Aplysia* neurons. *Aplysia* SA K^+ channels and S-channels were shown to be similar in many ways. They are both regulated by FMRF-amide, serotonin (5-HT), and cAMP in the same way and they exhibit identical kinetics (Vandorpe, et. al., 1994). Thus the S-channel was shown to be a type of SA K^+ channel, but is the reverse true? Are other SA K^+ channels in different preparations S-like in that they are modulated by neurotransmitters via second messengers?

iv) Molluscan Heart

SA K^+ channels of molluscan heart (Sigurdson *et al.*, 1987) are similar to those in neurons of the same organism (Sigurdson and Morris, 1989). Although it is possible that SA K^+ channels of *Lymnaea* ventricular cells are stimulated by extreme osmotic swelling (Morris and Moore, 1992), similar SA K^+ channels in *Lymnaea* growth cones are not (Morris and Horn, 1991). This issue is complicated though; TEA-insensitive whole-cell currents from *Lymnaea* neuron cell bodies were detected with cell swelling (Wan et al., 1994). Extreme osmotic swelling of the cell bodies resulted in currents which would amount to an open probability of only about 0.07 (Wan et al., 1994).

Serotonin is a neurotransmitter with excitatory actions in molluscan heart (Buckett *et al.*, 1990), similar to those in *Aplysia* neurons (Belardetti *et al.*, 1986; Shuster and Siegelbaum, 1987). Both mediate post-synaptic excitation by decreasing a K^+ conductance. Are these excitatory effects in molluscan heart mediated by an S-like channel? If so, does this S-like channel show stretch-sensitivity? Is it the SA K^+ channel already described in this tissue (Sigurdson *et al.*, 1987)?

SA K^+ channels have been described in insect somatic muscle (Zagotta *et al.*, 1988; Gorczyca and Wu, 1991). They have no known mechanosensory function. They are similar to molluscan SA K^+ channels. Octopamine and proctolin are contractility-modulating neurotransmitters whose effects are mediated by cAMP (Evans *et al.*, 1988). Is this SA K^+ channel S-like in that it is modulated by ligand-mediated second messengers? Is this S-like characteristic common among all SA K^+ channels?

CHAPTER II General Methods

1. Preparations Studied

(i) Aplysia californica Mechanosensory Neuron Culture

Aplysia californica from Marinus (Long Beach, CA) were housed at 15 ° C in aerated artificial seawater (Forty Fathoms, Marine Enterprises, Baltimore, MD). Animals (50-250 gm) were anesthetized by injecting them with about 50% of their weight of isotonic $MgCl_2$. An incision was made rostral to the antennae to expose the pleural and pedal ganglia (Fig. 2.1.A). The ganglia were cut out and placed in *Aplysia* culture media (ACM) with 1% protease (Sigma, St. Louis, MO) type IX and gently agitated for 4 to 6 hours. Following this enzymatic digestion, the ganglia were pinned down in a sylgard-coated 35 mm culture dish containing normal *Aplysia* culture medium (ACM) (Fig. 2.1B). The sheath surrounding the pleural ganglion was carefully cut away with fine forceps and micro-scissors to expose identified mechanosensory neurons of the ventrocaudal cluster of the pleural ganglion (Walters, et. al., 1983). Using a long-shanked micropipette, these neurons were teased away by hand from the ganglion and transferred to separate 35 mm culture dishes containing ACM. For some experiments which required small recording chambers, the petrie dishes were modified by placing a premolded form-fitting sylgard insert into the dish. The volume of the recording chamber and consequently the culture dish was either 60 or 300 µl depending on which size insert was used. Cells were left at room temperature in a small humid chamber for 1 to 6 days before use. The cells initially retracted any remaining axons before firmly adhering and sending out new

Fig. 2.1. ***Aplysia californica*** **mechanosensory neuron culture.** A) Schematic diagram of ganglia *in situ* from a dorsal perspective. B) Schematic diagram of the left pleural and pedal ganglia indicating the location of the pleural ventrocaudal (PVLC) cluster of mechanosensory somata (adapted from Walters et al., 1983). C) Videomicrograph of an *Aplysia* mechanosensory neuron left one day in culture. Scale 30 μm.

A

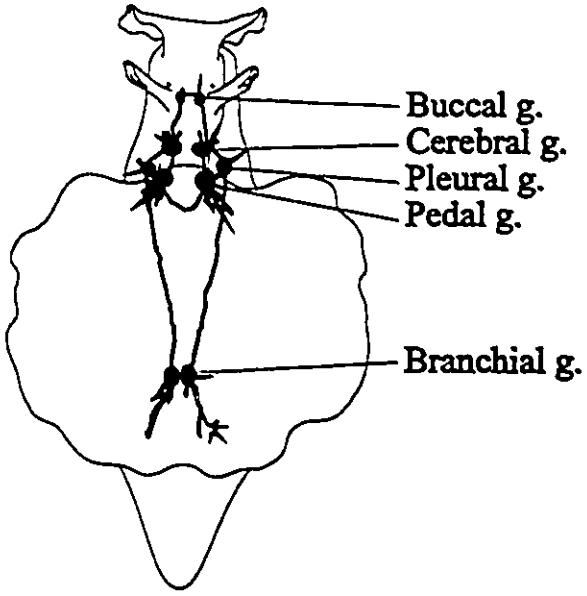
Buccal g.
Cerebral g.
Pleural g.
Pedal g.
Branchial g.

B

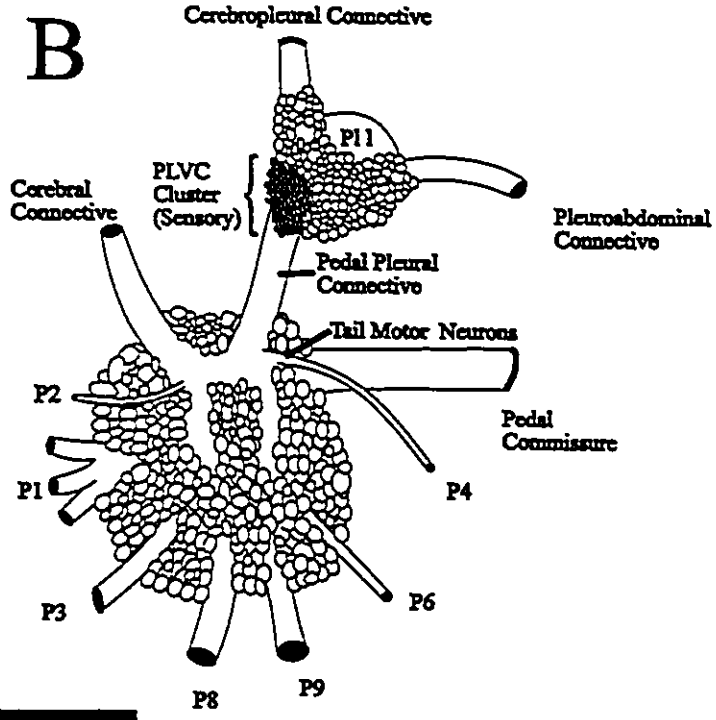
Cerebropleural Connective
P11
PLVC
Cluster
(Sensory)
Cerebral
Connective
Pleuroabdominal
Connective
Pedal Pleural
Connective
Tail Motor Neurons
P2
Pedal
Commissure
P1
P4
P3
P6
P8
P9

C

processes (Fig. 2.1C). New processes generally appeared after the first 24 hrs in culture.

(ii) Lymnaea stagnalis Neuron Culture

The shells of *Lymnaea* were removed and the snail was pinned ventral side down onto a flat piece of sylgard. An incision was made lengthwise just dorsal to the buccal cavity about 2 cm in length. A "T" was cut so that the flaps of skin could be pinned forward exposing the circumesophageal ganglionic ring (Fig. 2.2A). The esophagus was cut along with ganglionic connective tissue to allow the removal of the ring (Fig. 2.2B). The ring was then placed in a culture dish of *Lymnaea* culture medium (LCM) where the individual ganglia were separated and any connective tissue which remained was cut off. The ganglia were gently agitated in LCM containing 0.25 % protease type XIV (Sigma, St. Louis, MO) 40 to 60 minutes at room temperature at which point they were rinsed with 10 ml of LCM, then 10 ml of *Lymnaea* plating medium (LPM). The ganglia were plated in 35 mm culture dishes (usually one per dish) by pulling the remaining ganglionic sheath off the ganglion and then gently touching the ganglion to the bottom of the culture dish. Several cells would stick to the bottom of the dish when the ganglion was lifted from the bottom. This process was repeated until no more cells would come free from the ganglion. The cells plated in culture dishes, were left in humid chambers as were the *Aplysia* neurons for 1 to 6 days at room temperature at which time they were used for electrophysiological experimentation. The rate of growth was similar to the *Aplysia* neurons (Schacher and Proshansky, 1983), in culture. The morphology of the neurons varied, (Fig. 2.2C), not surprisingly, as the cells were a heterologous population of

Fig. 2.2. *Lymnaea* neuron culture. A) Photograph from dorsal perpsective of exposed circumesophageal ganglionic ring (arrowhead) which circles the esophagus. Scale 2.2 mm. B) Schematic dorsal view (left) (adapted from Slade, et al., 1981) and photograph of ventral view (right) of the circumesophageal ganglionic ring showing the arrangement of the central ganglia and nerves. a) left cerebral ganglia, b) cerebral commissure, c) right cerebral ganglia, d) left pleural ganglia, e) left pedal ganglia, f) right pedal ganglia, g) right pleural ganglia, h) left parietal ganglia, i) ventral ganglia, j) right parietal ganglia. Scale 630 µm. C) Series of videomicrographs illustrating variety of cell-types associated with enzymatic dissociation of circumesophageal ganglia. Cells shown at 6 days in culture. Unipolar (top left), bipolar (top right), "fried egg" (bottom left), and what I presume to be glial cells (bottom right)- I did not record from these cells- are all members of the resulting heterologous cultured cell population. Scale clockwise from top left; 37 µm, 55 µm, 28 µm, and 28 µm.

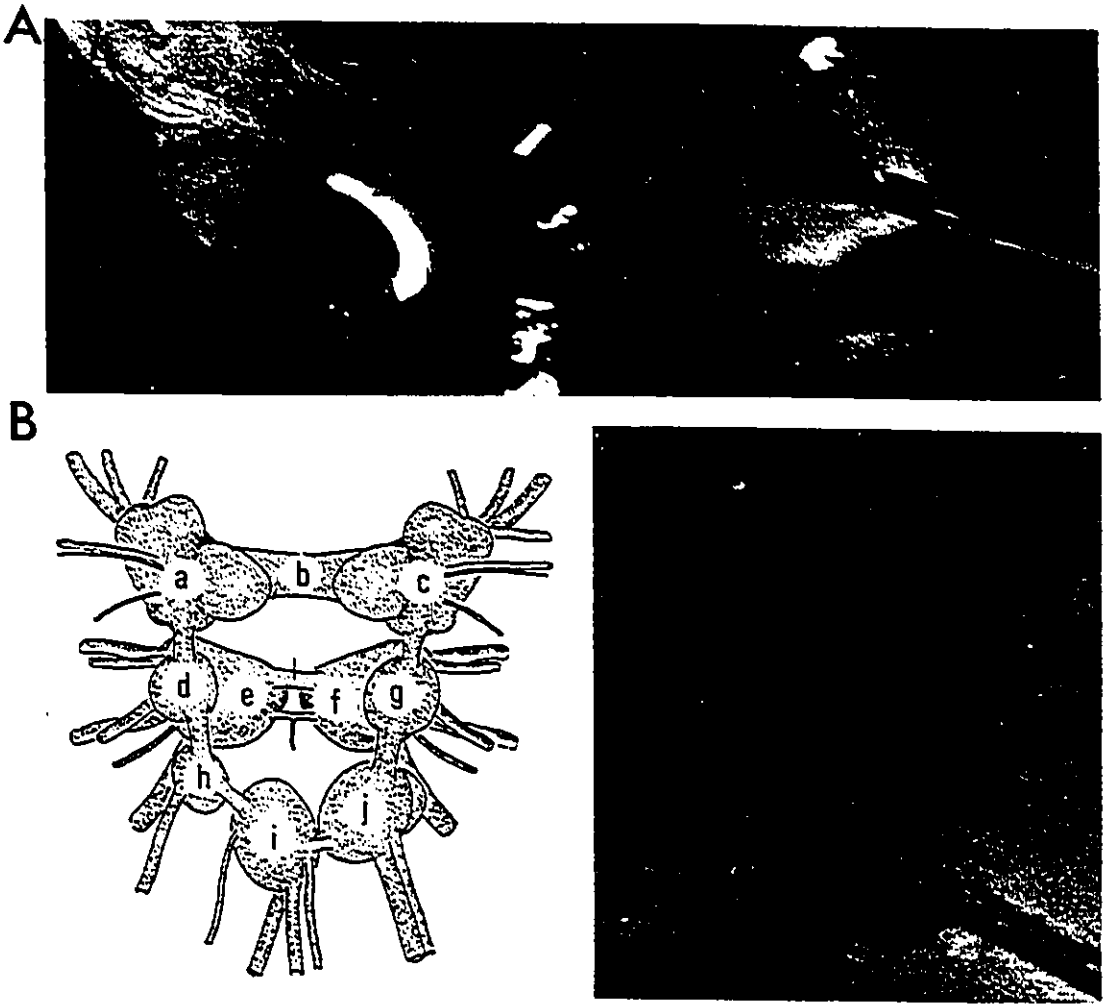
A
B
a
b
c
d
e
f
g
h
i
j
C

neurons representing cells from virtually the entire *Lymnaea* central nervous system.

(iii) Lymnaea stagnalis Ventricular Cell Culture

Hearts were removed from adult *Lymnaea stagnalis* as shown in Fig. 2.3. A-C (Brezden and Gardner, 1983). The atria and aortae were cut away and the ventricles were placed in LCM. The ventricles were cut into small (1mm) pieces with a scalpel and placed in 15 ml conical centrifuge tubes containing 5 ml of 0.25 % trypsin type XII-S (Sigma, St. Louis, MO) in LCM. The tissue fragments were treated at room temperature for 30 min and subsequently centrifuged at 115 g for 10 min. The trypsin was replaced with a 0.1 % solution of collagenase type II-S (Sigma, St. Louis, MO) and digested for a further 2 h. The tubes were gently agitated throughout this process. Following the collagenase treatment the tubes were centrifuged and the dispersed cells were resuspended in 5 ml LCM. The cells were plated in 35 mm Petrie dishes and used for patch-clamp experiments 2-4 days later (Fig 2.3 D and E).

(iv) Xenopus laevis Oocytes

Xenopus oocytes. Mature, wild caught female frogs (*Xenopus laevis*) were obtained from Xenopus I (Ann Arbor, MI). Frogs were anesthetized in a small container (500 ml) containing 0.35% MS-222 (the methane sulfonate salt of 3-aminobenzoic acid ethyl ester) (Sigma, St. Louis, MO)) for 15 to 20 min. They were maintained in an anethetized state by placing them, ventral side up, on a tray of crushed ice. A 1 cm

Fig. 2.3. *Lymnaea* ventricular myocyte culture. A) Diagramatic representation of the dissection procedure for the isolated heart preparation (adapted from Brezden and Gardner, 1983). The deshelled snail pinned down with the left side facing up. B) The exposed internal organs. AT, atrium; DA, distal aorta; F, foot; G, gut; PA, proximal aorta; V, ventricle. C) The isolated heart. D) Videomicrograph of freshly dissociated ventricular myocytes. Scale 73 μm. E) Videomicrograph of a cell-attached patch (arrowhead) of a venticular myocyte 3 days in culture. Scale 18 μm.

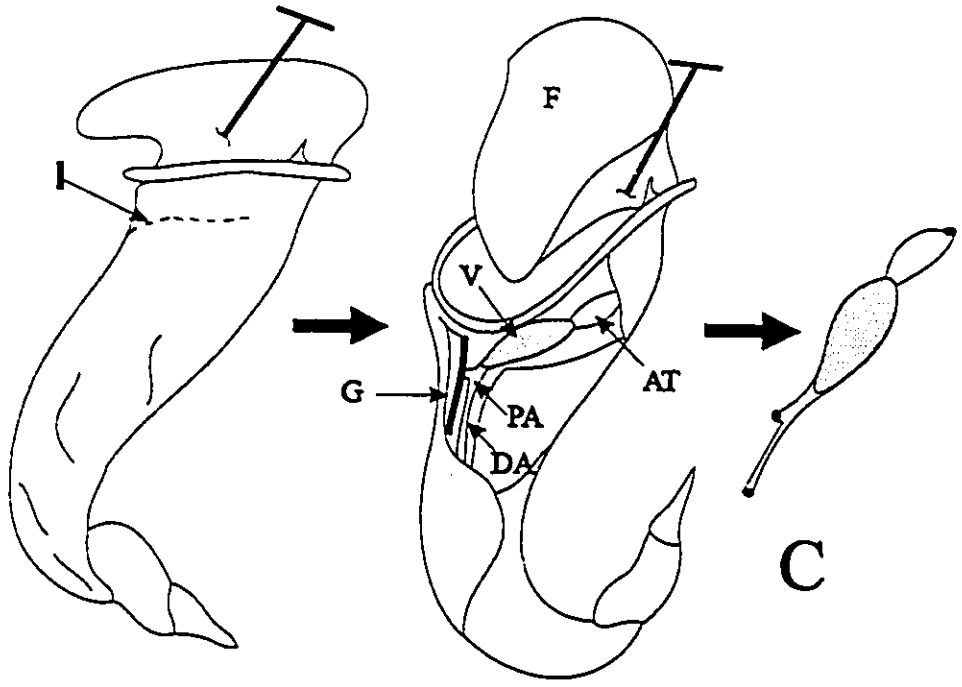

A B

D

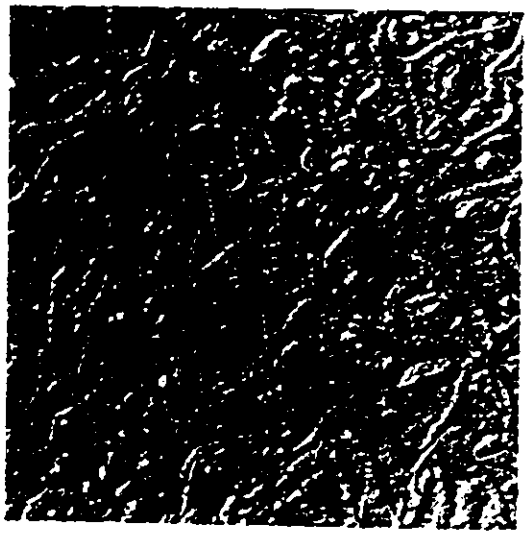

E

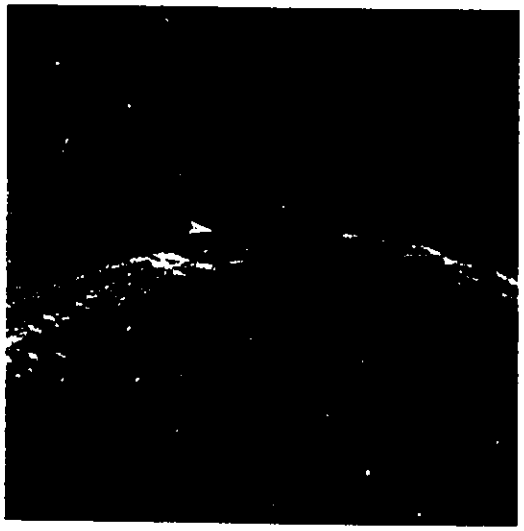

incision stretching diagonally from medial to lateral toward the head, was made in the skin and underlying fascia over the ovary. Oocytes were surgically removed to a small beaker containing OR2. The incision in the skin and fascia each was then sutured with 1 and 2 stitches, respectively, using #5 silk. Frogs were placed in 1 l of water in order for them to regain conciousness. Ovarian lobes were cut into smaller pieces, then gently agitated at room temperature in OR2 containing 2 mg/ml collagenase type IA (Sigma, St. Louis, MO) for 2-2.5 h checking periodically for defolliculation. Oocytes were washed in ND96 and type V and VI oocytes (Goldin, 1992), sorted and stored overnight in ND96 at 15 °C (Fig. 2.4. A). Just prior to patch-clamp recording, the vitelline was removed using fine forceps after first shrinking oocytes in hypertonic stripping solution (HYPER) (Methfessel, et al., 1986) (Fig. 2.4. B). Bare oocytes readily attach to any clean surface and stick resulting in damage if any attempts to move them are made. Therefore, they were transferred by micropipette from the devitilinizing dish to the recording dish immediately following removal of the vitelline and not moved again.

(v) Brachydanio rerio Embryos

One day prior to collecting embryos, 1-2 hr before the light period of the day, the fish were fed and the tanks cleaned. 4 males and 8 females were isolated in a small tank which had been lined with marbles; marbles keep the fish from eating their young. The next morning about 30 min after the beginning of the light cycle, embryos were collected from the bottom of the tank with a siphon consisting of a 1 cm i.d., 30-50 cm long glass

Fig. 2.4. Selection of *Xenopus* oocytes at various stages of development. Stage I (1), the earliest stage, oocytes are about 50-100 μm in diameter and appear transparent. Stage II (2) oocytes are 300-450 μm and appear either transluscent or white depending on the stage of development. Stage III (3) oocytes are 450-600 μm and can be distinguished by the appearance of pigmentation uniformly throughout the surface. Stage IV (4) oocytes are 600-1000 μm with differentiated hemispheres and a very dark brown animal hemisphere. Stage V (5) oocytes are 1000-1200 μm, with hemispheres clearly delineated. Stage VI (6) oocytes are 1200-1300 μm and can be distinguished by an unpigmented equatorial band between the two hemispheres. f) follicular cells appear red due to dense vascularization. Oocytes have been partially defolliculated enzymatically. Scale 1125 μm.

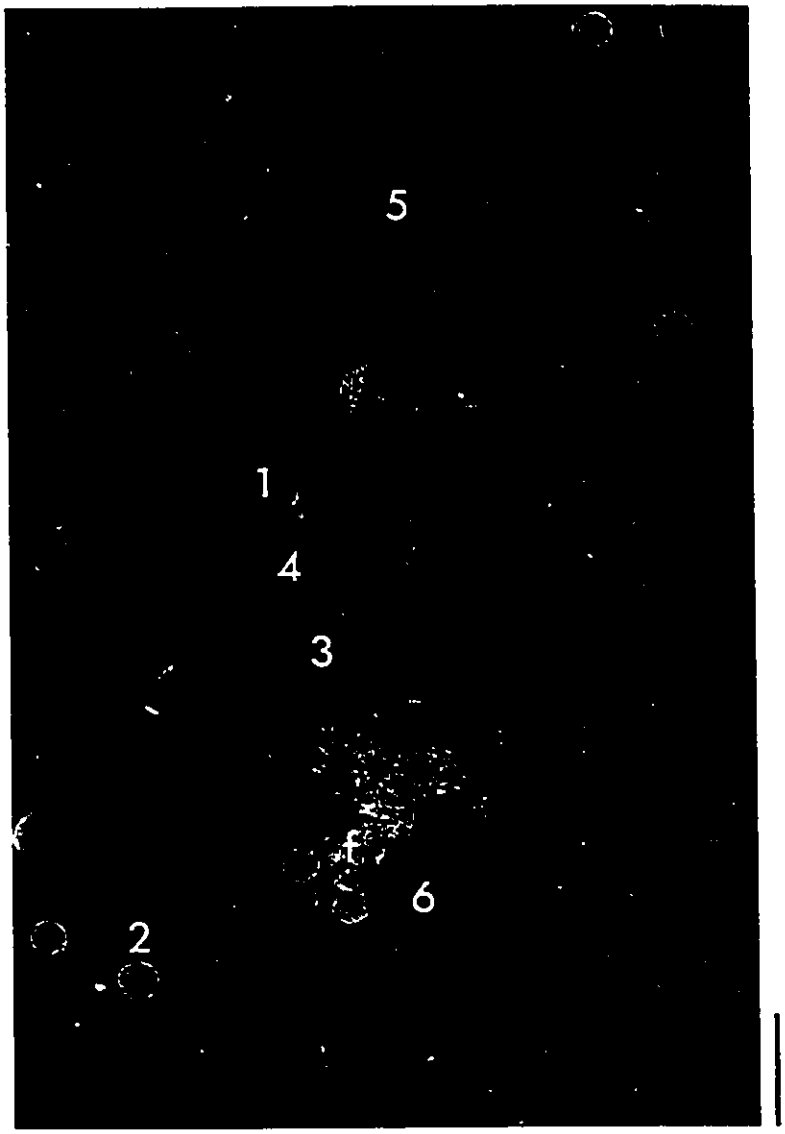
5
1
4
3
f
6
2

tube covered at one end with a piece of tygon tubing to protect it from breaking. The embryos are cleaned in 10 % Hanks saline and all feces and debris are removed. About forty min following birth the embryos will divide from a one cell stage to a two cell stage embryo. Another division occurs every 20 min. A 4-cell stage and an 8-cell stage embryo are shown in Fig. 2.5. A. and B. The rapidity with which these embryos developed necessitated working quickly. For experiments with dissociated embryonic cell culture, embryos were first dechorionated by soaking them in 0.5 mg/ml pronase in 10 % Hank's solution for five min. The dechorionated embryos were then washed in a calcium-free ZNS in which the yolk was cut away with a scalpel, then the remaining embryonic cells were triturated in fresh calcium-free ZNS until cells began to dissociate at which point they were transferred to ZNS in a 35 mm Petrie dish for patch-clamp experiments (Fig. 2.5. C).

2. Patch-clamp Recording

(i) Seal Formation

Before the pipette tip is submersed in the recording solution, a positive pressure (+10 to +20 mm Hg) is applied. This keeps debris from plugging the tip or interferring with the seal formation. Once the pipette tip is submerged in the recording solution, the junction potential is nulled manually and zeroed with the junction null zero or reset button. The junction null tracking is activated and the pipette tip is advanced toward the cell. The pipette resistance is monitored by repetitively applying a small (+10 mV) voltage step (seal test) to the pipette and measuring the resultant current. When the pipette touches the cell,

Fig. 2.5. *Brachydanio rerio* embryos and cultured cells. A) Videomicrograph of dorsal view of 4-cell embryo at 1 hr of development with intact chorion (black arrowhead). Nucleus (N) of an individual cell (white arrowhead) is visible and still quite large at this stage. Scale 280 µm. B) Videomicrograph of lateral view of 8-cell embryo at 1.2 hr of development with chorion removed with brief pronase treatment. A single cell is indicated with a black arrowhead. Scale 255 µm. C) Dissociated embryonic cells 1 day in culture. Cells are smaller yet have retained a visible nucleus (N) and cell "foot" (F) attachment sites have formed to anchor the cell to the petrie dish. Scale 20 µm.

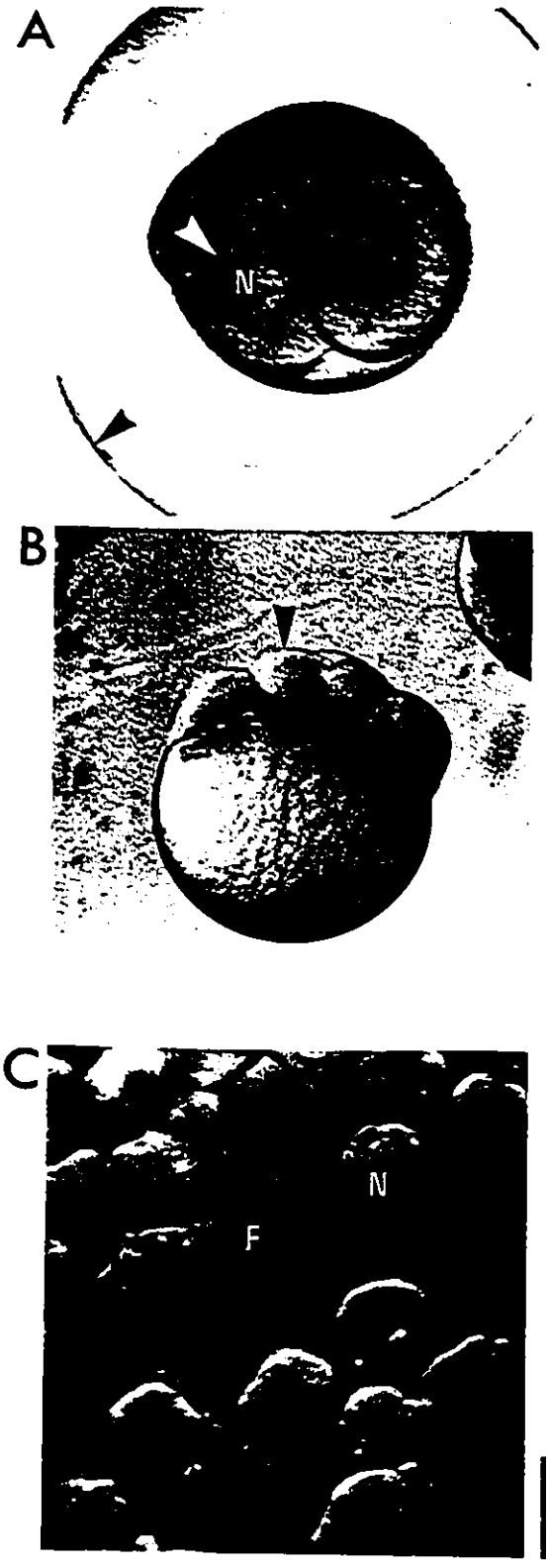
A
N
B
C
N
F

the seal test is turned off, the junction null is switched to hold and the positive pressure is released. The seal test is reactivated and suction is applied until seal formation. Generally, seals formed with a resistance of between 20 and 100 GΩ. This gigaohm seal means that the resistance to current flow between the glass recording pipette and the cell membrane is so high, any current that is recorded is essentially all passing through the patch of membrane, more specifically, through ion channels.

(ii) Pipette Fabrication

Recording pipettes were fabricated from a relatively soft glass, borosilicate glass tubing (N51A, OD 1.65 mm ID 1.15 mm; Garner Glass, Claremont, CA) and pulled using a List L/M-3PA puller (Darmstadt, FRG). Pipette tips were coated to within about 200 µm from the opening with sylgard to increase the dielectric constant and decrease recording noise. The sylgard was painted on with a toothpick and the sylgard was then cured by exposure to a heating element constructed from a modified pipette puller. At this stage the approximate size of the OD of the tip was 1-2 µm. Just prior to each experiment, tips were fire polished. The approximate size of the OD of the tip after fire polishing was 2-2.5 µm. The pipette resistances were 5-12 MΩ and 1-5 MΩ when filled with ANRM and LNRM respectively.

(iii) Recording Configurations

I used just two single channel recording configurations throughout this study; cell-attached patch and excised inside-out patch.

A) Cell-attached patch

In this recording configuration the cell remains intact, although the seal formation involves disruption of the cortical cytoskeletal associated with the membrane which is aspirated into the pipette. The net electrical potential across the membrane is equal to the transmembrane membrane potential with respect to the ground, minus the pipette potential. The polarity of the pipette potential is opposite to what the cell "feels" (i.e. applying a negative potential to the pipette depolarizes the patch of membrane). Currents flowing outward through the membrane into the pipette are considered positive currents with respect to the cell and negative with respect to the pipette. Convention dictates that current polarity is stated with respect to the cell. Because the resting membrane potential of a cell can oscillate or fluctuate within a modest range, "voltage-clamp" of the patch is subject to variation.

An advantage of this configuration is that the normal intracellular constituents and environment is disrupted less than in any other configuration. It could, however, be argued that the channels recorded in this configuration have had their cortical cytoskeletal environment disrupted whereas in a nystatin perforated patch, whole-cell configuration, this type of disruption would be minimized. Nonetheless, attempts at obtaining macroscopic mechanosensitive currents from this preparation almost always yield no MS K^+ current (Morris and Horn, 1991; Wan et al., 1994).

A disadvantage of this technique is that the solution at the intracellular face of the membrane patch cannot be manipulated and manipulation of the solution at the extracellular face by pipette perfusion is slow and fraught with difficulties.

B) Excised inside-out patch

The mechanical strength of the gigaseal permits removal of the patch from the cell by simply lifting the pipette up away from the cell with a quick jerky motion. If the motion is slow, it is likely that the membrane will get pulled into a tube formation and when the membrane patch finally separates from the cell, the sides of the tube of membrane seal to form a "vesicle" enclosing a small volume of bathing solution. To minimize the likelihood of vesicle formation one can excise the patch in low calcium solution (i.e. intracellular solution) and if a vesicle does form, brief exposure of the pipette tip to air can sometimes disrupt the vesicle while leaving the patch intact. If channel events are rounded as if by an RC filter, it is likely that a vesicle has formed. A change of solution at the intracellular face that should shift the reversal potential of K^+ currents can be used as a test of whether or not a vesicle has formed.

An advantage of this configuration, in addition to providing access to the intracellular face of the membrane patch, that the membrane patch can be reliably voltage-clamped. The membrane potential is no longer influenced by the cell's resting potential and is simply opposite in polarity to the pipette potential. The convention for polarity of membrane currents is identical to that of cell-attached patches: currents across the membrane into the pipette are positive currents. In spite of the fact that patch excision is a mechanically severe process, the excised patch does not consist solely of membrane. Cytoskeletal elements may also be present, as demonstrated by Sokabe and Sachs, (1990) and Sokabe et al., (1991).

C) Elimination of Ca^{2+}-activated K channel activity

To block the activity of Ca^{2+}-activated K channels (Shuster, et al., 1991), when recording from *Aplysia* mechanosensory neurons, I routinely used 10 mM TEA chloride in pipette solutions. The K_d for TEA block of *Aplysia* Ca^{2+}-activated K channels is 0.4 mM while the K_d for TEA block of S-channels was 40 mM (Shuster, et al., 1991). When recording from *Lymnaea* neurons or myocytes I routinely used 1 mM TEA to block Ca^{2+}-activated K channels. This concentration of TEA had a negligible effect on SA K channels as I showed that the K_d for TEA block of SA K channels is ~50 mM (Small and Morris, 1994b).

3. Data Analysis

i) Channel Kinetics

Channel currents were usually recorded on video tape (Sony, Beta) following pulse code modulation (PCM-1; bandwidth 0-16 khz; Medical Systems Corp., Greenvale, NY). Currents were analyzed by replaying the tape through an 8-pole Bessel filter (2 kHz; Frequency Devices, Haverhill, MA) connected to a microcomputer via a Labmaster A/D interface. Single-channel events were digitized at 10 kHz with FETCHEX, event lists produced with FETCHAN (FETCHAN uses a 50% threshold criterion for capturing events), and histograms generated with pSTAT, subroutines of the software package pCLAMP v5.5.1 (Axon Instruments). Given that the digitizing frequency was 5X the filter frequency, the 2 kHz filter constituted the final effective cutoff frequency and the deadtime for event detection was about 90 μs (that is, 0.9 times the sample interval of 100 μs) (Colquhoun & Sigworth, 1983). No correction for missed

events has been applied. Sub-conductance events were rare (as indicated by visual inspection of the records and from point-by-point amplitude histograms) in the recordings that I used for one-channel kinetic analysis and so mis-assignments associated with such events were ignored. pSTAT's non-linear, least squares curve-fitting method was used to fit Gaussian and exponential functions to the data. In a few cases, currents were recorded on-line via the A/D interface using FETCHEX.

ii) On-line Voltage-clamp/Pressure-clamp Studies

Channel currents were recorded using an Axopatch 1D (Axon Instruments, Foster City, CA) connected to a PC microcomputer via a TL-1 interface (Axon Instruments, Claremont, CA). pClamp 5.5 (Axon Instruments, Claremont, CA) was used to digitize and export records to Sigmaplot 4.1 (Jandel Scientific, Corte Madera, CA). Once in Sigmaplot 4.1 the records were analyzed then exported to Coreldraw 3.0 (Corel, Ottawa, Ont.).

For current/voltage (I/V) relations of single channel events from cell-attached patches the membrane voltage was taken to be $V_m=(V_{rest}-V_p)$, where V_p is the pipette holding potential and V_{rest} is the resting membrane potential, which was assumed to be -45 mV (Baxter and Byrne, 1990) for *Aplysia* neurons, -50 mV (Morris and Sigurdson, 1989) for *Lymnaea* neurons and -60 mV for *Xenopus* oocytes (Baud et al., 1982). To provide clear resolution of both inward and outward K currents, high K solutions were routinely used. Currents flowing into the pipette are illustrated as upward deflections.

The voltage-dependence of SA K channel open probability ($P_o(V_m)$) was

determined by dividing an ensemble average (I) of 30 consecutive 2 s voltage ramps by the maximum number of channels observed by eye in the patch (n) and the single channel current (i) at any given voltage.

$$P_o(V_m)=I/(n*i)$$

Results are reported as means±standard error, except where indicated. Paired or unpaired t-tests and chi-squared distributions were used, where appropriate and differences were considered significant when $p < 0.05$.

CHAPTER III

FMRF-amide and Membrane Stetch as Activators of the *Aplysia* S-Channel

Kinetic Analysis of Multichannel Patch Data

1. Introduction

The function of MS channels is unknown. Some stretch channels may serve mechanosensory functions, such as modulating the membrane potential in response to the tension of a cleavage cycle (Medina and Bregestovski, 1991). The evidence suggesting that SI Cat channels can function as cellular osmosensensitive proteins is good (Oliet and Bourque, 1993) but for others, stretch-sensitivity in patch configuration seems adventitious (Morris and Horn, 1991). Moreover, as I show in Chapter V, in *Lymnaea* neurons, SA K^+ channels seem to be buffered from membrane tension by cortical cytoskeleton and that stretch-sensitivity is a channel property which is normally kept in check.

It was recently demonstrated (Vandorpe and Morris, 1992) in identified mechanosensory neurons of the pleural ganglion of *Aplysia*, that a stretch-sensitive K^+ channel exhibits many of the characteristics of stretch-activated K^+ channels of neurons and heart cells from *Lymnaea stagnalis* (Sigurdson and Morris, 1989; Sigurdson et al., 1987). It was found that this *Aplysia* channel was indistinguishable from the *Aplysia* mechanosensory neuron channel characterized as the "S-channel" by Siegelbaum and colleagues (1982). Named for its modulation by serotonin (5-HT), the S-channel is also sensitive to the neurotransmitter, FMRF-amide, which activates it via an arachidonic acid pathway

(Belardetti, et al., 1987). It was hypothesized that the *Aplysia* mechanosensory neuron stretch-activated K^+ channel is the serotonin- and FMRFamide-sensitive K^+ channel.

Aplysia mechanosensory neurons exhibit both SA K^+ channel activity and S-channel activity; the two classes of events probably represent activity of the same channel entity (Vandorpe and Morris, 1992). Amplitude histograms for stretch-activated and FMRFamide induced currents in the same patch at the same pipette potential suggest that stretch and FMRF-amide activity represent currents through the same population of channels (Vandorpe et al., 1994).

If FMRFamide induced events and stretch events represent currents carried by different channels, it would be unlikely for the permeability characteristics of events activated by the different stimuli to match precisely. Any idiosyncracies of distinct K^+ channels should emerge in the form of distinct-shaped I/V relations when presented with a non-physiological permeating ion. The shape of the nonlinear I/V relation (inward thallium currents and outward K^+ currents) and its position along the voltage axis (and hence the reversal potential) did not change when channels in cell attached patches were stimulated first via FMRFamide then with stretch (Vandorpe et al., 1994). This is good evidence that the same channels (S-channels) are recruited by stretch and by FMRF-amide.

Single channel kinetics can be analysed in patches which possess just one channel. Stretch markedly decreases the proportion of long closed intervals of a stretch-activated channel in any record without substantially affecting the duration of open intervals. Analysis at several activating pressures from two patches from *Aplysia* neurons which contained only one stretch-activated channel (such patches are rare) and whose P_{open} increased substantially

with suction confirmed that this is also the case for the S-channel (Vandorpe et al., 1994). When assessed under otherwise identical conditions (same patch, pipette potential, recording solutions, filter settings, fitting routine), stretch-activated and FMRFamide induced events produce nearly identical kinetic "fingerprints"; they have the same collection of kinetic states in spite of the differences in the prevailing open probability (Vandorpe et al., 1994). Stretch and the FMRFamide pathway represent radically different activating stimuli for the S-channel; whether their effects converge on a single gating mechanism is not clear.

Like other stretch channels, S-channels remain stretch-sensitive in excised patches. Likewise S-channels in excised patches are directly activatable by an arachidonic acid metabolite in the FMRFamide/lipoxygenase pathway (Buttner, et al., 1989). A possibility consistent with the similar kinetic effects of stretch and FMRFamide on the S-channel is that stretch and the metabolite converge on a common gating process. Interestingly, a broad spectrum of free fatty acids and stretch can both activate K^+ channels in smooth muscle (Kirber, et al., 1990).

i) Multichannel Patch Analysis

The kinetically-identifiable states induced by FMRFamide and by stretch have been compared for single channel patches but a recurrent problem is that of dealing with several simultaneously active channels (the more usual case). I have therefore tested a new analysis program designed to reveal several kinetic aspects of multiple ion channel patches (Dabrowski and McDonald, 1992). First the program tests the stationarity of multiple channel data to determine its suitability for further analyses which are based on the binomial distribution of

current levels. The program then assesses whether the channel events contributing to a stationary section of data appear independent and identical. This process includes estimating 1) the number of channels in the patch, 2) open probability, 3) global means for open and closed times and 4) cumulative open and closed time distributions.

2. MATERIALS AND METHODS

Identified mechanosensory neurons from the pleural ganglion of *Aplysia californica* in primary culture were used 1-3 days after plating (Schacher and Proshansky, 1983). Single channel recordings were made from cell-attached or excised inside-out patches, as indicated. Unless otherwise indicated, pipette solutions were composed of ARS and 10 mM TEA chloride. The bath solution was the same but was pH 7.4 and had no TEA. In experiments involving FMRFamide (Phe-met-arg-phe-amide; Sigma, St. Louis, MO) induced channel activity, a 20 μM FMRFamide solution was perfused by macropipette over the patched cell. 100 μM serotonin hydrochloride (5-HT) (Sigma) was applied in the same manner (Belardetti, et al., 1986; Belardetti, et al., 1987) in some experiments. Any solution changes during an experiment were effected by changing the bath by perfusion with a macropipette.

i) ADaM analysis

For experiments which yielded current records with several simultaneously active channels, events lists generated by FETCHAN, as mentioned in general methods, were

analyzed by the program ADaM. The ADaM Channelyzer is a set of computer programs which implement the statistical techniques for ion channel kinetic analysis (Dabrowski, et al., 1990; Dabrowski and McDonald, 1992) and is available from A.Dabrowski or D.McDonald (Department of Mathematics, University of Ottawa). This program allows the analysis of multiple channel records from which information about the average duration of open and closed sojourns of individual channels is not normally obtained. ADaM uses current level, occupation density and downstep data (Figure 3.1) for the following purposes: to test for stationarity and then to provide estimates of N, the number of channels in a patch, of P_{open}, the open probability of a single channel, of τ_o, the mean open time of single channel events, and of τ_c the mean closed time of single channel events (these means are global averages for *all* the open or closed states of the individual channel, regardless of how many kinetically distinct open or closed states might exist). In certain cases, estimates of open and closed time cumulative probability distribution functions F(t) and G(t), respectively, can also be generated by the program. I examined only estimates of F(t) and, in keeping with convention, plotted the corresponding (estimated) survival function, 1-F(t).

More explicitly, ADaM uses the idealized multi-channel current record to produce a sequence of data vectors as illustrated in Figure 3.1. As in the case of single-channel data, statistical stationarity of the record over the period of observation is a prerequisite for analysis of its kinetics.

Within ADaM, both first and second order stationarity tests were conducted on multiple channel patches. First order stationarity simply requires that the mean behavior of a process (current density and number of downsteps per unit time) remains constant over

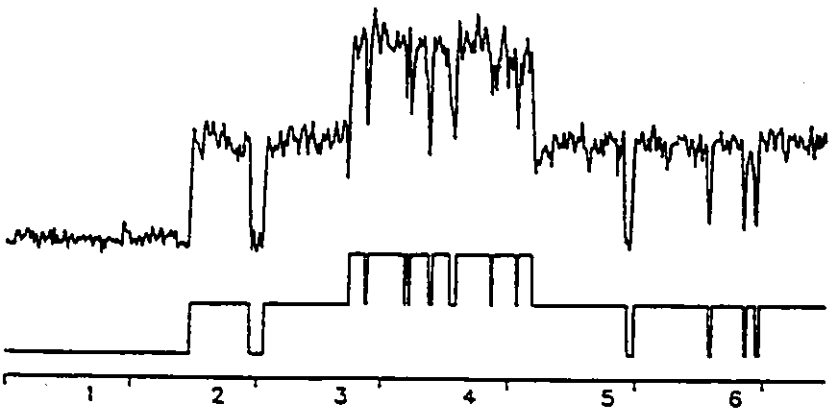

Chunk	1	2	3	4	5	6
Downstep Vector	0, 0	1, 0	0, 1	0, 5	1, 2	3, 0
Occupation Density	1.0.0	.48..52.0	0..71..29	0..10..90	.02..73..25	.09..91.0
Average Level	0	.52	1.29	1.90	1.23	0.91

Figure 3.1. Illustration of preliminary data analysis by the program, ADaM. The figure deals with a small subset of data; a 100 ms trace of raw current record is shown with its idealized record underneath. Data is typically divided into several hundred or up to a maximum of one thousand chunks of time. Six chunks of 15.43 ms duration are shown. They were analyzed to yield downstep vectors, occupation density vectors, and the average levels. Downsteps vectors contain a string of integers 0,1...z, (in this case 0...5) representing the number of downsteps per chunk from the current levels 1...n (in this case, 1,2; n is the highest current level visited during the entire analysis period). Occupation density vectors contain a string of real numbers, $0 \leq x \leq 1$, $\Sigma=1$, representing occupation densities for the current levels 0...n (in this case 0,1,2). Average level (for which the single channel current level has been normalized to 1) is computed from the occupation density data. The chunk duration should be chosen so that on average at least 2 downsteps are observed in each chunk.

time, whereas the second order stationarity requires that the variances and lag covariances (a lag(t) covariance is the covariance of a process X(s) with itself t seconds later, X(t+s)) of the process remain constant over time (Dabrowski and McDonald, 1992). ADaM provides tests on first and second order stationarity based upon a Kolmogorov-Smirnov-type test.

The test of independent and identical channels used by ADaM was a goodness of fit test (Dabrowski and McDonald, 1992) rather than, say, a likelihood ratio method (as used in (Belardetti, et al., 1987)). The goodness of fit approach is more robust, since it does not assume that the probability law governing the random variable is known (Larsen, 1974). If the ion channels in the patch are independent and identical, then the proportion of time that the total current record spends at each current level follows a binomial probability distribution with parameters N and P_{open}. This is true regardless of the precise probability law governing each channel. ADaM also uses the downstep rates in its analysis; this additional information permits the estimation of τ_o (and hence, of τ_c via the relation $P_{open} = \tau_o / (\tau_o + \tau_c)$) in addition to N and P_{open}.

ADaM estimates a covariance matrix of occupation times at the various levels, and the rate of downsteps from these levels. This matrix is used to define a quadratic form (expression 1 ref. (Dabrowski and McDonald, 1992)) in terms of the unknown values of N, P_{open} and τ_o. The values which minimize this quadratic form and which conform to a model of independent and identical channels (i.e. a binomial structure) are our estimators of N, P_{open}, τ_o and τ_c. The value of the quadratic form evaluated at this point is our test statistic, and measures the statistical distance between our data and a best-fitting model of independent and identical (iid) channels. Under this null hypothesis, the test statistic has a chi-squared

distribution. For data found to be comprised of the activity of iid channels, these estimates are used in a further stage of analysis to estimate the functions, 1-F(t) and 1-G(t).

A central feature of ADaM is that it explicitly tests the assumptions that the channels contributing to a multichannel record are, within a given level of confidence, iid. Given the nature of multi-channel records (they contain much less time-sequence information than single-channel records), a limitation imposed on the ADaM approach is that open states are aggregated or lumped together, as are the closed states. From single-channel records, it is possible to estimate the number of states and rate constants of each state. In a multi-channel setting, this is much more difficult. ADaM is not so ambitious, and attempts only to estimate τ_o (τ_c), the global mean open (closed) time. In the likely event that the channel has more than one open (closed) state, the mean open (closed) time, this τ_o (τ_c) is the average length of all open (closed) periods. Nonetheless, ADaM's ability to estimate these global means represents an improvement on just being able to estimate channel numbers and channel open probability.

ADaM implements the methods of (Dabrowski and McDonald, 1992) which is an improvement on (Dabrowski, et al., 1990). Whereas (Dabrowski, et al., 1990) uses the amount of time spent by the overall current record at levels 0,1,2...etc. (Dabrowski and McDonald, 1992) uses both this data and the record of downstep transitions. Regardless of the kinetic scheme of the channel, the record of current level occupation and transitions may be used to estimate the unknown parameters.

3. RESULTS

i) Stretch-induced channel activity is saturable

Because molluscan neuron patches often rupture at pressures not much greater than those which steeply activate the channels, it is ill-advised, on a routine basis, to directly determine N, the number of stretch-activatable channels in a patch, by applying super-saturating levels of suction. In a previous report (Vandorpe and Morris, 1992), only non-saturating stretch-activation curves for the S-channel were shown because, in each experiment, rupture preceded saturation. This leaves the impression a) that saturation might not be possible and b) that the reported density of 1-4 stretch-activatable channels per patch could have been considerably underestimated. Figure 3.2 illustrates that activation is, indeed, stretch-saturable, and that when saturation is achieved, N is not outside the range reported on the basis of the maximum number of simultaneously-active channels observed at sub-saturating suction. For activation curves (Vandorpe and Morris, 1992), I had used suction of fixed intensity for several seconds per intensity. Saturation is more readily achieved using continually increasing suction for several seconds as shown here, where the number of simultaneously open channels saturated at three. Though N can be rapidly checked by such super-saturating suctions (see Bedard and Morris, 1992), the risk of patch rupture is still considerable. In the illustrated case, the patch was especially robust. It ruptured at 175 mm Hg suction whereas many rupture at <100 mm Hg.

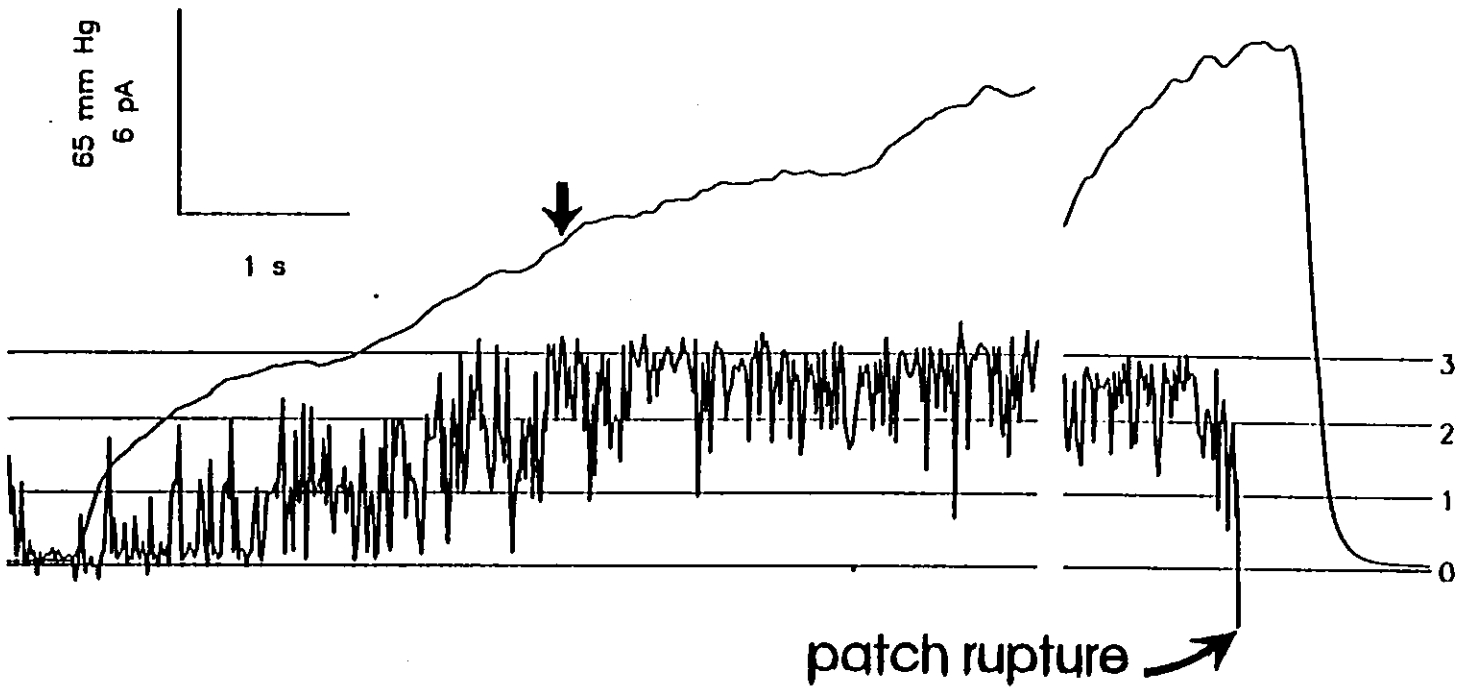

Figure 3.2. Saturation of stretch-activation. The current record indicates a maximum of 3 channels activated by suction (negative mm Hg indicated upward). The smoother trace is applied suction; beyond the downpointing arrow, suction was supramaximal. As the record beyond the interruption indicates, the membrane ruptured at -175 Hg.

ii) Mutiple channel kinetics: stationarity

The spontaneously active S-channel is noted for its tendency to exhibit non-stationary kinetics (Siegelbaum, et al., 1982), a tendency representing gating mode shifts among lower and higher open probability modes. Non-stationarity has hindered attempts at kinetic analysis of this channel. Figure 3.3 illustrates a 4 second piece of stationary data from a patch which showed a high level of spontaneous activity and which contained at least 3 S-channels; the record passed the stationarity tests incorporated in ADaM. Subsequent binomial analyses were carried out on such records if they passed first order and second order stationarity tests. However, it is worth recalling that individual channels in a given multichannel patch could be in different gating modes. If, say, two simultaneously active channels persisted in their different modes of activity, and a sufficiently long record was analysed, the record would be deemed stationary. At the next level of analysis, however, ADaM would (within established confidence limits) detect that the channels contributing to the record were not independent and identical.

iii) Stationarity over different time scales

The question of which sections of a multichannel record are likely to be usable for kinetic analysis is tricky. My experience was that it is difficult to tell by inspection of the current trace whether a given section of record of S-channel activity will prove stationary, presumably because of the slow processes that shift the channels among modes. Figure 3.4 (and Table 3.1) illustrates an objective method for finding stationary stretches of data. ADaM generates two cumulative functions which are related to the number of downsteps in a given

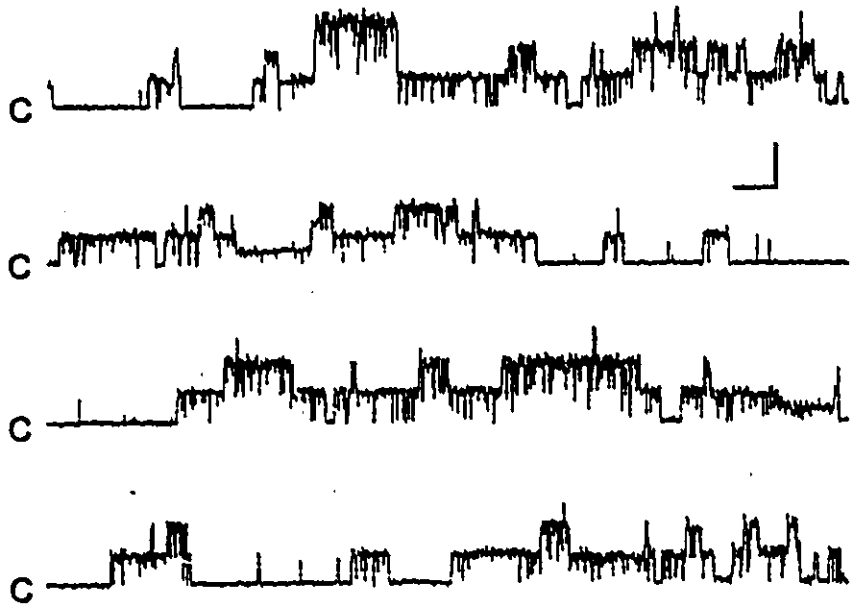

Figure 3.3. Four-second trace of spontaneous, stationary channel activity from a patch containing at least 3 channels. The first order stationarity test reported mean current level of 0.8, with $p = 0.29$. Average downstep frequency was 2.0, with $p=0.53$ ($p<0.05$ indicates that the data are non-stationary). Scales, 50 ms, 5 pA. C, zero-current level.

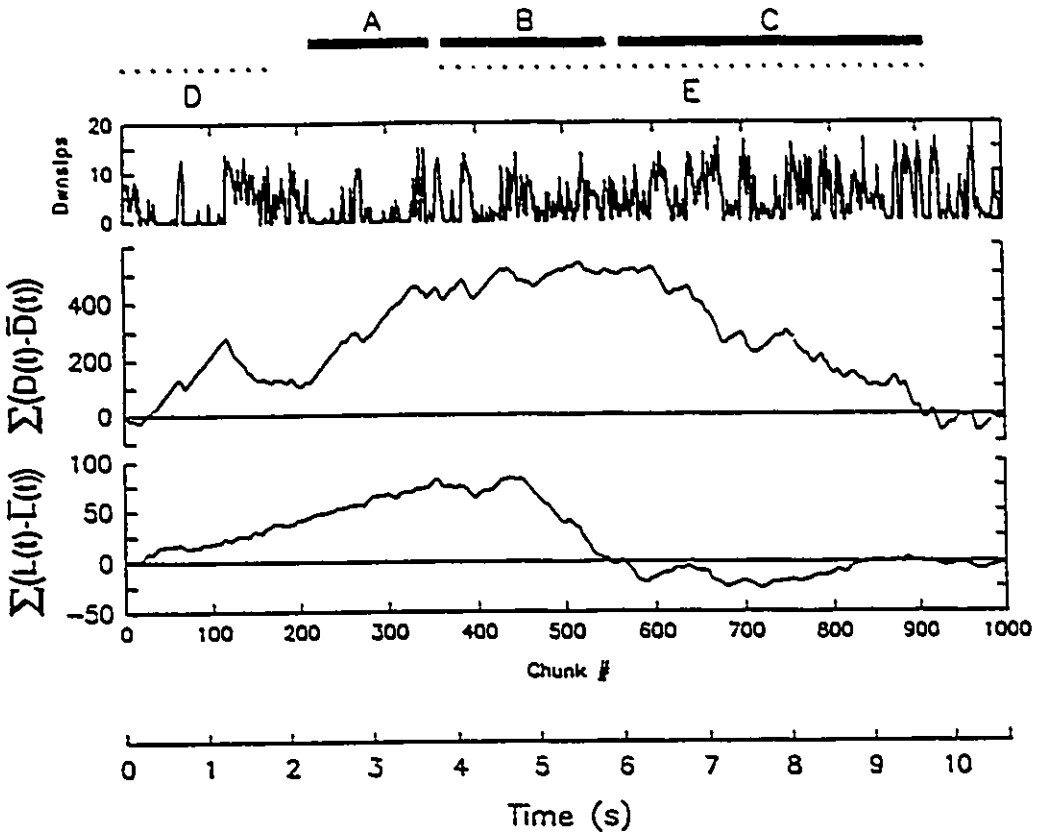

Figure 3.4. Exploring stationarity. This figure illustrates the procedure adopted to search for segments of record likely to be stationary. About 11 s of record with multi-channel activity were digitized and divided into 1000 chunks. The upper plot of downsteps/chunk summarizes channel activity over this period. The two plots below show the evolution, with time, of the cumulative downstep function and the cumulative levels functions for the data. Using the rule of thumb described in the text, we predicted that data stretches A,B and C would be stationary, whereas D and E would not. Table 3.1A indicates that these predictions were borne out. Note that segment E was not stationary, even though it encompasses two briefer stationary segments. The table also illustrates that segment C, though stationary, did not meet the criteria for independent and identical channels, and thus could not be used for further analysis.

chunk of time and the average current level per chunk of time. The downsteps function, $\Sigma(D(t)-\bar{D}(t))$, represents the cumulative sum of the difference between the number of downsteps in chunk t and the mean number of downsteps in all chunks up to chunk t. Likewise the levels function, $\Sigma(L(t)-\bar{L}(t))$, represents the cumulative sum of the difference between the mean level in chunk t and the mean level in all chunks up to chunk t (Dabrowski and McDonald, 1992). These cumulative sums, plotted over the period under consideration, are useful for searching for stationary subsections of data. The rule of thumb is that over the regions where the slope of the plots for both functions are roughly constant, the record should pass the first order stationarity test. Table 3.1, Part 1 shows that this was the case for sections A, B, C in Figure 3.4. D and E are examples of sections of the record which did not pass a first order stationarity test. Section E is comprised of the two contiguous stationary sections, B and C. It is as if the channels have undergone a mode change at the point at which the slopes of the two function plots change. Sections A, B, and C also passed second order stationarity tests which require that the variances and lag covariances of the two cumulative functions remain constant over time. Therefore, scanning the plots of the cumulative functions visually for constant slope provided a guide to stationarity that was far superior to visual inspection of raw data. Note that this general approach to the evaluation of stationarity is also applicable to records with only one channel active.

iv) Numbers of Channels in Patch Activated by Suction

The process of estimating the number of channels in a patch subjected to 40 mm Hg suction is illustrated in Figure 3.5. Before the application of suction, the activity of only one channel was apparent, while the application of suction resulted in the simultaneous activity of two channels in the patch. A binomial analysis conducted on this section of data supported the hypothesis that 2 independent and identical channels were operant.

From one-channel patch recordings of stretch channel data obtained at different applied suctions, it is by definition the case that suction increases P_{open} and not N. The ADaM analysis on multichannel recordings permits a wider range of possibilities, in that P_{open} and N could both potentially change. I expected to confirm that only P_{open} increases in patches subjected to suction. Disappointingly, an analysis of several patches (Table 3.2) indicated that increased NP_{open} in patches subjected to increased suction could be associated with a combination of changes: increased P_{open} only (Patches 1,2), increased N and P_{open} (Patch 3) and increased N, marginally decreased P_{open} (Patch 4). This array of possibilities convinced me that multiple-channel kinetic analysis of stretch channels (for example, to test stretch-sensitivity under various conditions) should not be undertaken without full binomial rigor. As Sokabe and Sachs (1990) have shown, patch suction is a problematic stimulus; sometimes it increases membrane area (potentially increasing N), other times, it causes vesicles to bud off (potentially decreasing N). Given these complications, it is understandable that the

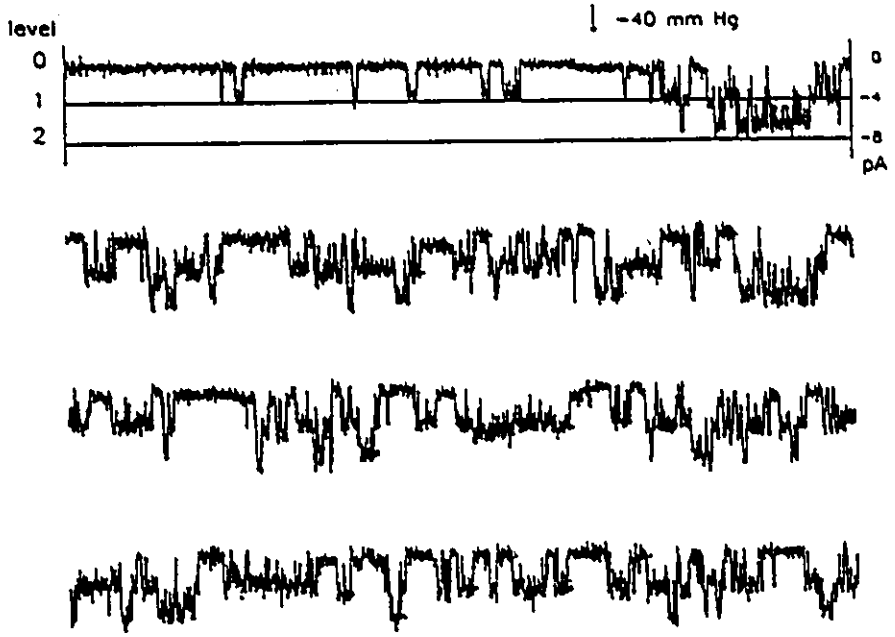

Figure 3.5. Multi-channel record showing the effect of suction. ADaM analysis indicated 2 independent and identical channels during application of -40 mm Hg suction. V_p -100 mV, NAS and 10 TEA in pipette, NAS in bath.

outcome of the present binomial analysis of stretch activation of the S-channel does not yield a story as straight-forward as that associated with FMRFamide activation (Belardetti, et al., 1987), in which NP_{open} changes were ascribed solely to increased P_{open}.

v) Open channel sojourns: within-patch similarities of S-channel and SAK$^+$ channel activity

Consistent with the idea that SA K^+ events and FMRFamide-induced events arise from the same channel population - the S-channels - was an analysis of activity in the only two patches (A,B in Table 3.3 and Figure 3.6) I obtained whose FMRFamide-induced and spontaneous activity, along with their stretch activity, were adequate for ADaM analysis.

Figure 3.6A shows, for a given patch, the estimated cumulative open distributions (F(t), plotted as the more familiar survival function, 1-F(t)) of FMRFamide and stretch activated events, respectively. Figure 3.10B compares spontaneous activity which was subsequently abolished by serotonin (5-HT), and stretch-induced activity recorded several minutes after 5-HT washout. The solid lines are estimates of 1-F(t) for a *single* channel, based upon the estimates of N and P_{open} obtained by ADaM in its test of independent and identical channels, and upon the lengths of time spent by the multi-channel record at varying current levels. The τ_o listed in Table 3.3 represents the mean open time for a single channel and is related to F(t) by τ_o = [INT(0 to INF)]tdF(t). Should the channel have but a single open state, F(t) would be an exponential function of mean τ_o; τ_o = [INT(0 to INF)]t$(1/\tau_o)(\exp(-t/\tau_o))$dt. Dotted lines in Figure 3.6 represent an estimate of 1-^F(t), for a hypothetical (but unlikely) case where a single open state with closing rate $1/\tau_o$ is assumed. Although the estimator ^F and the estimated F (as given by ADaM; see Methods) have the same τ_o, it is clear for all cases

Figure 3.6. Kinetic comparisons using F(t), as estimated by ADaM.

A. FMRFamide and stretch-activated current events from Patch A of Table 3.3. The solid line is the estimate for 1-F(t), one minus the estimated cumulative open time distribution derived from the non-model-specific analysis by ADaM. (see Appendix for explanation of the sawtoothed nature of the estimate). The single exponential plotted as a broken line has a decay constant equal to the global mean open time, τ_o, for this data (see Table 3.3), as derived from the goodness of fit test described in (Dabrowski and McDonald, 1992), which simultaneously fits N, P and τ_o (and hence τ_c). In these patches, the null hypothesis of independent and identical channels is not rejected, so N, P, and τ_o (and τ_c) are used to generate the estimated open time probability distribution function, F, by an algorithm described in (Dabrowski, et al., 1990). The difference between the 1-F(t) estimate and the single exponential reflect both the inherent error of the initial fit in the ADaM subroutine and the assumption that the channel activity can be adequately modeled as a first order process. ADaM analysis (see Table 3.3) indicated that N during both the FMRFamide-induced activity and during stretch was 3 (P_{open} during stretch and FMRFamide activation were similar). V_p -80 mV; NAS and 10 TEA in pipette and NAS in bath; suction, -88 mm Hg.

B. Spontaneous and stretch activated current events from Patch B of Table 3.3. Stretch was applied following 5-HT treatment (which "knocked out" all but one channel) , when 3 of the 4 channels (see Table 3.3) that were initially spontaneously active had recovered from 5-HT knock-out. V_p -100 mV; NAS and 10 TEA in pipette, NAS in bath; suction, -60 mm Hg.

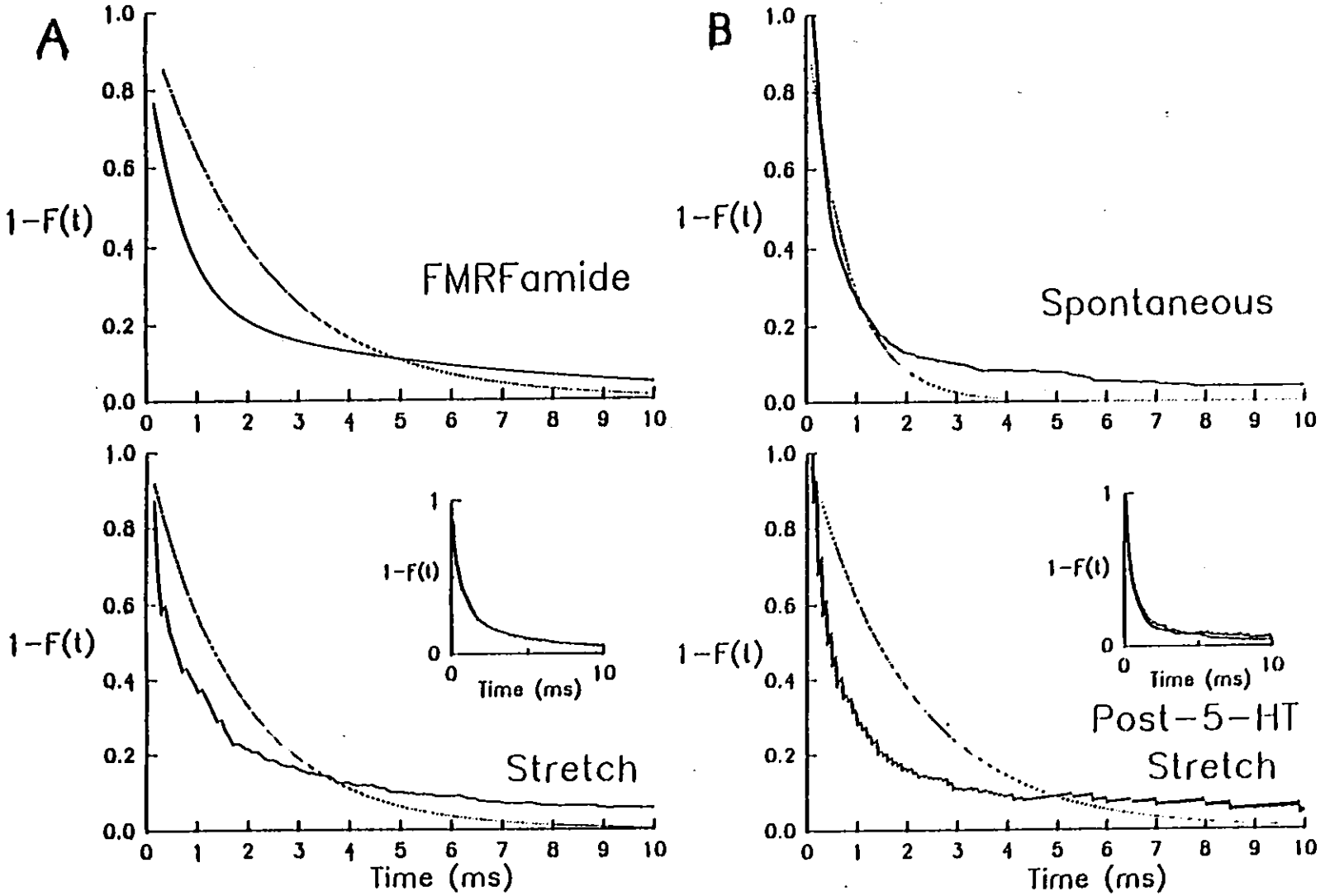
A
B
1-F(t)
FMRFamide
Spontaneous
Stretch
Post-5-HT
Stretch
Time (ms)
0.0
0.2
0.4
0.6
0.8
1.0
0
1
2
3
4
5
6
7
8
9
10

in Figure 3.6 that, not surprisingly, the single open-state model given by ^F is not a good model for the F estimated by ADaM. This issue can, however, be pursued a step further by examining the exponential substructure of the F estimates plotted in Figure 3.6 (that is, the estimated open time histograms for single-channel activity contributing to the multi-channel record). Are they, like the true one-channel records, double exponentials? The last two columns in Table 3.3 indicate that each estimated 1-F(t) curve is fitted well by two exponentials. In both patches and in all four conditions (stretch, FMRFamide, spontaneous, and post 5-HT stretch), τ_{o1} was the same - just under 1 ms. In the stretch/FMRFamide patch, τ_{o2} was indistinguishable for both modes of channel activation. Qualitatively, this pattern resembles the outcome from the direct one-channel analysis (i.e. two open times whose values are the same whether stretch or FMRFamide activate the channel), but quantitatively the time constants obtained by the one- and multi-channel methods cover different ranges. The multi-channel analysis detects a state of duration (τ_{o2}) intermediate to the two resolved by one-channel analysis, plus a longer-lived state. Note that, inevitably, multi-channel data are severely censored in a way that makes estimation of slow states poorer than with single-channel data. The most direct utility of these data is, therefore, for making within-patch comparisons for different test conditions, and not for establishing absolute kinetic parameters.

Although confidence bands are not provided for the estimates of 1-F(t) by ADaM, visual comparison of both sets of estimated 1-F(t) curves (see the almost completely overlaid curves in the Figure 3.6 insets) support the idea that for each patch (A and B), the two cases are the same. In other words, channels in Patch A which contributed FMRFamide-induced open events to the first multi-channel record had the same kinetic properties as those which

subsequently contributed stretch-induced open events to the second multi-channel record. Likewise for patch B; here, the spontaneous (subsequently shown to be 5-HT-inhibitable) and stretch-activated multi-channel records yielded remarkably similar 1-F(t) estimates. These within-patch 1-F(t) similarities are consistent with the earlier conclusion (one-channel kinetics section) that SA K^+ channels are S-channels and that, in activating the S-channel, stretch does not noticeably affect the length of its open channel sojourns. The multi-step ADaM analysis which yields an estimated 1-F(t) curve is, recall, carried out entirely independently for each experimental condition. Thus, when two independently determined curves (the estimated curves are sawtoothed; see Appendix C) from one patch prove to be indistinguishable (as in A) or extremely alike (as in B), the similarity is not trivial. These visual "fingerprint" comparisons do not, of course, constitute a statistical hypothesis test. Nevertheless, taken together and in conjunction with the one-channel patch analysis, they make it a notch harder to dismiss the conclusion that the stretch-activated channel is the S-channel.

4. DISCUSSION

It has been recently reported that in *Aplysia* mechanosensory neurons, a K^+ channel whose activity responds to FMRFamide and 5-HT is also sensitive to stretch (Vandorpe and Morris, 1992). This led to the conclusion that the so-called S-channel (Shuster, et al., 1991) is a stretch-activated K^+ channel analogous to those in other molluscan neurons. In light of the prodigious ability of neurons to make K^+ channel variants, this conclusion warranted closer inspection. To counteract problems of patch-to-patch variability, permeation and kinetic

traits of channels activated by FMRFamide and by stretch in a given mechanosensory neuron patch were compared. 5-HT reduces S-channel activity in a "knock-out" fashion (Belardetti, et al., 1987), so it is not possible to compare 5-HT-inhibited channels with stretch-activated channels in a parallel manner.

i) Multiple-channel patches versus one channel patches

Many cell types, including molluscan neurons contain several stretch channel varieties (Morris, 1993). In low activity multi-channel records, contributions from distinct channel types are sometimes evident by inspection of kinetics and/or conductance. Direct detection of heterogeneous contributions to current is not possible at high activity levels. By explicitly testing multi-channel data for its binomial character (i.e. testing the assumption that all contributing channels are identical and independent), one checks statistically for heterogeneity. In the patches that I was able to test, stationary stretch-activated data from Aplysia neurons usually met the binomial criteria, creating the impression that stretch did not routinely activate a kinetically mixed population of channels. An exception to this generalization is illustrated in Figure 3.4 (see also Table 3.1, Part 2); segment C was stationary but did not meet the binomial criteria of independent and identical channels.

Had suction of cell-attached patches seldom yielded binomial records, the explanation might have been outright channel heterogeneity or, more subtly, kinetic heterogeneity of a single channel type. Apparently it is possible for suction to produce sufficiently isotropic tension in channel-bearing membrane to activate channels identically.

The possibility of heterogeneous contributions to multi-channel data also needs checking

because S-channels can "spontaneously" switch between low and high probability gating modes (Seigelbaum, et al., 1982) and because it has been suggested for piscine SA K^+ channels that stretch-sensitivity itself is phosphorylation-dependent (Medina and Bregestovski, 1991). If individual channels had sufficiently different non-zero P_{open} values for a given stimulus, this would be detected during the ADaM analysis as "non-identical" channels. One possibility that was not controlled for is that the multi-channel analysis is best suited to deal with patches in which channels are not in a low probability gating mode; I may have applied ADaM more often to patches in higher probablility gating modes and the one-channel analysis to patches in lower probability gating modes (i.e. gating as determined by factors other than stretch). This would introduce systematic differences in the kinetics as revealed by one-channel or multi-channel analysis.

Siegelbaum and colleagues found that in patches with several spontaneously active S-channels, activity was binomial and that FMRFamide did not alter the number of active channels (N), but changed P_{open} (Belardetti, et al., 1987; Seigelbaum, et al., 1982). Analysis of our data for stretch-induced channel activity did not yield such a clean story; both parameters were changeable as suction changed. Suction-associated changes in N need to be noted, but are probably not biophysically interesting, in that they probably reflect patch mechanics (pulling of more membrane into the patch or budding off of vesicles for increased and decreased N respectively) and not channel responses to tension. Unfortunately this means that for stretch channels, suction induced NP_{open} changes cannot be safely attributed to P_{open} changes without a rigorous binomial analysis. Stretch-dependent kinetics obtained from one-channel patches, (assuming the analysis extends to P_{open} values approaching unity) constitute

the gold-standard. In such patches, by definition, changes in N are not possible, so increases in P_{open} must account for stretch-activation (Morris, 1990). Finding that N can change with stretch in larger multi-channel patches is disappointing because one-channel patches are rare, but it does not call into question the one-channel results.

Thus, I have illustrated the use of a set of programs that uses renewal theory as the basis for analysis of data from multi-channel patches. Ironically, in doing so, I have shown that the stretch-activated S-channel is not particularly amenable to this sort of analysis. This stems in part from a chronic problem encountered with stretch channels, namely that it is not possible to quantify the intended variable, membrane tension. Related points are that a) suction may produce effects other than tension changes and b) the system may not relax back to its previous condition upon release of suction. This, coupled with the tendency of the S-channel to spontaneously enter different modes, meant that truly stationary data had to be sought carefully (fortunately, ADaM provides a means of doing so). I also found that it was possible to contradict an assumption that has been derived from one-channel patch analysis, namely that the number of channels in the patch remains fixed at various intensities of applied suction. The caveats implicit in these remarks reflect the inherent difficulties of working with either stretch channels or strongly modulated channels, and the S-channel fits both categories. Nevertheless, the multi-channel analysis lent support to the hypothesis that the SA K^+ channel and the S-channel of *Aplysia* mechanosensory neurons are the same entity.

CHAPTER IV Search for Activators of Molluscan SA K^+ Channels

1. Introduction

Except for the S-channel of *Aplysia* mechanosensory neurons, SA K^+ channels in molluscs have no known function. Nevertheless, SA K^+ channels are ubiquitous in all molluscan neurons. Since 1) SA K^+ channels are relatively voltage independent in their gating behaviour, exhibiting a small increase in open probability with extreme (>+50 mV) depolarizations (e fold/ 70 mV) (Small and Morris, 1994a), 2) intracellular calcium does not affect gating (Sigurdson and Morris, 1989), and 3) membrane tension does not seem to be a physiological SA K^+ channel activator, it seems likely that there is some other activator(s) which modulates SA K^+ channel activity. Given the recent finding that S-channels are SA K^+ channels (Vandorpe et al., 1994), perhaps the converse is also true, namely, that all molluscan SA K^+ channels are modulated by the same second messengers as S-channels and thereby serve to modulate neuronal excitability?

It is unlikely that the activity of all molluscan SA K^+ channels is decreased by serotonin and increased by FMRF-amide given the large variety of neurotransmitter receptors present on neurons. Therefore I tested, at the next level down, whether the activity of all molluscan SA K^+ channels is increased by arachidonic acid (AA) and decreased by cAMP, the second messengers known to modulate S-channels. This didn't appear tenable however, as second messengers other than those which modulate S-channels could very well be acting to regulate SA K^+ channel activity and SA K^+ channels could still be S-like in that they are modulated by neurotransmitters via second messengers -- different groups of neurons might

enlist different second messengers following the activation of cell surface receptors. If this were true, applying just two different second messengers would be somewhat "hit and miss" using a heterologous cell population (all molluscan neurons).

To overcome this difficulty I chose to focus on a single cell type -- a homogeneous cell population. If, in this homogeneous cell population, I could establish a short list of potential candidates for modulating SA K^+ channels by assigning criteria based on similarities to S-channel modulation, it would increase the likelihood of successfully identifying a SA K^+ channel modulator. Although molluscan ventricular myocytes are not neurons, they are excitable cells which posses SA K^+ channels at high densities virtually identical to molluscan neurons (Brezden et al., 1986; Sigurdson et al., 1987). Furthermore, serotonin (5-HT) decreases a K^+ conductance via cAMP in these cells (Sawada et al., 1984) and 5-HT decreases S-channel activity in mechanosensory neurons via cAMP. The most convincing evidence to suggest that 5-HT decreases SA K^+ channel activity in these cells comes from a study (Morris and Moore, 1992) which has shown that extracellular 5-HT decreased efflux of radio-labelled Rb^+ from pre-loaded molluscan ventricular myocytes and that this efflux could be decreased by quinidine (a known SA K^+ channel blocker in this preparation). Single channel recordings are needed to ascertain whether this K^+ and Rb^+ current is via a SA K^+ channel.

Another way in which variablility due to the heterologous nature of the *Lymnaea* neuron culture might be reduced is by testing whether SA K^+ channels are modulated by second messengers which are further downstream in the transduction cascade. There is some evidence which suggests that the tail end of the second messenger cascade responsible for

modulating S-channel activity involves not only a protein kinase but a phosphatase as well (Endo et al., 1991). Purified PrP-1 and 2A have been isolated from *Aplysia* neurons, indicating that the phosphatases were present. Purified PrP-1 and PrP-2A in a microelectrode, permitted to slowly diffuse into an *Aplysia* mechanosensory neuron for 2 hrs, increased a potassium conductance in *Aplysia* mechanosensory neurons, suggesting that PrP-1 and PrP-2A are dephosphorylating a K^+ channel to decrease its activity. Given the results of Chung et al, (1991), which demonstrate that phosphatases and kinases can be closely associated with a channel and can therefore continue modulating channel activity in an excised patch configuration, it is desirable to ascertain whether this is the way in which the S-channel is regulated and if so whether this is how all SA K^+ channels are regulated--direct channel phosphorylation and dephosphorylation by kinases and phosphatases which reside in the membrane closely associated with the channel.

2. Methods and Materials

Three different preparations were used; cultured neurons and ventricular myocytes from *Lymnaea stagnalis* and identified mechanosensory neurons from the pleural ganglion of *Aplysia californica* see general methods for details. Single channel recordings were made from cell-attached or excised inside-out patches, as indicated. For *Aplysia* neuron experiments pipette solutions were comprised of ARS and 10 mM TEA chloride while for *Lymnaea* experiments pipette solutions were comprised of LNS and 1 mM TEA chloride. The bath solution was the same as the pipette solution but had no TEA and for *Aplysia* experiments

was pH 7.4. V_p, the pipette potential is reported.

3. Results

i) Normal Basal SA K^+ Channel Activity

Before testing the effects of agents which are suspected to modulate SA K^+ channel activity one must first establish what normal resting levels of channel activity are. Normal SA K^+ channel activity must be monitored for a sufficient period of time-- as long as any second messenger which is being tested might be acting. Cell-attached recordings were obtained of *Aplysia* mechanosensory neuron SA K^+ channel activity for a period of 30 minutes and an example of the normal basal activity level is shown in Fig. 4.1. Two features are immediately evident; 1) normal SA K^+ channel activity fluctuates considerably over time; 2) resting levels are quite low. These features are shared by SA K^+ channels of *Lymnaea* neurons and ventricular myocytes.

ii) Second Messenger Modulation of SA K^+ Channels in Heterologous Cell Population

Given that AA and cAMP increase and decrease the activity of *Aplysia* mechanosensory neuron S-channels, these were the two second messengers I focused on. When 50 μM AA (which is membrane soluble) was applied to the bath solution of cell-attached patches of *Lymnaea* neurons, there was a dramatic increase in SA K^+ channel activity as shown in Fig. 4.2. This increase was slow (~150 s).

When this procedure was repeated in 8 patches the results were inconsistent

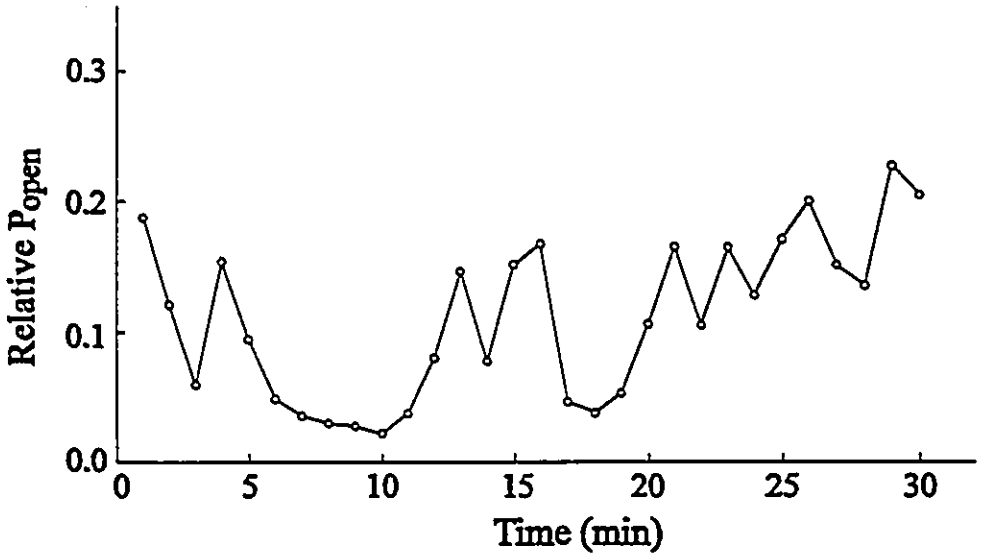

Figure 4.1. Continuous plot of relative P_{open} of 4 S-channels from an excised inside-out patch from a cultured *Aplysia* mechanosensory neuron. Vm=0 mV. Each symbol represents the P_{open} of a 60 s trace estimated using Fetchan.

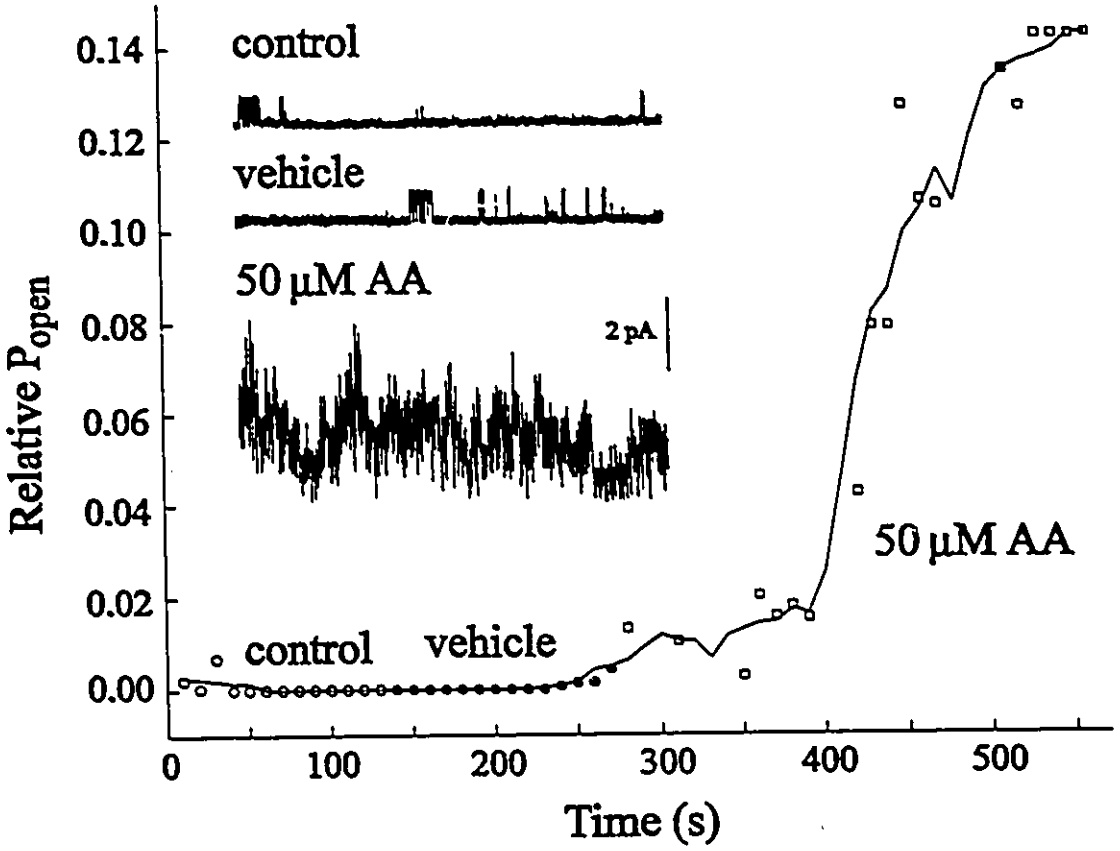

Figure 4.2. Continuous plot of P_{open} for 10 s records of SA K^+ channels a cell attached patch of a *Lymnaea* neuron; control (normal saline; open circles), vehicle (0.1 % DMSO; closed circles), and 50 µM AA in 0.1 % DMSO; open squares). Inset; 2 second records of channel activity while in control, vehicle, and AA solutions. P_{open} was estimated by integrating the area under amplitude histograms fitted with Gaussian distributions. Vp=-80 mV.

(Table 4.1). Bath application of AA resulted in an increase as great as 260 fold but also decreased SA K^+ channel activity in 2 cases. Using a membrane permeable analog of cAMP [dibutryl cyclic AMP (dbcAMP)] on cell attached patches of unidentified *Lymnaea* neurons, I asked whether the basal NP_{open} was decreased as it is in *Aplysia*. The effects of dbcAMP were variable; a large decrease in only one of five patches (Table 4.1). One attempt with double the concentration of dbcAMP resulted in less than a 40 % decrease in NP_{open}.

Table 4.1 Effects of AA and dbcAMP on P_{open} of SA K^+ channels in cell attached patches of *Lymnaea* neurons.

Relative change in P_{open}		
0.5 mM dbcAMP	1 mM dbcAMP	50 µM AA
1.0	0.61	9.3
0.29	----	4.2
1.0	----	0.43
0.85	----	3.1
0.87	----	260
----	----	1.3
----	----	50
----	----	0.27

iii) Modulation of SA K^+ Channels in a Homogeneous Cell Population

Bath application of 5-HT (10 and 100 µM) was carried out on cell-attached patches of *Lymnaea* cultured ventricular myocytes. In spite of an apparent increase in activity in the presence of 5-HT, this change was not significantly greater than the normal fluctuation about the basal levels of activity (Fig. 4.3). Moreover, whole-cell and nystatin patch studies on the effects of bath application of 5-HT on SA K^+ channel activity in *Lymnaea* cultured ventricular

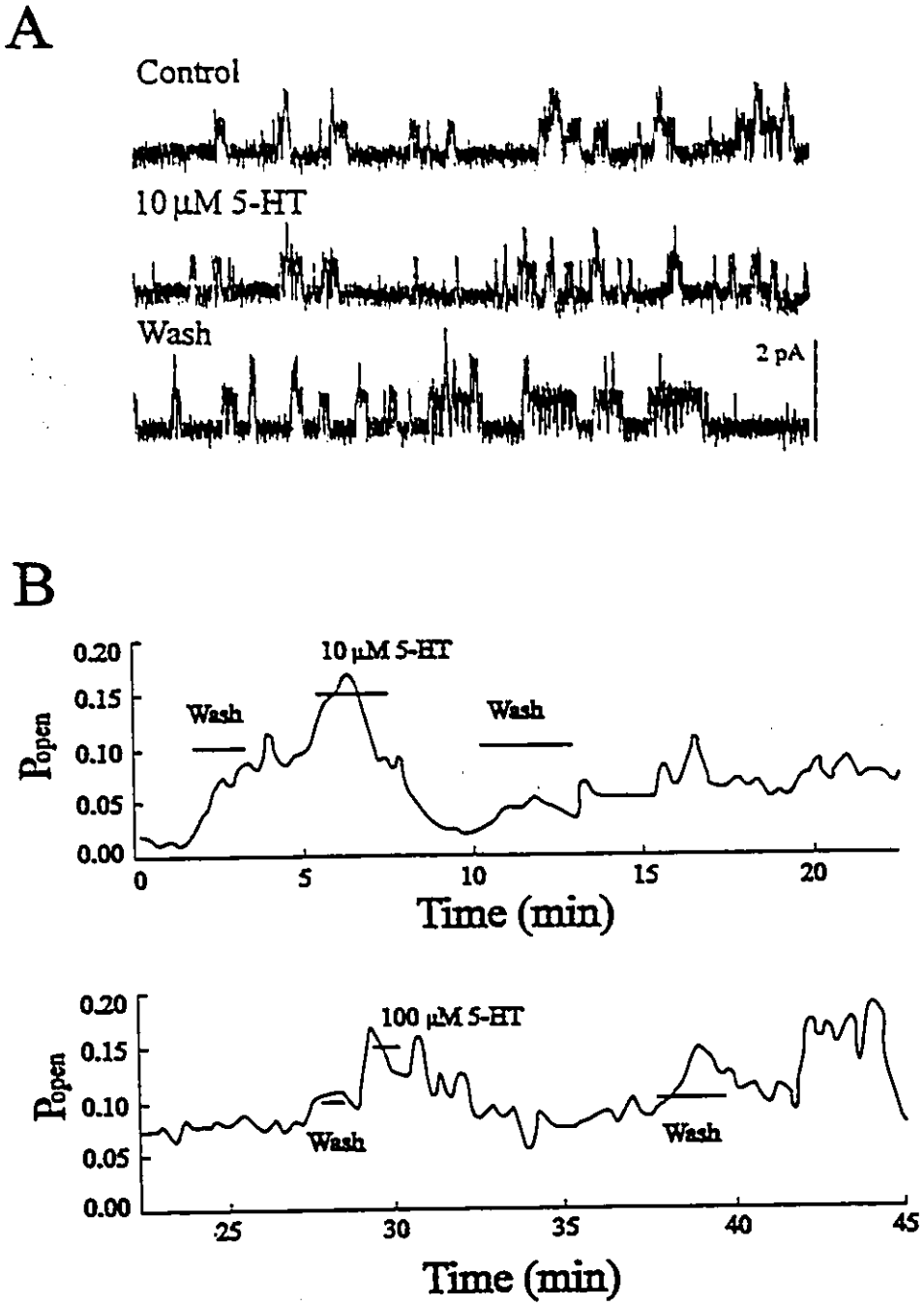

Figure 4.3. Lack of effect of 5-HT on cell-attached patches of *Lymnaea* ventricular cells. Above are three one second excerpts of channel activity at periods 4.5, 7.5, and 17.5 minutes into the recording representing the response following the application of normal saline (Wash), 10 µM 5-HT, and Wash again. The graphs below are continuous plots of P_{open} obtained from amplitude histograms constructed from 10 second records. Pipette holding potential was -60 mV and -15 mmHg was maintained over the 45 minute record. The above patch is representative of 9 other patches. No clear effect of 5-HT on SA K^+ channel activity was observed.

myocytes illustrated that there were no discernible effects on TEA-insensitive hypoosmotically activated macroscopic currents (Small, et al., 1992a).

iv) Direct Modulation of S-channel by (de)Phosphorylation

I applied potassium fluoride (KF) (50 mM) (a known, non-specific phosphatase inhibitor) to the cytosolic face of excised inside-out patches of *Aplysia* mechanosensory neurons. This would decrease the activity of endogenous membrane bound PrP's and, if the K^+ conductance which was decreased in the study by Endo et al., (1991), was the SA K^+ channel, the SA K^+ channel should decrease. I found that there was no significant difference in the P_{open} at basal levels of channel activity. The basal activity was, however, low (relative $P_{open} < 0.05$). Was this because SA K^+ P_{open} was already low and either could not be decreased beyond 0.05 or a decrease was just undetectable? Tabcharani et al., (1991) also were unable to decrease Cl^- channel P_{open} below 0.03 using an alkaline phosphatase which decreases channel activity by dephosphorylation. Carl et al., (1991), found that a phosphatase inhibitor had no effect on K_{Ca} P_{open} in the absence of PKA. Perhaps the system has to be "cocked" first. If the SA K^+ channel is already phosphorylated I would expect its P_{open} to be low. Blocking phosphatases which would dephosphorylate it, would further decrease its P_{open}. In order to overcome this potential difficulty of not detecting a decrease in a channel which had a very low P_{open}, I needed to somehow increase the P_{open} so that I could detect a decrease with a phosphatase inhibitor. I applied slight, sustained suction (10-20 mmHg) to the pipette to maintain a steady, increased SA K^+ channel P_{open} ($0.1 < P_{open} < 0.2$) (Fig. 4.4). Now when KF was added, there was a significant decrease in P_{open} (Fig. 4.5).

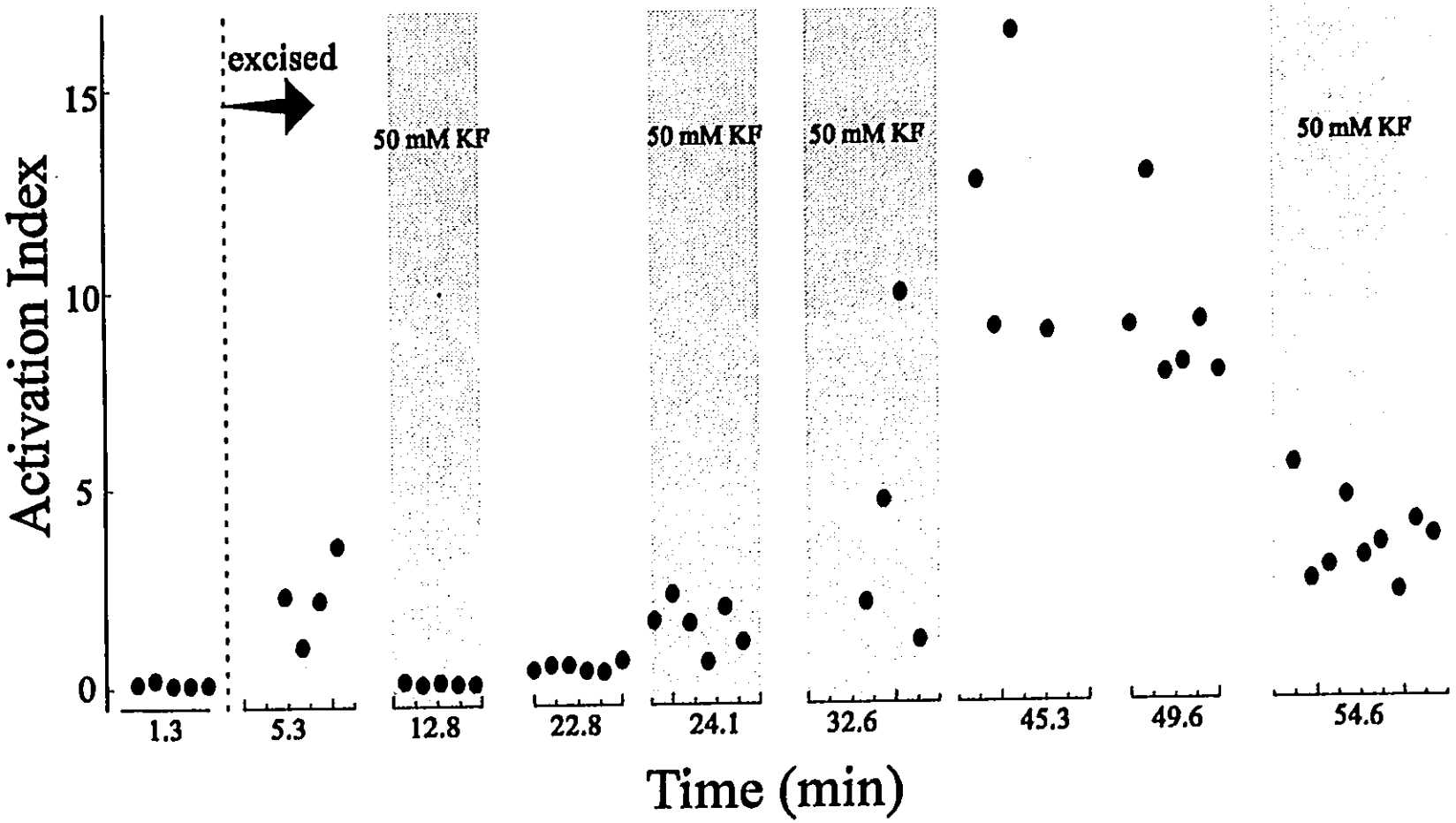

Figure 4.4. Effect of KF on P_{open} of SA K^+ channels in *Aplysia* mechanosensory neurons. 2 channel excised inside-out patch; Vm=0 mV. Activation index (filled circles) = (relative P_{open} / pressure (-mm Hg)) X 1000; shaded grey 50 mM KF present. Patch was excised at dotted vertical line. Each symbol represents analysis of a 10 s record. Time scale is interrupted; minor ticks are 3.8 s apart.

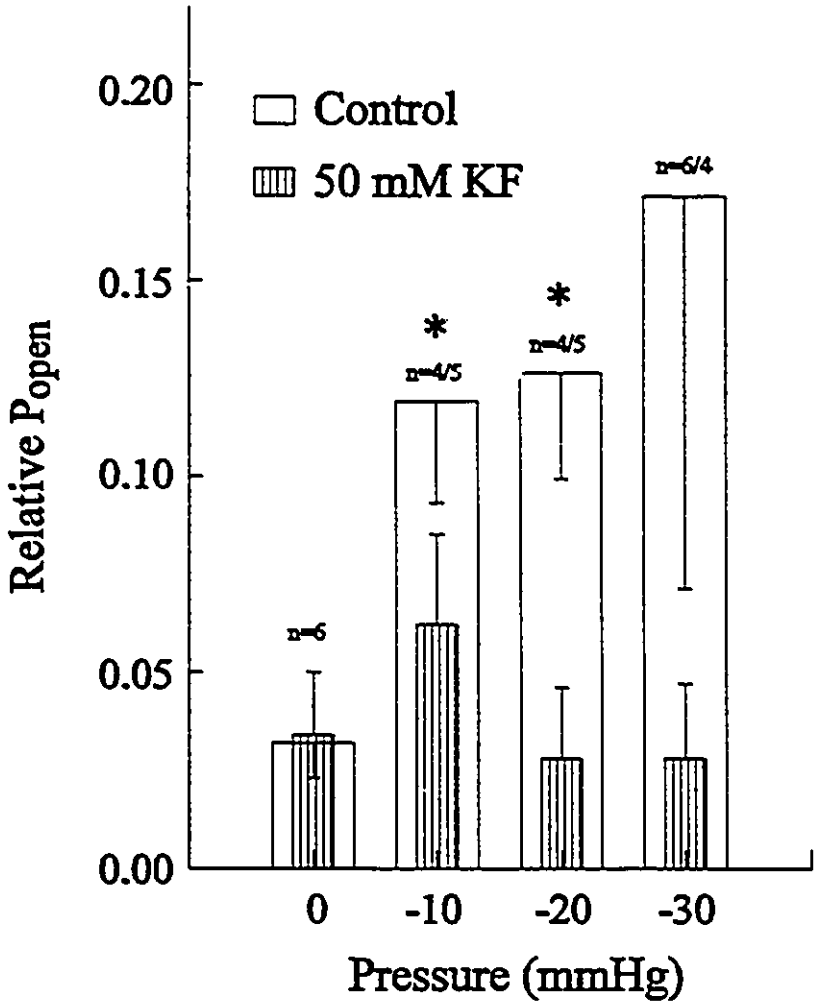

Figure 4.5. Bar graph summarizing effects of 50 mM KF on SA K^+ channels in excised inside-out patches of *Aplysia* mechanosensory neurons. Asterisks indicate significant differences in mean responses to suction in the presence and absence of KF using an unpaired student's t-test ($P<0.05$). Number of patches for control and KF treated patches are given above bars.

Attempts were made to stably activate the channels with stretch and then look for 5-HT inhibition, but stretch-induced activity is not sufficiently controllable in this preparation of cultured ventricular myocytes.

Is the low basal activity of *Aplysia* SA K^+ channels due to the fact that the channel resides in a phosphorylated state in normal resting conditions? This would explain the fact that the effect, on SA K^+ and S-channels, of FRMF-amide is more consistently observed and more pronounced than that of 5-HT (Vandorpe and Morris, 1992; Sweatt et al., 1989). Cl^- channels under this sort of dual regulation, when purified in reconstituted lipid bilayers, are found predominantly in the phosphorylated state (Finn et al., 1992). If this is the case for SA K^+ channels in *Aplysia* I should try to dephosphorylate the channel rather than inhibit the dephosphorylation. With this in mind, I applied an alkaline phosphatase (50 U/ml) to 4 excised inside-out patches. It had no effect on P_{open} (not shown).

4. Discussion

i) Normal Basal SA K^+ Channel Activity.

Given the low levels of activity it is likely that SA K^+ channels are heavily inhibited. The fluctuating levels of activity also suggest that the channels are under regulation by several converging agents under normal resting conditions. These regulatory agents could be neurotransmitters, second messengers and/or mechanosensitive enzymes.

ii) Second Messenger Modulation of SA K^+ Channels in Heterologous Cell Population

The variable results with AA and dbcAMP have been dealt with in terms of the

heterologous nature of the cell population itself with further experiments using a homogeneous cell population. Attempts to minimize the variability due to the loss in specificity concurrent with progression along a cascade of second messengers have also been made by using agents to address whether SA K^+ channels are modulated directly by phosphorylation and dephosphorylation.

The variability in responses to AA and dbcAMP could be a result of the fluctuations in modulation by endogenous agents which normally regulate SA K^+ channel activity. Furthermore, the lack of dbcAMP effect could be due to the fact that endogenous agents are capable of over-riding cAMP effects in the same way that the effects of FMRF-amide can override the effects of cAMP on S-channels (Belardetti et al, 1987). Because it is not known how the increase in P_{open} is caused by stretching the membrane, changes in membrane tension could override the cAMP effects. If this were the case, the spontaneous fluctuations in patch tension over time (Sokabe & Sachs, 1990; Sokabe et al., 1991), could account for the variability of dbcAMP effects. If there were a similar form of "cross-talk" between stretch effects and FMRF-amide effects the variability of AA effects might also be expected.

iii) Modulation of SA K^+ Channels in a Homogeneous Cell Population

The lack of consistent 5-HT effects on *Lymnaea* heart cell SA K^+ channels may be real or it may reflect a chronically inhibited state of the channels in this preparation. The same reasons for not seeing any dbcAMP or FMRF-amide effects in cultured *Lymnaea* neurons may explain my inability to record any significant 5-HT effects in the cultured *Lymnaea* heart cells. In spite of the convincing evidence to suggest that 5-HT modulates a resting K^+

conductance, the SA K^+ channel may well not be the channel underlying this 5-HT modulated conductance. There may be yet another neurotransmitter/receptor type which is responsible for modulating SA K^+ channels in this preparation. Because of these points I do not feel that the hypothesis that all molluscan SA K^+ channels are "S-like" has not been adequately tested by my attempts with heart cells.

iv) Direct Modulation of S-channel by (de)Phosphorylation

The fact that KF decreased SA K^+ channel P_{open} only when the channel was activated by membrane tension suggests that either the channel normally resides in a dephosphorylated state and that somehow, stretch results in the phosphorylation of the channel or the channel P_{open} is normally so low that a decrease by KF would not be seen. One difficulty with the idea that the channel is somehow phosphorylated by stretch is that in the excised inside-out patch configuration there was no obvious source of ATP because the intracellular solution was without ATP. This, therefore, leaves only the idea that the channel was normally so inactive that efforts to inactivate it further where fruitless. This hypothesis does not require that the channel be phosphorylated by membrane stretch but it does require that the channel be already phosphorylated prior to stretch-activation. This is in keeping with my results. Furthermore, it could mean that stretch somehow activates a membrane bound phosphatase and that direct channel dephosphorylation is the mechanism for stretch-activation.

My failure to observe an increase in SA K^+ channel P_{open} with alkaline phosphatase could be due to the fact that this phosphatase subtype is relatively non-specific and that PrP-1 or 2A were required, as is thought to be the case (Endo et al, 1991). Alkaline phosphatase

shares almost no characteristics with PrP-1 and 2A which are similar to one another. In spite of their similarities, it is possible that PrP1 and not 2A was effective. This is the case for calcium-activated K^+ channels (Carl et al., 1991). Unfortunately, PrP-1 is not yet commercially available to further test this hypothesis and synthesis of this protein is beyond my capabilities. It is also possible that the failure to observe any effects of alkaline phosphatase on SA K^+ channels resulted from the fact that the low channel activity was due not to phosphorylation but rather some other modulatory influence. This would not rule out the possibility that SA K^+ channels are modulated by phosphorylation and dephosphorylation.

v) Further Directions

It seems unlikely that serious progress can be made in understanding the mechanism of modulation of this channel without cloning the channel so that more precise tools can be designed to probe channel behaviour. This conclusion has prompted me to develop a cloning strategy aimed at using knowledge of channel behaviour to make predictions about channel structure. My attempts at cloning the channel with information already accumulated are described in Appendix A. Much of the remainder of this thesis describes experiments which were carried out to further characterize SA K^+ channels in the hopes that the observations will facilitate the cloning of these channels and eventually aid in the characterization of heterologously expressed putative cloned channels.

CHAPTER V Dynamic Behaviour of MS Channels

1. Introduction

Mechanosensitive (MS) ion channels are present in abundance in many cell types including nonsensory cells (Morris, 1990). They are classified based on whether they are stretch-activated (SA) or stretch-inactivated (SI) and on the basis of their selectivity [cation-selective (SA Cat), K^+-selective (SA K^+) and anion-selective]. Given the mechanosensitivity of these channels under single-channel recording conditions, it seems plausible that some of their physiological roles relate to mechanotransduction (Morris, 1992). In osmosensitive magnocellular neurons the case for mechanosensitive channels behaving as physiological mechanotransducers is especially good (Oliet and Bourque, 1993).

A common feature of mechanoreceptors like hair cells and Pacinian corpuscles is adaptation in response to a maintained stimulus. It is therefore a matter of considerable interest that some MS channels show adaptation at the single channel level. The response of SA Cat channels in ascidian oocytes to a step change in suction was shown to be highly phasic, with channel open probability initially increasing rapidly then decreasing over several hundred milliseconds to a nonzero steady-state level (Moody and Bosma, 1989). In yeast protoplast plasma membrane too, (Gustin et al., 1988) SA Cat channels showed adaptation in response to pressure steps at the high end of the stimulus range tested.

Until recently, MS channel kinetics have been studied mostly under equilibrium conditions; protocols which gave stationary MS channel responses to constant pressure

stimuli were used with the result that dynamic MS channel behavior (Gustin, 1992; Moody and Bosma, 1989) was de-emphasized. Studies using voltage-clamp and concentration jump techniques have been invaluable in describing voltage- and ligand-gated channels (i.e. *Shaker* K^+, Na^+, delayed rectifier, and glutamate-gated channels) and in understanding their physiological roles. McBride and Hamill (1992; 1993) developed a similar technique (pressure-clamp) to study the transient nature of MS channel behavior in more detail. SA Cat channels in *Xenopus* oocytes and in myotubes from dystrophic (*mdx*) mice showed a rapid adaptation similar to that demonstrated previously for MS channels of yeast and ascidian oocytes (McBride and Hamill, 1992). These findings led Hamill and McBride to speculate about SA Cat channels as physiological mechanotransducers, and to attempt an explanation for reported discrepancies between MS currents recorded in the whole-cell and patch modes. Referring to the fact that snail SA and SI channels exhibit little mechanosensitive gating under macroscopic recording conditions (Morris and Horn, 1991), they proposed that MS channel adaptation (still present in whole-cell, but lost in the patch), "would result in an underestimation of whole cell current when extrapolated from patch currents". They felt that their findings might "complicate the interpretation of SI channels reported in snail growth cones (Morris and Sigurdson, 1988) and dystrophic muscle (Franco and Lansman, 1990)". Potential misinterpretations about SI channel activation are not trivial since SI channels seem to be what magnocellular neurons use in responding to osmotic signals (Oliet and Bourque, 1993).

Since I have mostly studied our channels under conditions which, in *Xenopus* oocytes, tend to abolish transient aspects of mechanosensitive gating, I felt it was important to

determine whether predictions by Hamill and McBride about snail MS channels were correct and whether I have overlooked a dynamic aspect of MS channel behavior which might explain discrepancies between macroscopic and single channel MS currents. Therefore, I characterized the dynamic properties of SA K^+ channel responses to rapid steps of suction applied to membrane patches of *Lymnaea* neurons so that a comparison could be made between these channels and SA Cat channels of *Xenopus* oocytes. I found that the response of single SA K^+ channels to rapid jumps of suction was markedly delayed unlike the rapid activation of SA Cat channels with similar stimuli. SA Cat channel adaptation was observed only at hyperpolarizing potentials while the delayed response of SA K^+ channels was observed at both depolarizing and hyperpolarizing membrane potentials. The delay decreased with increasing suction and was irreversibly lost with repeated stimuli just as the rapid adaptation of SA Cat channels is lost with repeated stimuli. Thus, although activation kinetics of SA K^+ and SA Cat channels in naive patches challenged with a suction step are different, the dynamic characteristics of both types of MS channels are fragile and dependent on patch history.

2. MATERIALS AND METHODS

Lymnaea stagnalis neurons and *Xenopus laevis* oocytes were studied using cell-attached patches as described in the general methods.

i) Pressure Steps

The pipette holder's sideport was connected to two pressure transducers (Biotek Instruments, Winooski, VT), in series, T1 and T2 (Fig. 5.1A). The transducers were

considered to be in series because the distance between valve B and T2 was only the distance

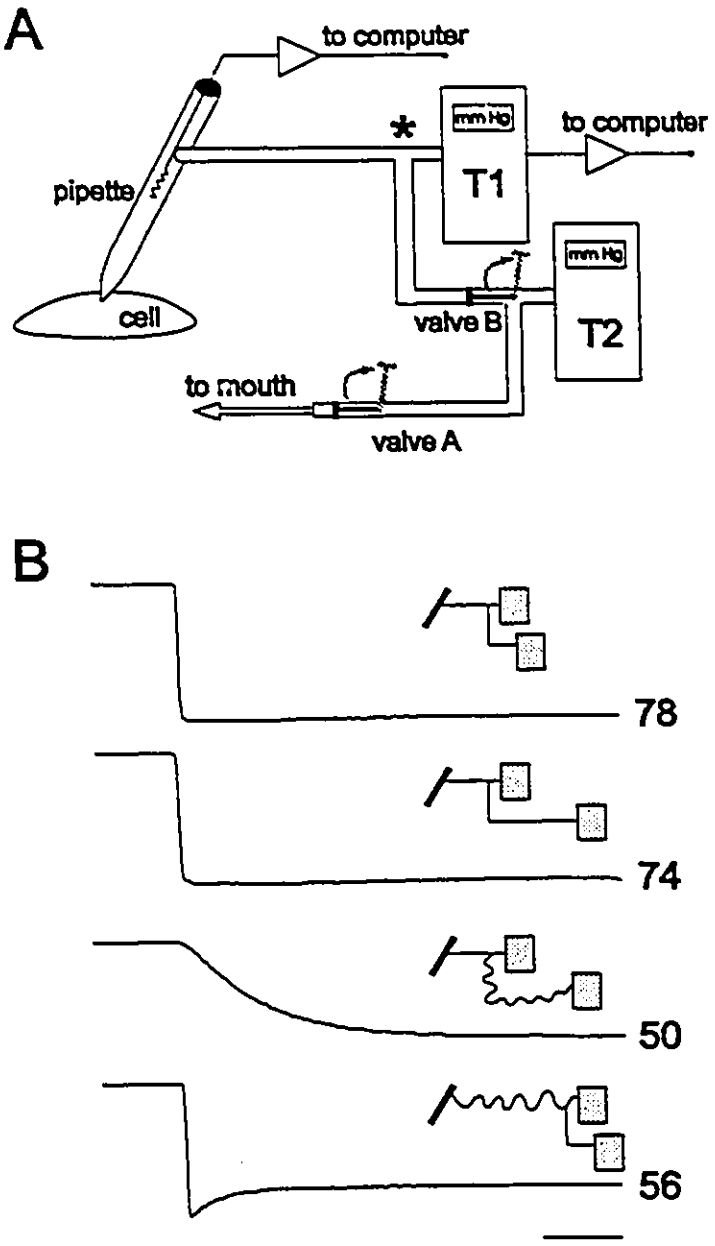

Fig. 5.1. Schematic representation of the set-up used to effect pressure steps (A). T1 and T2 are pressure transducers. T1 was used only to measure pressure; its output was connected through an amplifier to the computer. T2 was used to apply pressure. The two valves were operated manually. The branch point (asterisk) represents the port of transducer T1. (B) Representative traces measured at T1 when pressure steps of -180 mm Hg were applied at T2 for various tubing lengths (see inset cartoons). From top to bottom trace: the lengths (cm) of tubing between the patch pipette and T1, and between T1 and T2 were as follows: 75/75, 75/150, 75/900, 900/75. Pressure plateau magnitudes are indicated to the right of the traces (-mm Hg). Scale, 375 ms.

of the valve screw itself (1 cm). At T1, likewise, there was 1 cm from the branch point to the transducer itself. With valve A and B both closed, thereby isolating T2, a desired pressure was dialed up on T2 using the thumb wheel. To effect a pressure step, valve B was opened. Thus, the pressure acting on the patch was measured by T1; this transducer was adapted for connection through an amplifier to the computer. The pressure step was terminated by opening valve A, thus returning the system to atmospheric pressure.

The length of tubing between T1 and the patch pipette was 75 cm as was the length of tubing between T1 and T2. Traces representing pressure steps as measured at T1 are illustrated in Figure 5.1B. Because valves A and B were operated manually it was impractical to arrange a valve any closer to the patch itself. When valve B was opened a pressure wave began to propagate towards the patch.

In order to assess how well the pressure wave at T1 approximated that at the patch, I looked at the effect of changing tube lengths. I increased the length of tubing between T1 (*) and T2 by an additional 75 cm (the same distance between T1 and the patch). The resulting waveform (second trace) was virtually the same as the standard configuration (top trace) except for a ~ 5 % decrease in the steady-state pressure. The third trace illustrates the effect of an unacceptably long length of tubing in the same portion of the system. The fourth does the same for an unacceptably long length of tubing between the monitoring transducer and the patch. Given the large pressure drop observed when valve B was opened (e.g. -180 mm Hg at T2 dropping to -76 mm Hg at T1 as in trace 1, Fig. 5.1B), the volume of the total system must be more than twice that of the section between valves A and B. Large increases in tubing length (e.g. traces 3 and 4, Fig 5.1B) had a minor effect on the steady state

magnitude of the pressure step. Evidently, the tubing volume contributed minimally to the total system volume. Nevertheless, because pressure induced at T2 must propagate to the patch, long tubing was unacceptable because it degraded the transient (step).

ii) Analysis

Ideally, first latency would have been used to describe the delay in SA K^+ channel responses. However, SA K^+ channels have a low resting level of activity which meant that sporadic events occurred during what I characterized as the delay time (from initiation of the pressure step to the onset of activation). Therefore, in lieu of using first latencies to quantify the pressure-dependent delay in current activation, a running average of the current was obtained (Fig. 5.2A*ii*). This running average used a window of 50 data points and was taken over the entire pressure step (about 1-2 s). The resulting smoothed record contains the same number of data points as the original record. For the initial and final points in the smoothed record, the running average was computed by appending (50-1)/2 additional initial and final values to their respective ends of range. The data points were sampled at a frequency of 3 ⅓ kHz (pClamp sampling 3 channels, current, voltage and pressure, at 100 μs intervals). The delay (t_d) was estimated from this running average as the time from the beginning of the pressure step to the beginning of the current activation as judged by eye. The rate of activation ($1/\tau$) was determined from a single exponential fit (Sigmaplot 4.1) of the running average of the current using the equation $y=a+e^{(-t/\tau)}$ where y is current, t is time, a represents the offset from zero current at the beginning of the exponential and τ is the exponential rise time of the current. The offset a was necessary to account for sporadic events during the

delay prior to activation. First hits (the very first pressure stimulus delivered to a patch) were used for all patches unless indicated otherwise. Fig. 5.2B and 5.4D represent patches with a "non-gentle" history, i.e. repeated pressure steps. For Fig. 5.3D and 5.5 A-D, if the first hit did not elicit a response, the second pressure step (usually of a greater magnitude) was used for analysis. If there was no response to a second hit within 4.5 s but it became clear from subsequent stimuli: (3^{rd}, 4^{th} hits) that channels existed in the patch, a delay of 4.5 s was arbitrarily recorded for Fig. 5.5.

3. RESULTS

i) Characterizing transient effects in snail neurons

As previously (Morris and Sigurdson, 1989), SA K^+ channels were observed in every patch and sometimes SI K^+ channels were also evident (Fig. 5.2A). When evident, SI K^+ channels were spontaneously active and turned off only with suction. Suction also turned on SA K^+ channels. Upon termination of suction, SI K^+ channels turned on again and SA K^+ channels turned off. SA K^+ and SI K^+ events could be seen together throughout the record indicating that distinct channels were responsible for the two types of events. Furthermore, SI K^+ and SA K^+ events had different unitary conductances and kinetics (Fig. 5.2A *i* and *ii*).

On the time scale of Fig. 5.2A*i*, both channel types seemed to respond "instantly" and did not appear to exhibit any special dynamics. This particular patch had been treated in a manner routine for studying ion channels (Hamill et al., 1981), that is, suction of a magnitude

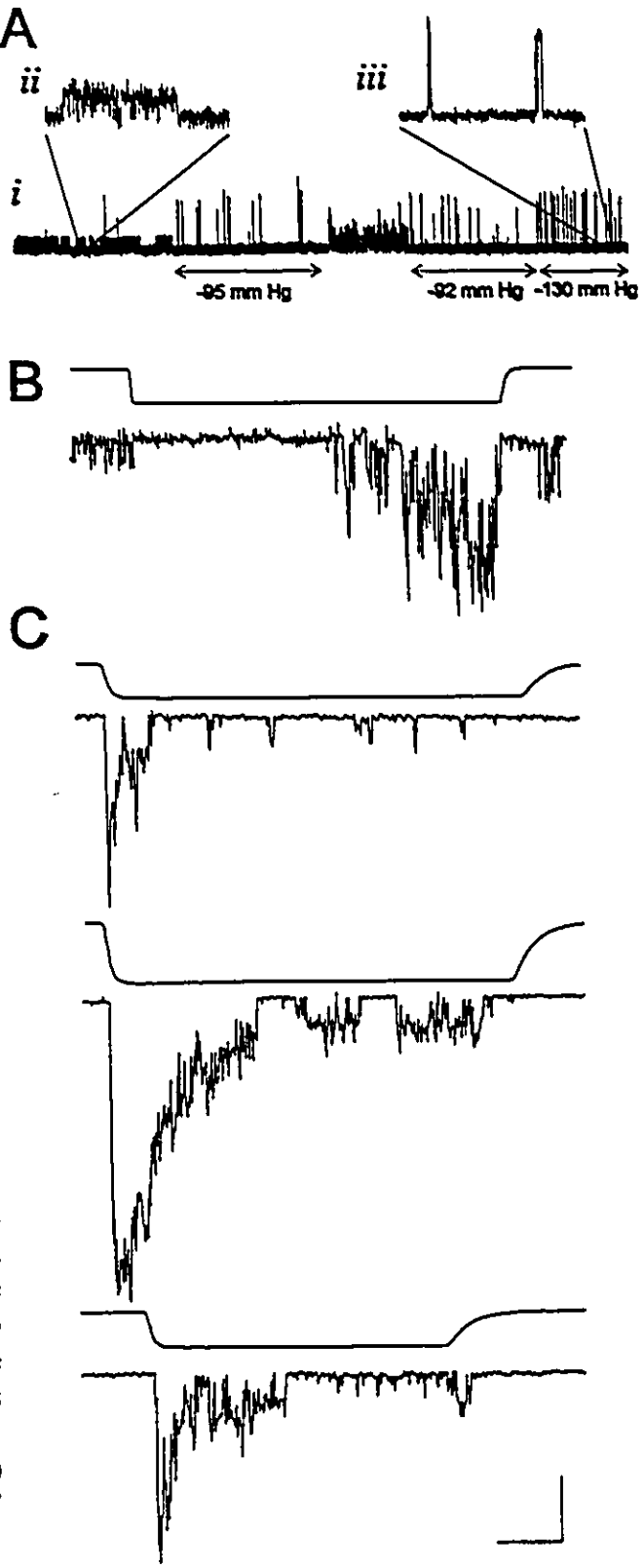

Fig. 5.2. Comparison of the dynamic responses to suction of three different channels; SI K^+ and SA K^+ channels in *Lymnaea* neurons and SA Cat channels in *Xenopus* oocytes. In A the suction was applied at the places indicated by arrowed lines and in B and C the suction pulse wave form is shown in the top trace. Pipette potential was -100 mV for A, 60 mV for B and 60 mV for C. Inset A *ii* and *iii* show examples of SI K^+ and SA K^+ channel activity on expanded scales. This example is representative of patches which were treated in a normal "non-gentle" manner similar to those of previous studies of SA K^+ channels of *Lymnaea* neurons. (B) In a day-3 neuron, SI K^+ channels turned off immediately following a pressure step. SA K^+ channels didn't activate in response to a pressure step for almost 1.25 s, at which point there was a gradual increase. (C) Three separate examples illustrating SA Cat channels turning on rapidly in response to a pressure step and turning off within 1 s of their initial activation. The compliance of the tubing used in the system to test the oocyte responses was greater than that used on neurons in order to exaggerate any limitations in the system used to compare the two. In spite of the shorter rise time in the pressure steps (more rounded) due to tubing with greater compliance, the rapid adaptation phenomenon is evident. Scale (A)*i* 3 pA, 6 s; (A)*ii* 1 pA, 200 ms (A)*iii* 2 pA, 200 ms; (B) 5 pA, 165 mm Hg, 400 ms; (C) 17 pA, 84 mm Hg, 300 ms.

and duration sufficient to induce giga-ohm seal formation was used. Moreover, as is customary in studying stretch channels, the patch had had a history of repeated pressure applications. When gigaohm seals were made gently (see Methods) and pressure steps made in a fashion similar to that described by McBride and Hamill (1992; 1993), the response, on a timescale of seconds, was not instantaneous. As shown in Fig. 5.2B, SA K^+ channels began to activate after a delay of just over a second and they did so in a gradual manner. It might be argued that this response was due to a delay in the arrival of the pressure wave at the patch. This could not have been the case because this behavior was special to patches that had been treated gently; generally, channels responded "instantaneously" (as viewed at this timescale). Supplementary evidence was provided by patches like those in Fig. 5.2B, which contained SI and SA K^+ channels. SI K^+ channels are more sensitive to pressure than SA K^+ channels (Morris and Sigurdson, 1989), but I note that within a few tens of milliseconds, the patch experienced sufficient pressure to turn off SI K^+ channels.

The delayed activation of SA K^+ channels was dissimilar to the dynamic behavior of SA Cat channels in a variety of preparations (see Introduction) including *Xenopus* oocytes, where, using a pressure clamp with rapid feedback control, pressures as low as 10 mm Hg will elicit adaptation (Hamill and McBride, 1992). A step of pressure applied to membrane patches containing SA Cat channels caused, within tens of milliseconds, a rapid activation, which then decayed over the next second. I was concerned that the striking difference in the response of molluscan SA K^+ channels was a peculiarity of our methods, especially since I had no feedback system for pressure application. That this was not the case is illustrated in Fig. 5.2C, which shows responses to pressure steps in *Xenopus* oocytes. Note that even

though the pressure steps were rounded compared to the standard step in Fig. 5.2B, (I used softer tubing which, because of its mechanical compliance, degrades the step response), activation transients like those seen by others [eg. (Hamill and McBride, 1992)] were observed.

ii) Quantifying transient effects of SA K^+ channel responses

Is the delayed response of SA K^+ channels to pressure steps a fixed property of the patch or does it depend on the magnitude of applied suction? The delay (t_d) was measured from smoothed records (Fig. 5.3A) (see Methods) of patches responding to two consecutive pressure steps (Fig.5. 3B). The first step of -130 mm Hg always preceeded the smaller step of -80 mm Hg. Given that the delay decreases with repeated pressure steps, an underestimation of the relationship between delay and the magnitude of the pressure step would result by giving the smaller of the two steps second. The delay of responses to consecutive steps of patches of 15 cells plotted in Fig. 5.3C indicates a negative correlation between the magnitude of the time delay and the magnitude of the pressure step. The rate ($1/\tau$) at which, following the delay period, SA K^+ channels activate in response to a pressure step was measured (Fig. 5.3A) from another 15 patches and plotted for various pressures (Fig. 5.3D). In contrast to the case for the delay, t_d, there was no discernible relationship between the magnitude of pressure steps and rate of activation, $1/\tau$.

iii) Stimulus strength and duration

As previously (Morris and Sigurdson, 1989; Sigurdson, 1990), I found that there

Fig. 5.3. The relationship between the pressure step magnitude and both the delay and the rate of activation of SA K^+ channels in *Lymnaea* neurons. (A)*i* The upper trace shows a typical delayed response of SA K^+ channels from a day-2 neuron to a pressure step (lower trace). (A)*ii* A running average of the current trace above. This shows both how t_d was measured and the single exponential fit used for estimating τ. Scale, *i* 6 pA, 135 mm Hg, 500 ms *ii* 2.2 pA. (B) Examples of SA K^+ channel responses of a day-4 neuron to two consecutive pressure steps whose magnitude (mm Hg) is indicated at the left of the current trace. By using the first step for the analysis in part C (bargraph) I eliminated the possibility that the measured delay was affected by patch history (i.e. decreased because of repeated stimuli). The arrow marks the beginning of the pressure step. The delay was less for the larger pressure step. Scale, 5 pA, 1s. (C) Bargraph of the time delay, t_d, of SA K^+ channel responses to paired pressure steps effected on 15 patches of day-4 neurons held at pipette potentials of 60 mV. (D) Scatterplot of $1/\tau$ as a function of pressure for SA K^+ channels in 15 day-1 patches. τ was estimated as described above. 1^{st} and 2^{nd} hit responses were significantly different (paired t-test).

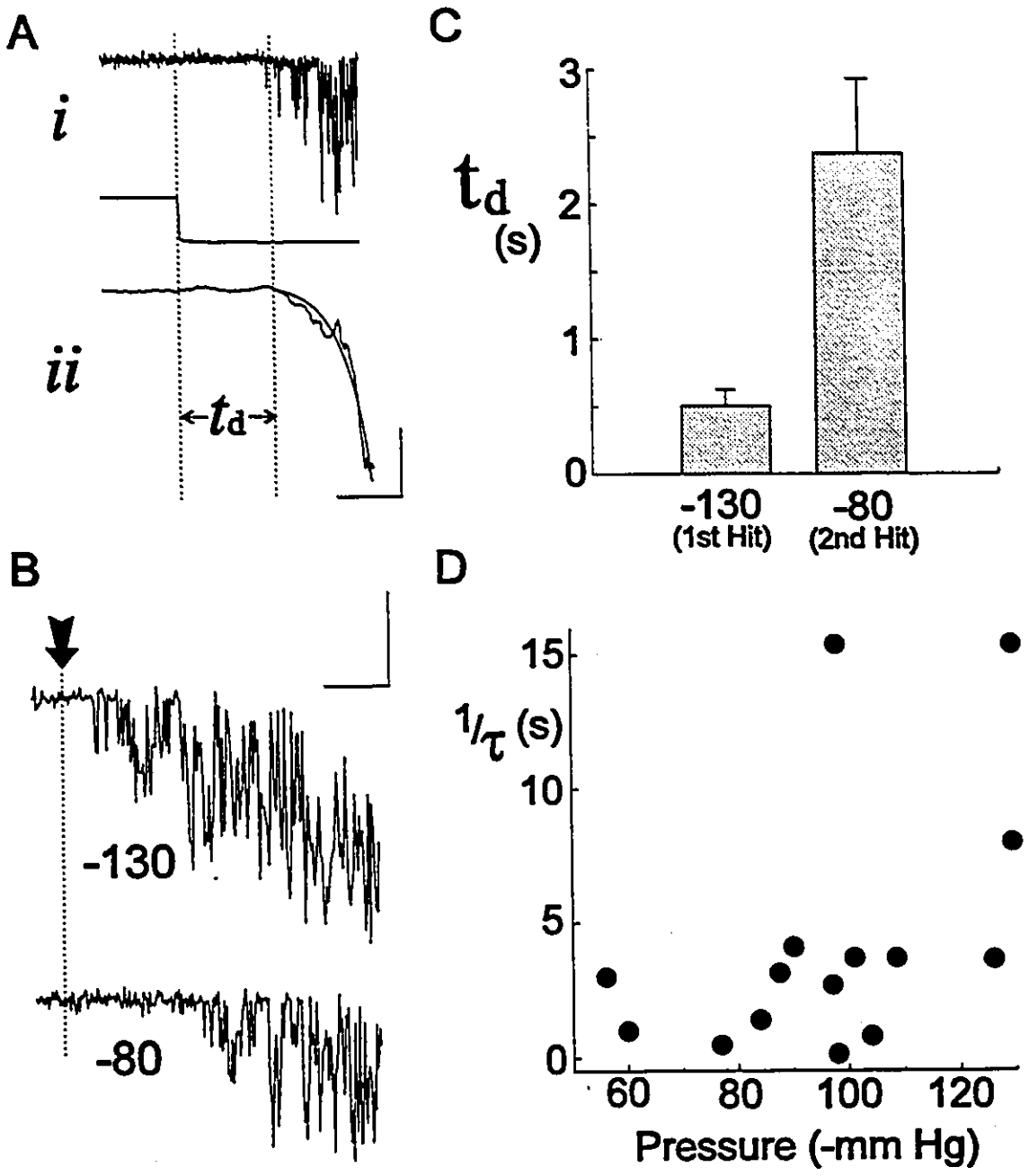
A
i
ii
t_d
B
-130
-80
C
t_d (s)
3
2
1
0
-130
(1st Hit)
-80
(2nd Hit)
D
$1/\tau$ (s)
15
10
5
0
60
80
100
120
Pressure (-mm Hg)

was a threshold for eliciting a response from SA K^+ channels. It was possible, however, that subthreshold cases (no channel activation), reflected a delay longer than the stimulus duration. To assess whether the phenomenon of threshold was real or only apparent, I did a series of 15 experiments sustaining the first pulse until activation occurred. 13 of the 15 patches of day-6 neurons responded in 3.8 s or less, while 2 responded after a delay of about 35 s. The magnitude of pressure steps used for this were similar to those used routinely for activation of the channels (-80 to -130). Perhaps if steps of smaller magnitude were maintained for a greater duration even longer delays would be observed. A physical limitation that would be encountered in attempting to determine the delay for a minimal stimuli is the changing geometry of the patch under such experimental conditions. A small pressure for an extended period of time (minutes) could pull more membrane into the pipette thus increasing the area of the patch and possibly the number of channels in that patch.

In Fig. 5.3C I showed a correlation indicating that the delay of channel activation decreases with increasing pressure. Does this correlation extrapolate to a delay of zero at sufficiently high pressure? Efforts to answer this question were hampered by the fact that patches routinely ruptured following large pressure steps. The magnitude of pressures that patches withstood without rupture seemed to vary with the age of the cell in culture; day-1 patches, for instance, ruptured at lower pressures than day-4 patches. I was, however, able to observe some patches which responded instantaneously with sufficiently large pressure pulses.

iv) Fragile nature of the SA K^+ channel's dynamic behavior

The dynamic behavior of SA K^+ channels (the delay phenomenon and the slow exponential rate of activation) are fragile and depend on patch history. If the gigaohm seal was made too forcefully (see Methods) these phenomena were absent. Repeated pressure steps of the same magnitude would also irreversibly abolish the dynamics while the basic mechanosensitivity of the SA K^+ channels was left intact (Fig. 5.4A, 5.4B). With repeated pressure steps the delay is lost and the activation rate begins to appear instantaneous. The fragile nature of these dynamics was common to both SA K^+ channels and SA Cat channels. Like Hamill and McBride, (1992) I found, in *Xenopus* oocytes, that a repeated pressure step caused a change in the character of the response from a large transient to a small steady-state response. In contrast to SA Cat channels, SA K^+ channels in molluscan neurons characteristically responded to repeated pressure steps of fixed magnitude with an increased degree of activation (for example, see the effects of repeated -130 mm Hg steps in Fig. 5.4A). Thus, SA K^+ channel sensitivity to stretch increases as the channel's dynamic behavior wanes. This behavior is in distinct contrast to that reported for SA Cat channels. The data presented by Hamill and McBride [Fig. 2 of (Hamil and McBride, 1992)] is consistent with the findings of Gustin [Fig. 5 of (Gustin, 1992)] that SA Cat channels exhibit hysteresis, in the form of a rightward shift of the "dose-response" curve. In addition, *Xenopus* showed a decreased maximum. Our data for molluscan SA K^+ channels, by contrast would lead to a leftward shift and an increased maximum.

v) Fragile nature of the SI K^+ channel responses

SI K^+ channel events were seen in 26 patches (of 56) in which gigaohm seals had been

Fig. 5.4. Characterization of the fragile nature of the time delay and of the voltage-dependence of SA K^+ channel behavior of *Lymnaea* neurons. (A) The current responses to the first, third, fourth and fifth hit pressure steps of -130 mm Hg effected at the arrow. Successive hits were separated by about 10 s. Note the loss of the delay with repeated pressure steps. Day-4 neurons at Vp=60 mV. Scale, 4 pA, 1 s. (B) Bargraph of time delay of current response to the indicated hits, using -130 mm Hg on 15 patches of day-4 neurons at Vp=60 mV. In pairwise comparisons (1-3, 1-4, 1-5) all were significantly different from each other (t-test). (C) Current traces (with associated pressure steps) representing SA K^+ channel responses of two patches held at the indicated pipette potentials. Scale, 4 pA or 270 mm Hg, 1 s. (D) Voltage-dependence of SA K^+ channel open probability. Upper graph is a current response to a single 2 s voltage ramp from a membrane potential of -50 to 120 mV used to establish SA K^+ single channel conductance (the line i(v) was fit by eye). Middle graph is an ensemble average of the response to 30 consecutive 2 s voltage ramps. Bottom graph is a plot of SA K^+ channel open probability (P_o) as a function of voltage for 5 patches (see methods for description of P_o determination); means are reported with their standard error (mostly within symbols). A fixed pressure was sustained throughout each experiment in order to activate the channels.

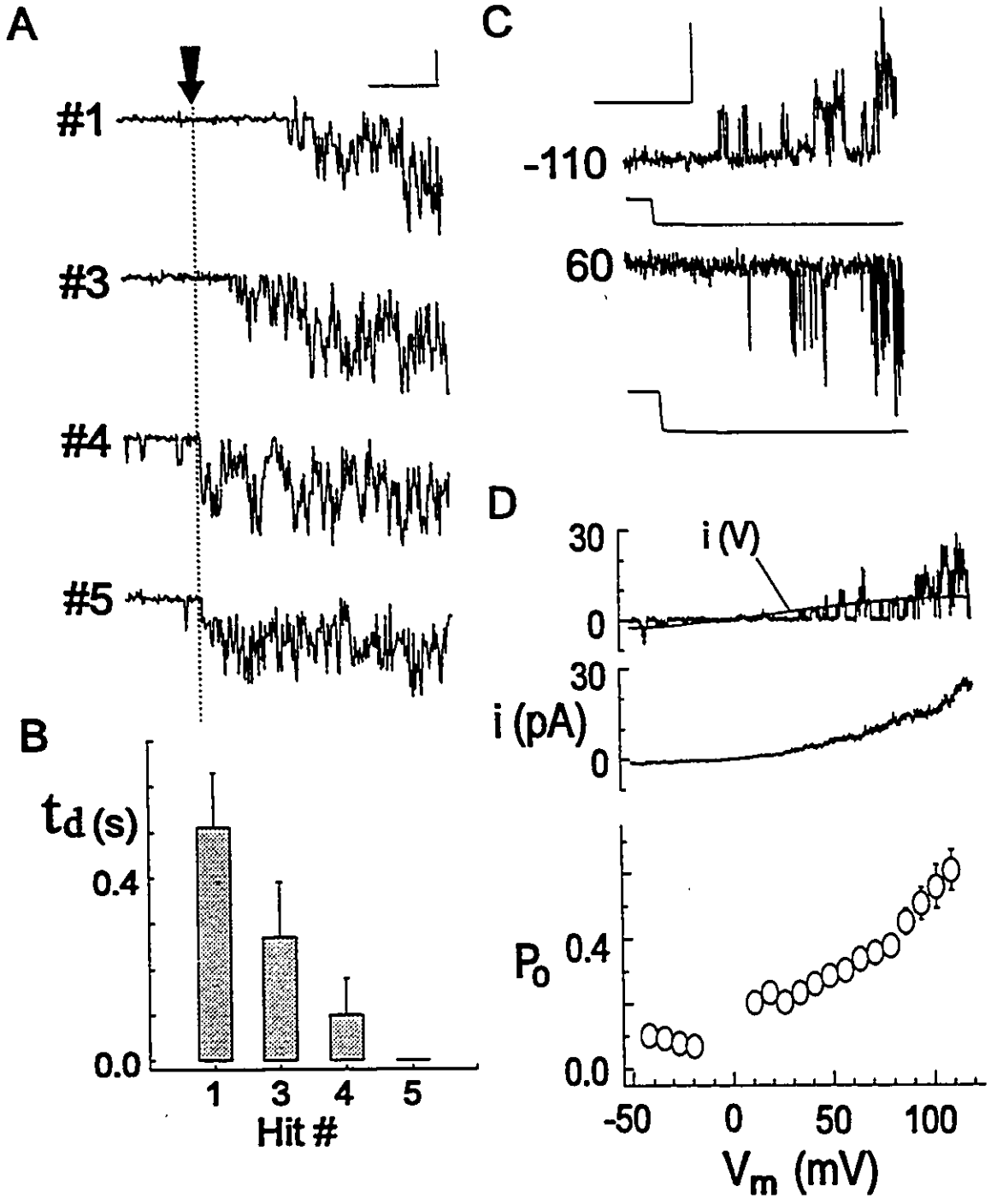
A
#1
#3
#4
#5
B
t_d (s)
0.4
0.0
1
3
4
5
Hit #
C
-110
60
D
30
i (V)
0
30
i (pA)
0
P_o
0.4
0.0
-50
0
50
100
V_m (mV)

made gently. In patches on which a gigaohm seal formed without suction, SI K^+ channels were present in large numbers (>5). Their small conductance (Morris and Sigurdson, 1989) and normally high basal level of activity made then hard to quantify. It is worth noting, however, that in a few gentle patches, immediately following seal formation, SI K^+ channel activity was seen to first increase then decrease with increasing suction. (An explanation for this complex behavior is posited in the Discussion.) For those patches which did not exhibit SI K^+ channel activity, part of the explanation might be a downward shift of their mechanosensitivity as a result of normal (i.e. "non-gentle") gigaohm seal formation. Such a shift could ensure that the channels were chronically inactivated by the resting membrane tension. Consistent with this possibility, activity in gentle patches was lost in 22 of the 26 cases with repeated pressure steps.

vi) Voltage-dependence of MS channel responses

The P_o of SA Cat and SI K^+ channels is weakly voltage-dependent, increasing with depolarization (Yang and Scahs, 1990, Sigurdson, 1990). Fig. 5.4D shows that SA K^+ channel activity increases substantially at high (non-physiological) depolarizations. This voltage-dependence of SA K^+ channels was not affected by patch history; recordings were obtained from patches in which SA K^+ channel activity was elevated for several minutes beyond the basal level by applying a sustained suction. There was no evidence that the voltage-activation changed with time as a result of this prolonged mechanical stimulation.

Unlike SA Cat channels in yeast plasma membrane (Gustin et al., 1986), in *Xenopus* oocytes and in *mdx* myotubes (McBride and Hamill, 1992), all of which exhibit dynamic

behavior only at hyperpolarizing membrane potentials, SA K^+ channels demonstrated dynamic behavior at both positive and negative membrane potentials (Fig. 5.4C). I do not, however, rule out the possibility that there are quantitative differences in the dynamic behavior at the voltage extremes. In three patches, t_d was determined at depolarized potentials using the indicated first-hit pressure (-56 mm Hg, 0.5 s; -58 mm Hg, 0.7 s; -76 mm Hg, 0.65 s) ; the delays observed from these first-hit steps were less than would have been expected on the basis of t_ds determined for first-hits on hyperpolarized patches (Fig. 5.3C).

vii) Cytoskeleton-dependence of SA K^+ channel responses

Neurons in culture reorganize their cytoskeleton and regenerate processes as they change from rounded newly-isolated cells to rearborized neurons; the slower response of day-4, 5 and 6 cells (Fig. 5.5A) might be dependent on cytoskeletal reorganization. In order to address whether a cortical cytoskeleton which has had longer to reestablish itself, contributed to the delayed response of SA K^+ channels, I treated the cells with 50 μM cytochalasin D (cyt D). The cyt D-treated cells responded with a significantly shorter delay than those treated with either DMSO or just NS. Furthermore, the cyt D-treated patches were also more mechanosensitive than control patches. Following the delay, the channels responded with a greater level of activity. The cyt D-treated patches all responded to the first hit and the magnitude of the steps needed to evoke responses was less. This is consistent with the idea that the delay was due to some cytoskeletal protein(s) which had been disrupted in the patch-clamp configuration under normal "non-gentle" recording conditions.

Fig. 5.5. Cytoskeleton-dependence of SA K^+ channel responses. (A) Bargraph of time delay of current response to pressure steps illustrating an increasing delay as neurons age in culture. Days 4, 5, and 6 neurons responded with a significantly longer delay than day 1 or 2 neurons (unpaired t-test). The number of day 1, 2, 4, 5, and 6 neurons were 8, 6, 23, 13, and 8 respectively. All patches were held at 60 mV pipette potential and all responses measured were from first or second hits only (see text). (B) Bargraph showing comparison of the time delay of current responses to pressure steps of day-6 patches treated prior to patch formation with NS, NS+1% DMSO or 50 μM cytochalasin D (Cyt D) in 1% DMSO for ≥ 105 minutes. The cyt D-treated patches responded with a significantly (unpaired t-test) shorter delay than both control and DMSO-treated patches. 8 control, 6 DMSO and 10 cyt D patches were all held at 60 mV (Vp). (C) Effect of cyt D on current activation. In the left panel the integral of the current, i, (shaded area) was divided by the corresponding pressure, p, integral to obtain an activation index. This index is plotted in the bargraph, right, for day-6 neuron patches of 10 control and 10 cyt D-treated (≥ 105 min) all held at 60 mV (Vp). There was a significantly greater activation of cyt D-treated patches (unpaired t-test). Scale, 5 pA, -80 mm Hg, 1s.

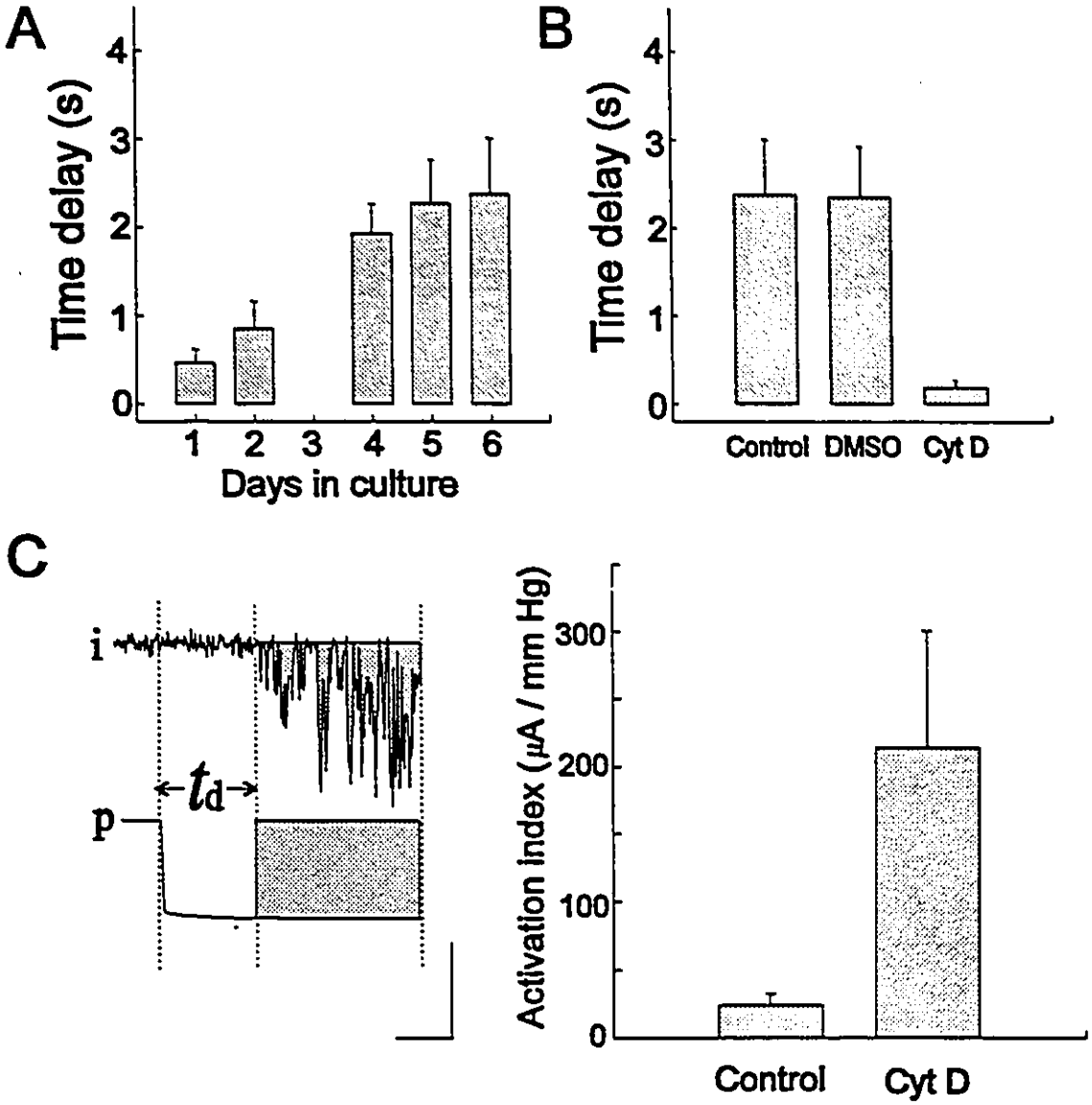
A
Time delay (s)
0
1
2
3
4
1
2
3
4
5
6
Days in culture
B
Time delay (s)
0
1
2
3
4
Control
DMSO
Cyt D
C
i
p
t_d
Activation index (μA / mm Hg)
0
100
200
300
Control
Cyt D

4. DISCUSSION

Previous studies of snail neuron SA and SI channels did not explore the possibility of dynamic responses to pressure steps, but since dynamics have proved to be an interesting aspect of SA Cat channel behavior, this oversight has now been redressed. Using the appropriate protocol, I did, in fact, observe dynamic behavior in SA K^+ channels. Following a suction jump there was a delay in the response by SA K^+ channels. This delay shortened if the step was either augmented or applied repeatedly. Once activation began, it proceeded with an exponential timecourse. The magnitude of the response was increased by greater suction but, surprisingly, the activation rate was unaffected. This dynamic SA K^+ channel behavior was fundamentally different from that reported for SA Cat channels (Hamill and McBride, 1992). SA Cat channels show immediate activation followed rapidly by an adaptation. This adaptation is not to be confused with a process analogous to inactivation in voltage-gated channels because, as Hamill and McBride, (1992) showed, channels that had adapted during a near-maximal stimulus could be "reactivated" by increasing the magnitude of suction.

In our hands, SA Cat channels in *Xenopus* oocytes showed the same adaptive behavior reported by Hamill and McBride. Since I used the same protocol in snail neurons, differences in dynamic responses of SA Cat and SA K^+ channels are likely to reflect real differences in the mechanics of the patches in the two preparations.

i) Discrepancies between patch and whole cell results

"Gentle" seal formation has revealed that SI K^+ channels are present in almost half the patches studied. This revelation should facilitate further study of SI K^+ channels. The fragile nature of SI K^+ channel behavior, however, remains an obstacle to further study of these channels. If SI K^+ channels are, indeed, even more abundant than previously reported (Morris and Sigurdson,, 1989), then the discrepancy between patch results and whole-cell results (Morris and Horn, 1991), rather than being resolved, is exacerbated. The fragility of the SI K^+ channel responses combined with their sensitivity to small applied pressures may, however, offer an explanation. In an earlier paper (Morris and Sigurdson, 1989), they showed that "bell-shaped" activation curves could be obtained for SI K^+ channel activity. They argued that residual tension in the patch had to be offset in order to achieve true zero for applied pressure. It is possible, however, that true zero required even more positive pressure than I assumed. If so. the SI K^+ channels would more appropriately be seen as mechanosensitive channels which goes through an activation maximum as tension increases from zero. This would be consistent the experimental results of Oliet and Bourque (1993) for mechanosensitive channels in osmosensory neurons. The effect of fragility would be to shift our experimental operating range to pressures that chronically inactivate the SI K^+ channels.

The discrepancy between single channel and macroscopic recordings of SA K^+ and SI K^+ channels (Morris and Horn, 1991) remains problematic. Could the dynamic behavior of SA K^+ channels I have now uncovered account for this discrepancy? Since I saw no adaptation (fast or otherwise), a fast decay of channel activity following mechanical stimulation during macroscopic recording is unlikely. I did, however, observe a delay.

What might the implications of this type of dynamic behavior be at the macroscopic level? If, in an intact cell, delays (instead of being several seconds or as much as half a minute, as in cell-attached recordings) typically lasted several minutes or more after the onset of tension, SA K^+ channels could act as steady-state or low frequency tension detectors. Since there is almost no evidence for such channel activation (Morris and Horn, 1991; X. Wan and C.Morris, unpublished observation), the discrepancy remains unresolved. It may be that, normally, in intact snail neurons, the structures that are responsible for delayed activation in patch recording conditions are able to fully buffer the channels from experiencing substantial tension changes.

An observation made for swelling-activated Cl^- currents in other cell types may be relevant to this issue. In these cells [leukocytes (Stoddard et al., 1993; Ross et al., 1994), epithelial cells (Kubo and Okada, 1992; Okada et al., 1992), bovine chromaffin cells (Doreshenko and Neher, 1992)], whole-cell recordings consistently yield delays of 5 s to 2 min between the onset of swelling and the activation of Cl^- channels. Since the mechanism by which swelling activates these Cl^- channels is unknown, it remains possible that direct (but delayed) stretch-activation is involved.

A discrepancy also exists between single-channel recording and macroscopic recordings of Xenopus oocytes. Although SA Cat channels are readily observed in cell-attached and excised patches, an exhaustive study of hypotonicity-activated currents in *Xenopus* oocytes (1) revealed no evidence for involvement of these channels during swelling. The rapid adaptation of SA Cat channels might account for part of this discrepancy, although it should be remembered (Hamill and McBride, 1992) a) that adaptation occurs only at

potentials hyperpolarized beyond rest and b) that adaptation does not fully eliminate MS channel activity in patch clamp experiments.

ii) Voltage-dependence

Under normal (non-gentle) recording conditions, I found that SA K^+ channel P_o increased with depolarization; in this respect SA K^+ channels resemble SA Cat channels (Yang and Sachs, 1990). A peculiar aspect of SA Cat channel adaptation is that it is only evident upon hyperpolarization. Two further complications are 1) that although SA Cat channels are depolarization- and stretch-activated channels, under the conditions of adaptation experiments [e.g. Fig. 5.1D of (Hamill and McBride, 1992)], stretch activation (in the moments prior to adaptation) is most pronounced at hyperpolarized potentials, and 2) that adaptation to a pressure can be delayed by a depolarization. No such complicated voltage-pressure interactions were observed in association with the SA K^+ channel dynamics. The delayed response of SA K^+ channels occurred at both positive and negative membrane potentials, though the delay was shorter with pressure steps at depolarized potentials.

iii) Fragile nature of dynamic behavior

Both the dynamic phenomena I detected in SA K^+ channels and the adaptive phenomenon of SA Cat channels were irreversibly lost with repeated pressure pulses while leaving the channels' basic mechanosensitivity intact. Hamill and McBride, (1992) showed that the voltage-dependence of SA Cat channel adaptation was also lost. Thus the dynamic behaviors are fragile; it is interesting to realize that once patches have received considerable

mechanical perturbation, there is no longer any substantial qualitative difference in the stretch-activation or voltage-activation properties of SA K^+ and SA Cat channels. This suggests that the unadorned channels may operate in similar ways, but that they have different types of secondary links to their immediate environment.

Gustin, (1992) stresses that MS channel adaptation in yeast is readily apparent in whole-cell recordings but rarely so in patches. This would be in keeping with Hamill & McBride's general interpretations of the fragility of adaptation, given that yeast patches do not seal easily (Gustin et al., 1986); if mechanical disruption of the channel environment is greater in patches than in the whole-cell configuration, one would predict that adaptation would be more readily lost in the patch.

This raises the possibility that even our gentlest patch forming conditions abolished some aspects of SA K^+ channel and SI K^+ channel dynamics in snail neurons. The whole-cell configuration is more mechanically disruptive than perforated patch recording; it would therefore be ideal to look for adaptation in macroscopic recordings under perforated patch conditions.

I am unaware of any other explicit studies in which delay is reported to be a dynamic feature of MS channel activation. I note, however, that Stockbridge and French (Fig. 3 of (1988)), in illustrating adaptation of fibroblast SA Cat channels, showed what seems to be a delay prior to a transient activation. Also, a preliminary report by Sachs suggested that there is a delay prior to activation of MS channels in (presumably) chick muscle SA Cat channels (Sachs, 1987).

There continues to be uncertainty about the mechanism of MS channel transduction

(Gustin et al., 1991). Gating tension may be exerted through the lipid bilayer (Martinac, et al., 1990) or through underlying cytoskeleton (Sachs, 1990; Guharay and Sachs, 1984). The dynamic behavior of SA K^+ channels is dependent on cortical cytoskeletal elements. The longer delays observed in SA K^+ channels from older neurons may depend on cytoskeletal networks that become progressively denser with age in culture (Vale et al., 1992). In that case tension would be "filtered" through cortical cytoskeleton, and fragility could be explained by gradual disruption of cortical cytoskeletal elements with repeated suction, as suggested in Fig. 5.5. The elements destroyed by extensive mechanical manipulation or cyt D are those responsible for dynamic behaviors, those maintained are those (if any) involved in mechanosensitivity per se.

CHAPTER VI

Pharmacology of Stretch-Activated K^+ Channels in *Lymnaea* Neurons

1. Introduction

A wide variety of mechanosensitive (MS) channels have been described in eukaryotic cells (Morris, 1990), of which two major types, based on ion selectivity, are cation- and K^+-selective stretch-activated channels. The role of most of these channels is unknown (Morris, 1992), but there is growing evidence that some may function as cellular mechanotransducers, with the strongest case being that for MS channels in supraoptic neurons functioning as osmo-mechanical transducers (Oliet & Bourque, 1993).

Since they are most mechanosensitive in mechanically-disrupted membrane (Morris & Horn, 1991; Small & Morris, 1994), SA K^+ channels may act to signal incipient cell trauma but they show little promise of serving as physiological transducers. Moreover, it has been shown that a channel with a well-defined non-mechanical function, the *Aplysia* S-channel (a serotonin and neuropeptide modulated K^+ channel whose activation reduces neuronal excitability), behaves as a stretch-activated K^+ channel in cell-attached and excised patch recordings (Vandorpe et. al., 1994). Stretch-activation is facilitated by the actin reagent, cytochalasin-D, suggesting that SA K^+ channel mechanosensitivity is normally held in check by cytoskeletal restraints (Small and Morris, 1994). This observation raises the possibility that mechanosensitivity is transduced via the phospholipid bilayer as suggested for bacterial mechanosensitive channels (Martinac, et. al., 1990).

In general, the physiological functions of channels are difficult to assess if the channel

cannot be selectively disrupted. What is required for MS channels, therefore, is a high affinity blocker or a cloned channel whose function could be manipulated. Although a MS channel from *E.coli* has recently been cloned (Sukharev, et. al., 1994), its behaviour is unlike any MS channel in eukaryotes and its structure does not resemble any other cloned channel, making it unlikely that it is similar to MS channels of eukaryotes. We note, among eukaryotes, that SA Cat channels but not SA K^+ channels often appear in a cell type of one species while SA K^+ channels but not SA Cat channels appear in the same cell type of another species (Table 6.1). This, along with the fact that site-directed mutagenesis studies (Heginbotham et. al., 1992) have shown that a two amino acid deletion readily can convert K^+ and Cat channels, suggest that SA K^+ and SA Cat channels might be closely related.

TABLE 6.1 Distribution of K^+- and cation- selective SA channels.

Cell Type	+ SA Cat - SA K^+	- SA Cat + SA K^+
CNS neurons	• leech[1]	• mollusc[2]
cell body of mechanoreceptor neurons	• crayfish stretch-receptor[3]	• molluscan mechano-sensory neuron[4,5]
somatic muscle	• amphibian[6] • avian[8]	• *Drosophila*[7]
oocytes or 2 egg embryos	• amphibian[9] • tunicate[11]	• fish[10]

References:
1. (Pelligrino, et. al., 1990); 2. (Sigurdson & Morris, 1989); 3. (Erxleben, 1989); 4. (Vandorpe & Morris, 1992); 5. (Vandorpe, et. al., 1994); 6. (Kirber, et. al., 1988); 7. (Zagotta, et. al., 1988); 8. (Ruknudin, et. al., 1993); 9. (Yang & Sachs, 1990); 10. (Medina & Bregestovski, 1991); 11. (Moody & Bosma, 1989).

Additionally, permeation studies of SA Cat channels revealed pore characteristics more like those of a K^+ channel than, for instance, those of ligand gated non-selective cation channels like the nicotinic AChR (Yang & Sachs, 1990).

Several groups have been developing a pharmacological profile for SA Cats as a prelude, it would be hoped, to designing strategies for the molecular cloning of the channels (Hamill et al., 1992; Lane et. al., 1991; 1992; 1993). In this study we describe the pharmacology of SA K^+ channels in *Lymnaea* neurons with the hope that a pharmacological profile will facilitate comparisons of other cloned channels and assist in the molecular cloning of MS channels.

2. Methods

Cell-attached and excised inside-out membrane patches of cultured *Lymnaea stagnalis* neurons were recorded as described in the general methods. Data analysis and patch-clamp recording were carried out as described in the general methods. All drugs were used the same day they were put into solution (none were stored). Amiloride solutions were sonicated to aid in dissolving any particulate matter.

3. Results

i) Amiloride

Cell-Attached Patches External amiloride (2 mM) decreased SA K^+ single channel currents in cell-attached patches of *Lymnaea* neurons without affecting the apparent P_{open} of the channel (Fig. 6.1A-E). A fast-flickery amiloride block of SA K^+ channels was evident

Figure 6.1. Effects of extracellular amiloride on SA K^+ channels in cell-attached patches. SA K^+ channel current responses to three 2 s voltage ramps from -100 to 100 (-Vp, mV) in the absence **A)** and presence **B)** of 2 mM amiloride. SA K^+ channel responses to a 2 s voltage step to -100 (top) and 100 (bottom) (-Vp, mV) in the absence **C)** and presence **D)** of 2 mM amiloride. Scale bar: 10 pA for a-d. **E)** Superimposed ramp I-V data (as in a, b) from 4 patches were fit by eye to give average single channel current levels (solid line). At the extremes, single channel current was measured from step recordings (symbols as in B, C). Standard error bars are mostly within the symbols (n=12). **F)** Concentration response curves for amiloride block of SA K^+ channels at -100 (closed circles) and 100 (open circles) (-Vp, mV). 3, 4, 12, 3 and 3 patches were used for concentrations of 0.5 to 10 mM amiloride respectively. **G)** Hill plots of data in **F)**. The x-intercepts indicate IC_{50}s (for negative and positive membrane potentials) of 2.0 and 2.3 mM. Slopes give Hill coefficients (for negative and positive potentials) of 1.5 and 1.7, (correlation coefficients, 0.99 and 0.97).

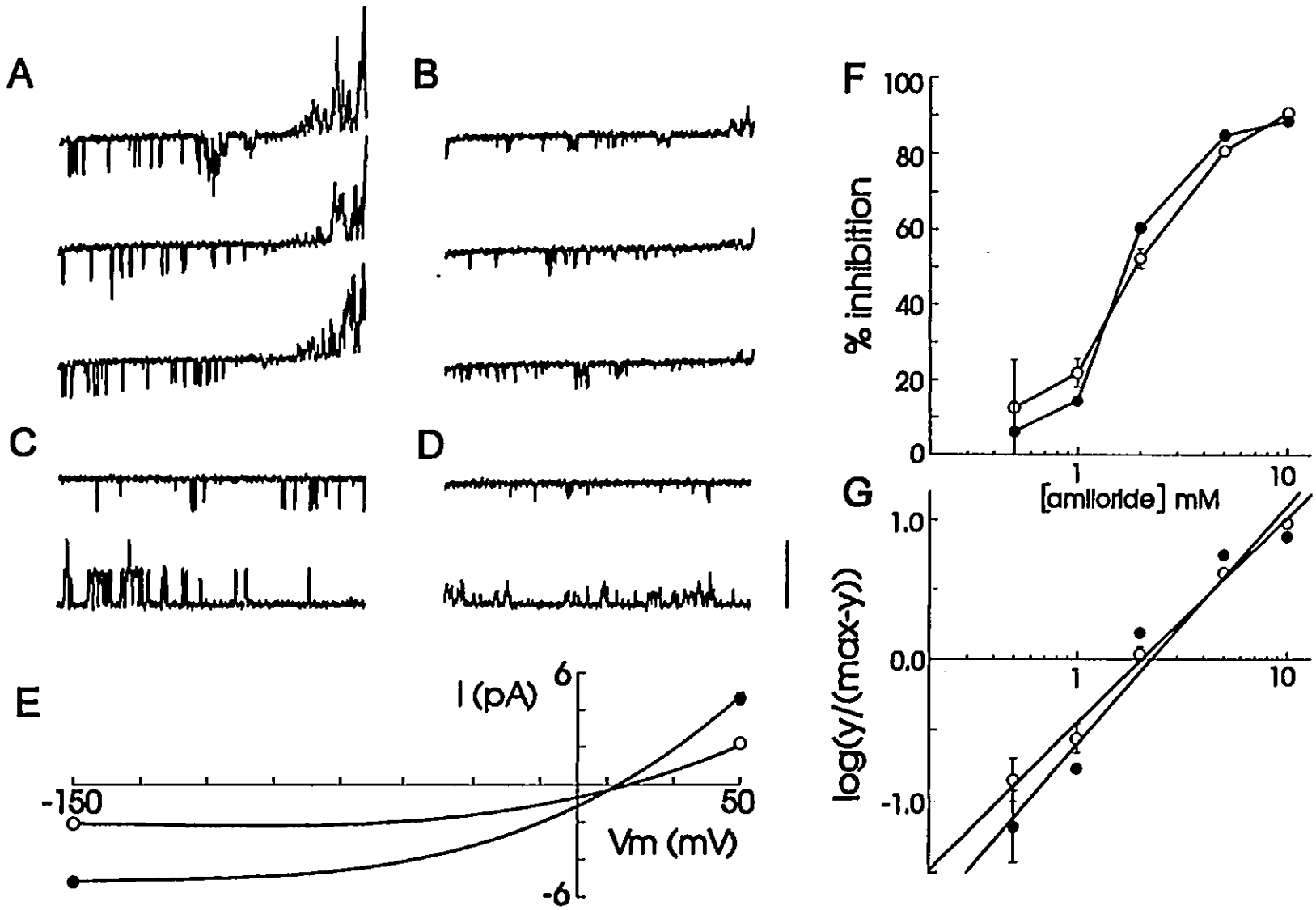
A
B
C
D
E
I (pA)
6
-6
-150
50
Vm (mV)
F
100
80
60
40
20
0
% inhibition
1
10
[amiloride] mM
G
1.0
0.0
-1.0
log(y/(max-y))
1
10

over a wide voltage range. Although some of amiloride's actions on other membrane proteins are steeply voltage-dependent (Lane et. al., 1991), the extent of SA K^+ channel block by amiloride was similar at the extremes of positive and negative voltage we tested (Fig. 6.1E). The concentration response curves (Fig. 6.1F) demonstrate that amiloride's effect on single SA K^+ channel current at both positive and negative membrane potentials was concentration dependent. Hill plots of amiloride block for both positive and negative membrane potentials (Fig. 6.1G) yield similar IC_{50} s (2.3, 2.0) and Hill coefficients (1.7, 1.5) for positive and negative membrane potentials, consistent with a voltage-independent block. Given that the Hill coefficients are closer to 2 than 1, and that block is not voltage-dependent, a mechanism of amiloride block of SA K^+ channels involving the binding of 2 amiloride molecules at sites external to the transmembrane voltage field seems likely.

Excised Inside-Out Patches Excised inside-out patches were formed with high K^+ in the pipette and single SA K^+ channel conductance was examined using 2 s voltage ramps from -50 to 170 (-Vp, mV). On 4 patches, channel activity was recorded before and after the addition of amiloride to the inside face of the patch. No effect was detectable on either the conductance or kinetic properties using concentrations as high as 10 mM (not shown). Thus, unlike the case for *Xenopus* oocyte MS channels (Lane et. al., 1991), amiloride did not block SA K^+ from the internal side.

ii) Gadolinium

Cell-Attached Patches Gadolinium (Gd), a cation with a complex blocking action on SA Cat channels (Yang & Sachs, 1989) was tested. With Gd (100 μM) in the recording

pipette of 5 cell-attached patches, 2 s voltage ramps from -50 to 170 (-Vp, mV) yielded single SA K^+ channel I-Vs which were compared to control patches. The single SA K^+ channel conductance and apparent kinetics of ramp responses from both groups of patches were indistinguishable (not shown).

iii) Diltiazem

Cell-Attached Patches Using the same protocol, but with 100 μM diltiazem (diltiazem has been shown to block one type of SA Cat channel (Ruknudin, et. al., 1993)) in the pipette, 4 cell-attached patches were tested. Single SA K^+ channel conductance and apparent kinetics of these patch responses were not detectably different from control patches (not shown).

iv) Tetraethylammonium (TEA)

Cell-Attached Patches TEA has been a useful probe for K^+ channels and though it is a poor blocker of molluscan SA K^+ channels (Vandorpe et. al., 1994), it does interact to some extent with these channels. To explore this interaction further, we tested external TEA on cell-attached patches by including it in the recording pipette at concentrations from 5 to 200 mM and ramping V_m from -50 to 170 mV over 2 s. TEA produced a fast flickery block of SA K^+ channels, associated with a decreased single channel amplitude (Fig. 6.2), as measured from 2 s steps to the indicated pipette potentials. The single channel I-Vs (Fig. 6.2A) and the corresponding Woodhull plots (Fig. 6.2B) both indicate that this block was not voltage dependent. The effects of increasing concentrations of TEA on block of SA K^+

Figure 6.2. Effects of extracellular TEA on SA K^+ channels in cell-attached patches. **A)** Single SA K^+ channel I-V relations. Symbols are as follows; control (1 mM TEA) (open circles) n=7, 5 mM TEA (closed circles) n=7, 10 mM TEA (open down triangles) n=7, 25 mM TEA (closed down triangles) n=3, 50 mM TEA (open squares) n=3, 100 mM TEA (closed squares) n=4, 200 mM TEA (open up triangles) n=3. **B)** Woodhull plots of TEA block of SA K^+ channel. Symbols are as above. First order linear regressions fit to data gave slopes (and corresponding correlation coefficients) for 5 through 100 mM TEA of 0.0010 (0.96), 0.0005 (0.90), -0.0002 (0.84), -0.0025 (0.34) and 0.0065 (0.87). **C)** Concentration response curves for TEA block of SA K^+ channels at -50 (closed circles) and 170 (open circles) (-Vp, mV). 7, 7, 3, 3, 4 and 3 patches were used for concentrations of 5 to 200 mM TEA respectively. **D)** Hill plots of TEA block of SA K^+ channel. Symbols are as in **C)**. IC_{50}s for negative (and positive) membrane potentials were 54 (and 48) mM. Hill coefficients for negative (and positive) membrane potentials were 1.4 (and 1.2). Correlation coefficients to fits were 0.99 and 0.99. Asterisks indicates no error bar possible.

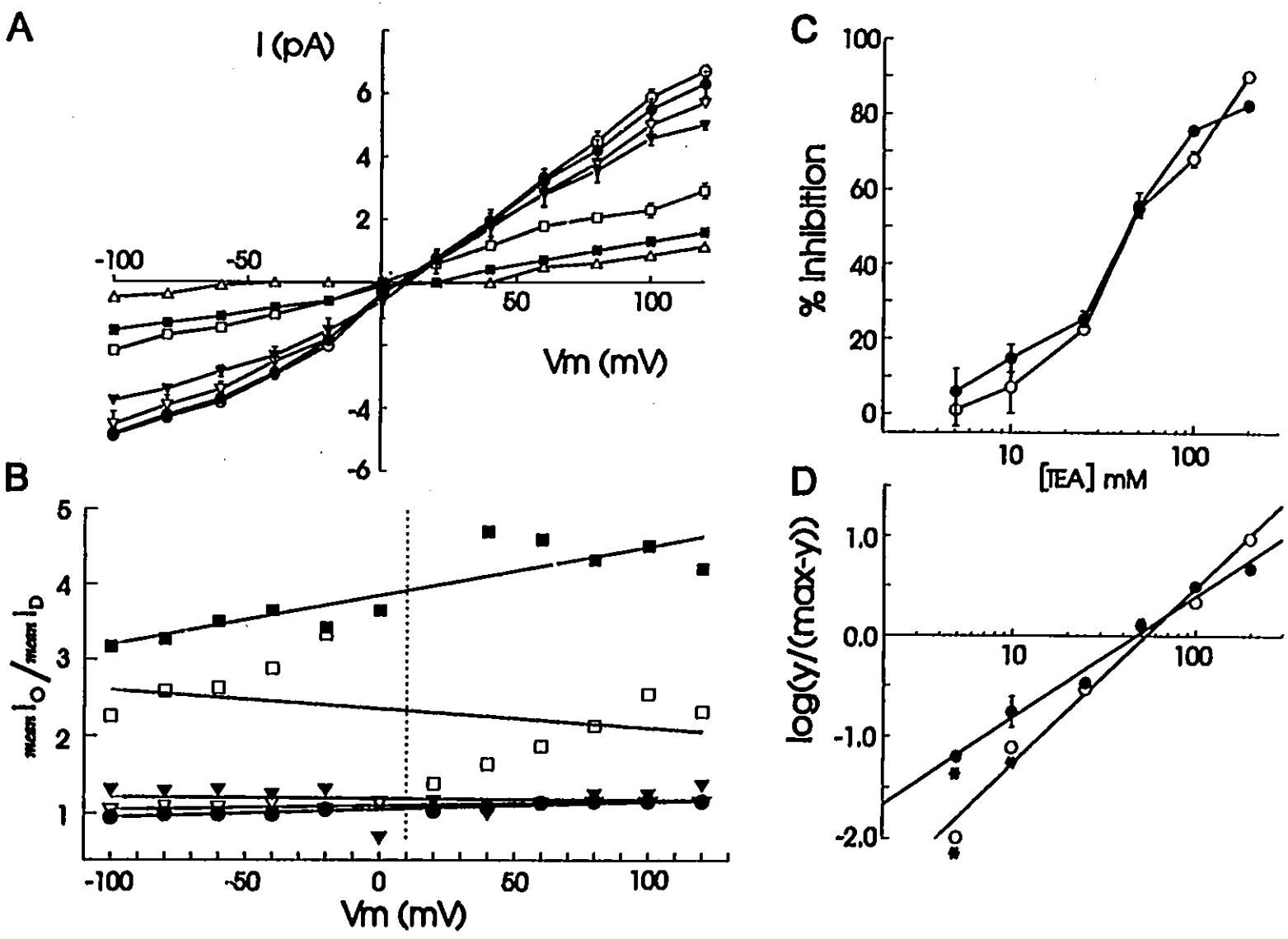
A
I (pA)
6
4
2
-4
-6
-100
-50
50
100
Vm (mV)
B
5
4
3
2
1
-100
-50
0
50
100
Vm (mV)
C
100
80
60
40
20
0
% Inhibition
10
100
[TEA] mM
D
1.0
0.0
-1.0
-2.0
log(y/(max-y))
10
100

channels were evident at both positive and negative membrane potentials, giving IC_{50}s of 48 and 54 mM at the voltage extremes (Fig. 6.2C). The Hill plots of the concentration dependence data at the voltage extremes suggest that a single TEA molecule is sufficient to produce the block, since the Hill coefficients are closer to 1 than 2 (1.2, 1.4) (Fig. 6.2D).

Excised Inside-Out Patches On 4 patches, the effect of internal TEA was tested on single SA K^+ channels by examining the responses to 2 s voltage ramps before and after bath application of TEA. Concentrations as high as 200 mM had no apparent effect on conductance or kinetics (not shown).

v) Quinidine

Cell-Attached Patches External quinidine (1 mM) was shown to reduce currents through single *Lymnaea* heart cell SA K^+ channels (Brezden et. al., 1986). Here we show that external quinidine produces a concentration-dependent block of the neuronal SA K^+ channels (Fig. 6.3A). With quinidine in the pipette, 2 s voltage ramps from -50 to 170 (-Vp, mV), and 2 s voltage steps to the indicated potentials were applied to cell-attached patches. The quinidine block resulted in a reduction in single SA K^+ channel amplitude at all membrane potentials. Woodhull plots of quinidine block I-V data (Fig. 6.3B) have slopes close to zero indicating a voltage-independent block. The reduction in current amplitude obtained from voltage steps to -50 and 170 (-Vp, mV) (Fig. 6.3C) was identical, consistent with the Woodhull plots. Hill plots constructed from concentration response data (Fig. 6.3D) revealed IC_{50}s of 0.8 and 0.7 mM at positive and negative membrane potentials respectively. Hill

Figure 6.3. Effects of extracellular quinidine on SA K^+ channels in cell-attached patches. **A)** Single SA K^+ channel I-V relations. Symbols are as follows; control (open circles) n=7, 0.1 mM quinidine (closed circles) n=3, 0.2 mM quinidine (open triangles) n=3, 0.5 mM quinidine (closed triangles) n=5, 1 mM quinidine (open squares) n=3, 2 mM quinidine (closed squares) n=3. **B)** Woodhull plots of quinidine block of SA K^+ channel. Symbols are as above. First order linear regressions fit to data gave slopes (and corresponding correlation coefficients) for 0.2 through 2 mM quinidine of -0.00094 (0.88), 0.00064 (0.88), 0.00198 (0.79), and -0.002 (0.31). **C)** Concentration response curves for quinidine block of SA K^+ channels at -50 (closed circles) and 170 (open circles) (-Vp, mV). 3, 3, 4, 3, 3, 3 and 3 patches were used for concentrations of 0.01 to 12 mM quinidine respectively. **D)** Hill plots of quinidine block of SA K^+ channel. Symbols are as in C). IC_{50}s for negative (and positive) membrane potentials were 0.7 (and 0.8) mM. Hill coefficients for negative (and positive) membrane potentials were 1.6 (and 1.5). Correlation coefficients to fits were 0.99 and 0.98. No points were possible for 0.01 mM because the mean % inhibition was < 0 so that the transformed value to be plotted in **D)** was undefined.

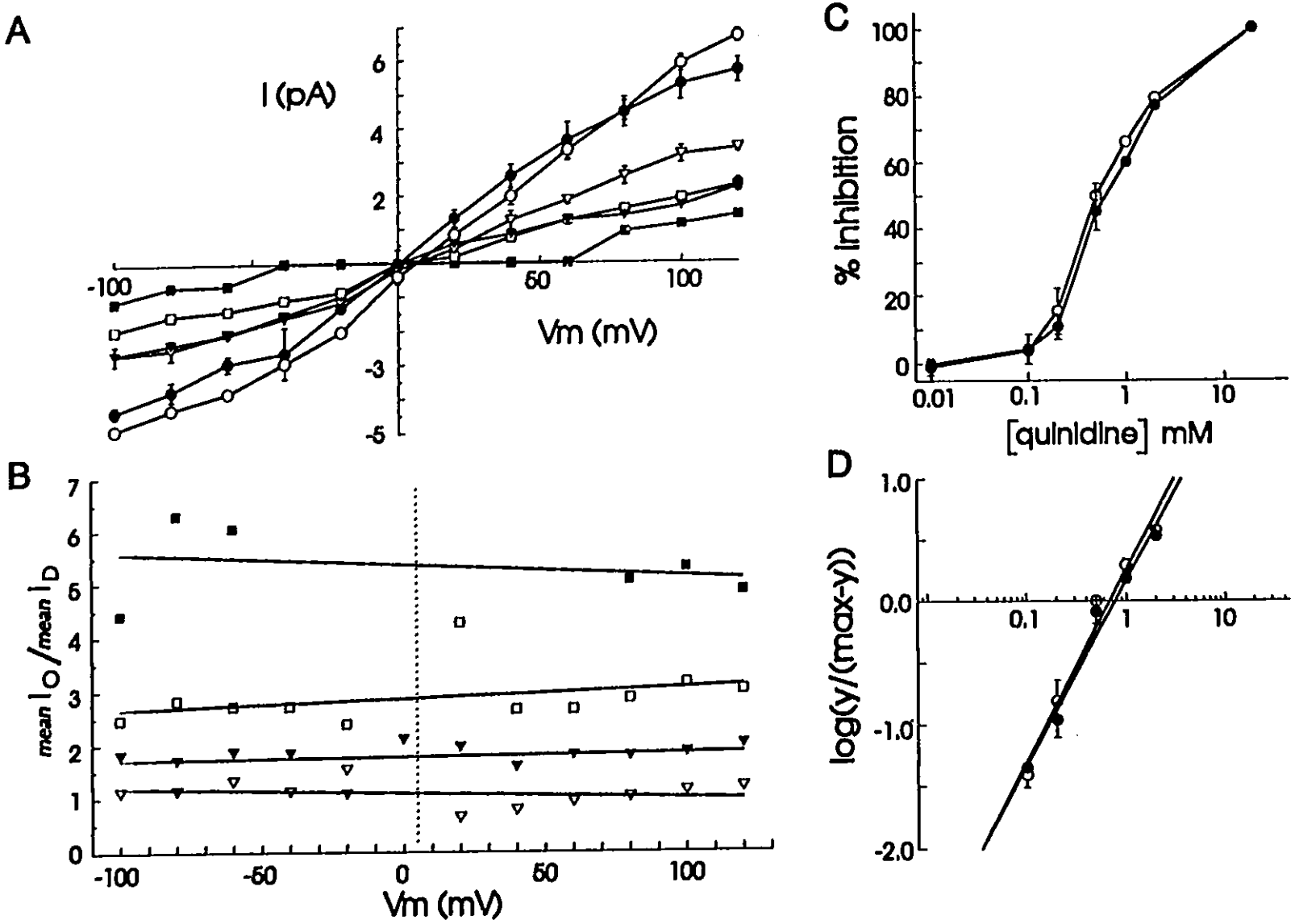
A
I (pA)
6
4
2
-3
-5
-100
50
100
Vm (mV)
B
mean I_O / mean I_D
7
6
5
4
3
2
1
0
-100
-50
0
50
100
Vm (mV)
C
% Inhibition
100
80
60
40
20
0
0.01
0.1
1
10
[quinidine] mM
D
log(y/(max-y))
1.0
0.0
-1.0
-2.0
0.1
1
10

coefficients closer to 2 than 1 (1.5 and 1.6) at these potentials suggest that binding at two sites may be necessary for quinidine block of SA K^+ channels.

Excised Inside-Out Patches Quinidine was also applied to the intracellular face of excised inside-out patches. Voltage ramps were used as usual to examine single SA K^+ channels' conductance before and after the addition of quinidine. In all 4 patches tested, internal quinidine was without effect; there was no discernible difference in the single channel conductance or the apparent kinetic properties of the SA K^+ channel with internal quinidine at concentrations as high as 10 mM (not shown).

vi) Ethanol

Cell-Attached Patches We tested the effects of 3% (v/v) ethanol, a concentration that significantly increases the fluidity of membranes (Goldstein, 1986; Silberman et. al., 1990), on the behaviour of SA K^+ channels. The ethanol was applied in the pipette and patches were exposed for at least 5 min prior to testing. Ethanol did not cause SA K^+ channels to lose their mechanosensitivity; no difference in the activation of SA K^+ channels by 20 to 40 mm Hg suction was noted. The responses of ethanol treated patches to 2 s voltage ramps (V_m = -50 to 170 mV) were indistinguishable from control patches (not shown). Likewise, the single SA K^+ channel I-V relations obtained using 2 s steps to various voltages (Fig. 6.4), were not significantly different between control and ethanol treated patches.

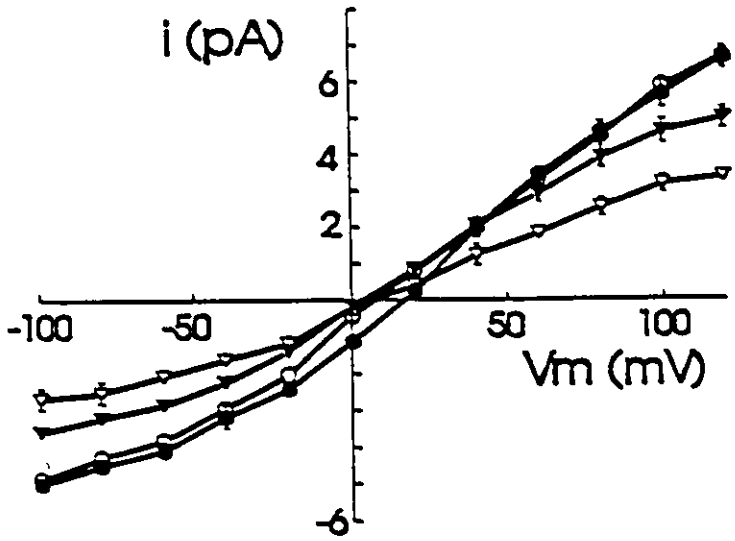

Figure 6.4. Effects of 3 % ethanol, quinidine and both together on SA K^+ channels in cell-attached patches. SA K^+ channel I-V relations. Symbols are as follows; control (open circles) n=7, 3 % ethanol (closed circles) n=4, 0.5 mM quinidine (open triangles) n=3, 0.5 mM quinidine in 3 % ethanol (closed triangles) n=10.

vii) Quinidine with Ethanol

Cell-Attached Patches The I-V relationship of single SA K^+ channels in patches exposed simultaneously to 0.5 mM quinidine and 3 % ethanol in the recording pipette was examined. The single SA K^+ channel current amplitude was measured during 2 s voltage steps (Fig. 6.4). Although ethanol alone did not affect SA K^+ channel characteristics, it decreased the efficacy of SA K^+ channel block by external quinidine. In the presence of ethanol, quinidine still produced a flickery block of SA K^+ channels but the extent of block decreased from 52 to 25 % and from 50 to 33 % at positive and negative membrane potentials respectively (i.e. ~50 % and ~34 % reductions in quinidine's efficacy) (see Fig. 6.4).

4. Discussion

i) Amiloride

Although amiloride's highest affinity is for epithelial Na channels, it, along with

structurally related analogues, has been used in constructing a pharmacological profile of MS channels in *Xenopus* oocytes (Lane et. al., 1992). On these channels, amiloride appears to have two distinct types of binding site, one type (Hill co-efficient 2) is accessible from the external side, causes a distinctly voltage-dependent flickery block and has K_d 0.5 mM at -100 mV and another type of lower affinity that is voltage-independent and accessible from the inner face (Lane et. al., 1991). Amiloride blocks MS currents of hair cells (Jorgensen & Ohmori, 1988) with even greater potency (K_d 50 μM); the suggested binding reactions are complex. We found no published reference to amiloride blockade of K^+ selective channels in the mM range, so we cannot say whether a voltage-independent block with a K_d of 2 mM - the result we obtained for *Lymnaea* SA K^+ channels - is normal or unusual for K^+ channels. Nevertheless, given the paucity of known blockers for SA K^+ channels, knowledge of amiloride's action may eventually be helpful, in a biophysical context, as a distinguishing characteristic.

ii) Gadolinium and diltiazem

External gadolinium (Gd^{3+}) can fully block cation-selective MS channels at 10 μM; it is not specific for MS channels, however, since it inhibits some Ca channels (Yang & Sachs, 1989). Do SA K^+ channels share the sensitivity of SA Cat channels to Gd^{3+}? It has been reported anecdotally (Yang & Sachs, 1989), that a rat astrocyte SA K^+ channel is not Gd^{3+}-sensitive at 10 μM, and we have now shown that 100 μM had no discernable effect on molluscan SA K^+ channels. Evidently, being sensitive to membrane tension does not in itself render channels susceptible to Gd^{3+}.

The antiarhythmic, diltiazem blocks a wide spectrum of channels including cyclic

nucleotide gated cation channels (Chen et. al., 1993), L-type Ca channels (Budavari, 1989), *eag*-type K^+ channels (Nguyen et. al., 1994) and an avian Cat channel of marginal mechanosensitivity (Ruknudin et. al., 1993) with K_ds in the micromolar range. Nevertheless, on SA K^+ channels, 100 μM extracellular diltiazem had no effect. Since it was reported (Ruknudin, et. al., 1993), that 20 μM external diltiazem inhibited a vertebrate "stretch-activated" cation channel, we tested 100 μM on *Xenopus* oocyte SA Cat channels but found that it had no effect (Small & Morris, unpublished observation).

iii) Tetraethylammonium

The classic K^+ channel blocker, TEA, binds to K^+ channels with a 1:1 stoichiometry, usually producing a voltage independent block from the outside and, from the inside, a voltage dependent block at ~20 % across the electric field (Pongs, 1992).

For external TEA block, K_d varies from 0.1 mM (Rettig et al., 1992) to >200 mM (Tasaki & Hagiwara, 1957) in many types of K^+ channels (i.e. delayed rectifiers: 0.3 (Dubois, 1981) to >200 mM (Tasaki & Hagiwara, 1957); calcium-activated K: 0.14 (Bokvist, et. al., 1990) to 52.2 mM (Wong & Adler, 1986); inward rectifiers: <10 mM (Schachtman, et. al., 1992)). Site-directed mutagenesis experiments on cloned K^+ channels suggest that external TEA sensitivity is determined by the residue at "position 19" in the mouth of the pore (Hartmann, et. al., 1991). Basic residues yield high K_ds for external TEA blockage. Hydrophillic residues (tyrosine>cysteine>threonine) yield TEA sensitive channels (Pongs, 1992). SA K^+ channels of *Lymnaea* neurons are shown here to have a high K_d for external TEA block (~50 mM). Other K^+ channels which exhibit relatively high external K_ds are listed

in Table 6.2.

Table 6.2 K^+ channels blocked by high (>15 mM) concentrations of external TEA.

Channel	K_d (mM)	References
stretch-activated		
SA K^+ *Lymnaea* neuron	50	
S-channel *Aplysia* MS neuron	90	(Shuster & Siegelbaum, 1987)
K_{ST} *Drosophila* muscle	35	(Gorczyca & Wu, 1991)
others		
K_{ATP}	22	(Bokvist, et. al., 1990)
K^+ persistent *X. laevis* axons	19	(Koh, et. al., 1992)
$K_{delayed\ rectifier}$ squid axons	>200	(Tasaki & Hagawari, 1957)
K_{Ca} (maxi) anterior pituitary	52.2	(Wong & Adler, 1986)
cloned		
RCK 3	50	(McCormack, et. al., 1990)
RCK 4	>100	"
RCK 5	129	"
Shaker	17	(Pongs, 1992)
reag	28	(Ludwig, et. al., 1994)

Among the SA K^+ channels (Table 6.2), Hill coefficients for external TEA block are all less than 1.5, consistent with 1:1 stoichiometry for TEA-channel binding. For the *Aplysia* (Shuster & Siegelbaum, 1987) and *Drosophila* (Gorczyca & Wu, 1991) channels, Hill coefficients were not originally given, but the data were sufficient to make the calculation, which yielded 0.9 and 1.3. In both cases, the block is voltage independent. For *Lymnaea* channels, our average Hill coefficient was 1.3 and block was voltage independent.

The intracellular TEA pharmacology of the two molluscan SA K^+ channels differed, however. Intracellular TEA blocks the S-channel with K_d 40 mM (Shuster & Siegelbaum, 1987), whereas 200 mM intracellular TEA was without effect on *Lymnaea* SA K^+ channels. No information is available for the *Drosophila* channel on this issue.

iv) Quinidine

Quinidine is another agent commonly used to block K^+ channels. In the 10 to 100 μM range it blocks delayed rectifiers, transient outward A-currents, Ca-activated K^+ channels, as well as voltage-gated sodium channels. Extracellular quinidine produced a voltage-independent block of SA K^+ channels with K_d 0.8 mM. This is comparable to quinidine's efficacy on the newly-cloned *reag* channels which are blocked by quinidine with IC_{50} 0.4 mM (Ludwig, et. al., 1994).

Since quinidine is a tertiary amine of pK^+ 8.9 (Rich, et. al., 1994a), 95% would be cationic in a pH 7.6 aqueous solution. Because quinidine's actions on some channels occur in the 10 to 100 μM range, it is possible that the micromolar quantities of the neutral form (eg. the bath concentration of neutral quinidine would be ~40 μM at the K_d we determined for SA K^+

channels) are responsible for SA K^+ channel block. If the neutral form blocked the channel via the bilayer, quinidine should have been equally effective presented from either side. We found, however, that quinidine blocked exclusively from the outside. This establishes that the site is external and accessed from the aqueous medium, but does not rule out the possibility that the neutral form is the effective species.

At the pH of our solutions (7.6) quinidine was predominantly cationic; blockade by a cation should be voltage-dependent unless it occurs outside the voltage field. Because extracellular quinidine blocked SA K^+ channel independent of voltage, we must conclude either that the neutral form is effective or the cation acts at an external site. Since, a quaternary cationic form of quinidine blocks hKv1.5 by binding to a site in the mouth of the channel (Rich, et. al., 1994b), the second hypothesis seems more likely.

A two-state channel with open channel block (Fig. 6.5A) would be consistent with our observations of a dose-dependent reduction of channel amplitude in the presence of quinidine (Fig. 6.4). Simulated single channel currents as they would appear during open channel block without and with filtering for various conditions on the blocking and unblocking rate constants are shown in Fig. 6.5A. In both conditions of k_{on} big, the filtered single channel amplitude is decreased. This behaviour is typical of fast open channel blockade (Moczydlowski, 1992), and seems the likeliest explanation for the effect of quinidine on SA K^+ channels.

v) Ethanol

It is thought that by binding to the phospholipid head groups, ethanol interferes with

the packing of acyl chains in the bilayer (Mitchell & Litman, 1994), thereby increasing membrane fluidity (Goldstein, 1986). For native membranes exposed to < 2% ethanol, fluidity increases of as much as 12% have been measured (Silberman, 1990). Alcohols can affect ligand-channel interactions. On acetylcholine channels, ethanol (1.8 %) causes the channel to open more readily and stay open longer (Dilger, et. al., 1994); the efficacy of the agonist increases, not the agonist's affinity for the channel. In another case, phencyclidine (PCP) binding to acetylcholine channels is competitively inhibited by hexanol (Lin & Wang, 1994).

On SA K^+ channels, 3 % ethanol had no effect on conductance but decreased the efficacy of 0.5 mM quinidine block. According to the interpretation of Fig. 6.5A, ethanol decreased the k_{on} for quinidine block.

Two possible explanations for our ethanol/quinidine interaction data are depicted in the cartoon in Fig. 6.5B. One is based on the somewhat exotic possibility that quinidine binds at the lipid/protein/aqueous interface, where the interactions of ethanol with the phospholipid headgroups (Mitchell & Litman, 1994) could hinder quinidine's action. The other is based on the more likely possibility (Rich, et. al., 1994b) that there is a quinidine binding site in the mouth of the channel.

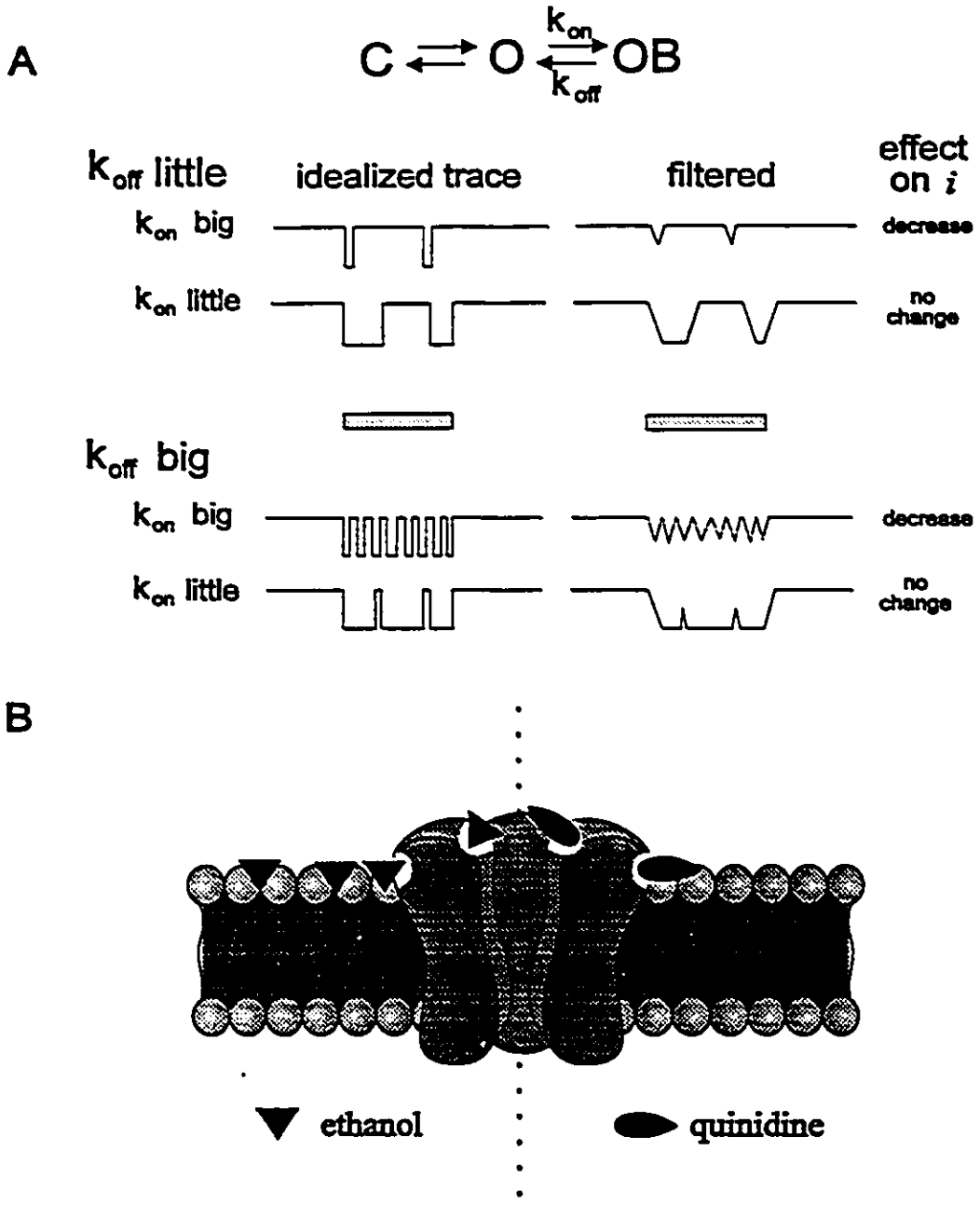

Figure 6.5. A) Two-state channel with open channel block. Simulated single channel currents as they would appear during open channel block without and with filtering for various conditions on the values of the blocking and unblocking rates. Shaded bar represents a period of time when the channel is open and therefore subject to open channel block. K_{on} and K_{off} represent the on and off rates of the blocker. **B) Cartoon depicting two possible explanations for our ethanol/quinidine interaction data.** Ethanol binding sites are indicated on the left and quinidine sites on the right. The two possible sites where both ethanol and quinidine might bind on the channel are marked by white areas.

CHAPTER VII

Pore Properties of *Lymnaea* Neuron SA K^+ Channels

1. Introduction

The *Aplysia* S-channel in mechanosensory neurons is a stretch-activated (SA) K^+-selective channel, (Vandorpe & Morris, 1992; Vandorpe et al., 1994), which modulates resting membrane conductance in response to neurotransmitters via second messengers (Seigelbaum et al., 1982). SA K^+ channels similar to this are found in all molluscan neurons (Morris and Sigurdson, 1989; Bedard and Morris, 1992), *Drosophila* somatic muscle (Zagotta, et al, 1988; Gorczyca and Wu, 1991), rat heart (Kim and Duff, 1990; Kim, 1992) and fish embryos (Medina and Bregestovski, 1991). Given that SA K channels are insensitive to intracellular calcium (Sigurdson and Morris, 1989), insensitive to physiological membrane voltages (Small and Morris, 1994a), and are persistently active with a low open probability (Vandorpe et al, 1994), it seems likely that SA K channels primarily modulate resting membrane conductance. Furthermore, SA K channels in early teleost embryos activate cyclically during cell cleavages and are regulated through cAMP-dependent phosphorylation (Medina and Bregestovski, 1988).

The mechanosensitivity of some of these channels seems to be an adventitous feature which is only readily apparent when the plasma membrane is decoupled from cortical cytoskeleton (Small & Morris, 1994a). Though neuronal mechanosensitive ion channels do appear to be physiological mechanotransducers, (Oliet and Bourque, 1993a; Oliet and Bourque,1993b), membrane tension in molluscan neurons is buffered by the cortical cytoskeleton in a way that "protects" SA K^+ channels from mechanical

stimulation. For this reason, perhaps SA K^+ channels should be thought of as K^+-selective channels with an additional feature which renders them mechanosensitive only under extremely disruptive situations.

Pore properties of *Aplysia* S-channels from identified mechanosensory neurons have been described in some detail (Shuster et al., 1991). It is the focus of this chapter to describe the pore properties of a related channel -- the K^+-selective SA channel of *Lymnaea* neurons. SA K^+ channel pore properties will be discussed in relation to other K^+ channels.

2. Methods

Lymnaea stagnalis cultured neurons were used to form cell attached and excised inside-out patches as described in General Methods. Cell-attached recordings were made in a bath solution of NS. Pipette solutions contained only KCl and/or the test cation salt as indicated and did not contain any $MgCl_2$, $CaCl_2$, HEPES or glucose in order to minimize interference by these agents on test cation permeation while measuring channel selectivity and unitary conductance. Experiments depicted in Fig. 7.5 did however contain a high K^+ version of NS (no NaCl, and 50 mM KCl instead of 1.6 mM KCl). Excised inside-out patches also had only KCl and/or the test cation indicated. In the case of thalium (Tl), the chloride salt is insoluble so I used Tl-acetate and substituted K-acetate for KCl. The resulting large offsets at the silver-silver chloride electrode (Raynauld, 1994), could however, be zeroed out. With symmetrical TlAc/KAc conditions, I assumed a V_{rev}

of 0 mV. Bath solution changes were made by perfusing 9 ml of test solution at ~4 ml/min into 2 ml recording chamber (excess was aspirated from top of recording chamber).

Unitary chord conductance was measured and current-voltage relations (I-Vs) constructed by measuring the single SA K^+ channel amplitude in response to 2 s voltage ramps from -100 to 120 mV (V_m) and 2 s voltage steps at the these voltage extremes. Linear I-Vs were fit by eye to three or four ramp responses. The end points of the I-Vs (symbols) are means and s.e.m.. Paired student's t-tests were carried out to determine statistical significance of difference between means. The end points were obtained by measuring the current amplitude of responses to 2 s voltage steps to -100 and 120 mV (V_m). To test the hypothesis that the Kms obtained from the hyperbolic fits to inward and outward conductances with increasing symmetrical K^+ concentrations in Fig. 7.1 were different, the hyperbolas were linearized using $(1/\text{conductance})=(1/\gamma_{max})+(K_m/\gamma_{max})*(1/[K^+])$ and a t-statistic regression analysis was performed. For cell-attached patches membrane voltage was taken to be $V_m=(V_{rest}-V_p)$, where V_p is the pipette holding potential and V_{rest} is the resting membrane potential, which was assumed to be -50 mV (Morris and Sigurdson, 1989) for *Lymnaea* neurons. Currents flowing into the pipette are illustrated as upward deflections.

3. Results

Effect of Symmetrical K^+ Concentration on Single SA K^+ Channel Conductance

Single channel current amplitude was measured over a range of voltages with symmetrical K^+ concentrations. The effect of K^+ concentration on SA K^+ channel activity

is illustrated in Fig. 7.1. At different concentrations there was no change in channel kinetics as judged by the appearance of SA K^+ channel responses to voltage ramps (Fig. 7.1A). The single channel current-voltage relations (I-Vs) at lower K^+ concentrations appeared linear over the entire voltage range. At K^+ concentrations ≥ 50 mM, the I-Vflattened at extreme membrane depolarizations. Chord conductances were determined between 0 and 120 mV (outward), zero and -100 mV (inward) and -100 and 120 mV (overall). Applying the Michealis Menton equation, hyperbolic fits to the mean conductances using $\gamma=\gamma_{max}/(1+K_m/[K^+])$ (Fig. 7.1B) yielded dissociation constants (K_m) of the channel for K^+ of 28.0 ± 4.0 mM, and 91.0 ± 35.0 mM for inward (obtained by measuring chord conductance from 0 to -100 mV) and outward currents (chord conductance from 0 to 120 mV), respectively, with an overall K_m for both inward and outward currents (chord conductance from -100 to 120 mV) of 35.0 ± 7.8 mM. These hyperbolic fits yielded asymptotic maxima (γ_{max}) representing concentrations at which the K^+ binding site(s) within the pore saturates. For inward and outward currents, γ_{max} was 180.0 ± 11.0 pS and 160.0 ± 33.0 pS, respectively, with a value from conductances over the whole voltage range of 140.0 ± 12.0 pS. The fact that different K_m values were obtained for inward and outward currents suggests that the SA K^+ channel pore contains more than one binding site for K^+. This is not what is expected from only one binding site. Likewise, the Michealis Menton formalism applies to a single association, dissociation reaction but the K_m values here represent one or more sites with which K^+ interacts as it permeates the pore.

Figure. 7.1 Effect of K^+ concentration on single SA K^+ channel unitary conductance. Excised inside-out patches with symmetrical K^+ concentrations as indicated. *A*, Examples of SA K^+ channel responses to 2 s voltage ramps from -100 to -120 mV (V_m). K^+ concentrations indicated at left of each trace. Each trace is from a different patch. Scale 10 pA; 25 mV; 225 ms. *B*, Plot of SA K^+ channel unitary conductance versus K^+ concentration. ▼, ▲ and ● represent chord conductance from 0 to -100 mV, 0 to 120 mV and -100 to 120 mV (V_m), respectively. Means (symbols) and s.e.m. (mostly within symbols) are shown of 3, 4, 5, 7, and 4 patches for 1, 5, 10, 50 and 100 mM KCl, respectively. Lines are best hyperbolic fits to mean data (symbols) using $\gamma=\gamma_{max}/(1+K_m/[K^+])$.

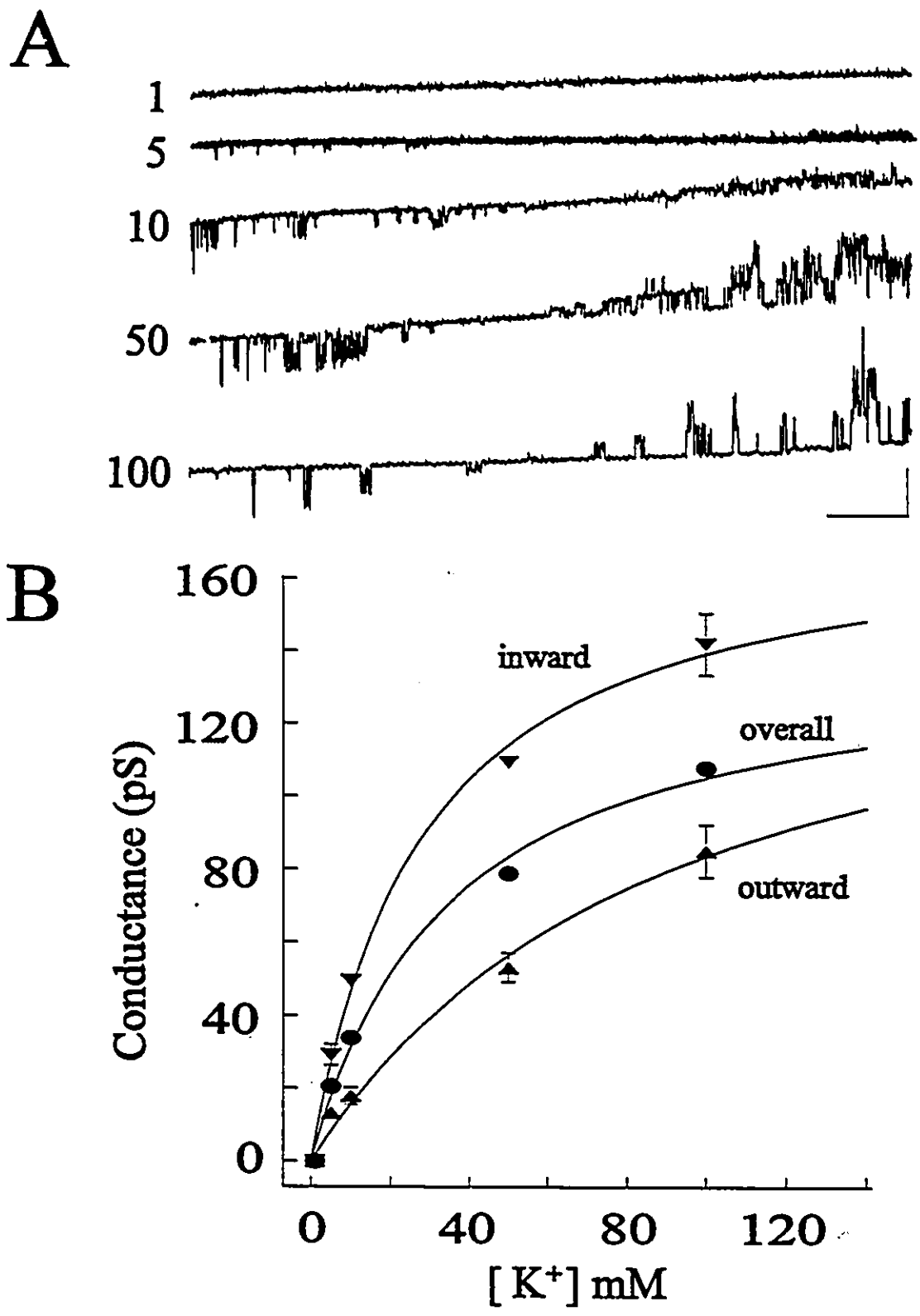
A
1
5
10
50
100
B
160
120
80
40
0
Conductance (pS)
inward
overall
outward
0
40
80
120
[K+] mM

Anomalous Mole Fraction Effect With Mixtures of Rb^+ and K^+

When an ion channel contains more than one ion at a time, ion-ion repulsion can occur inside the pore destabilizing ion binding, resulting in rapid transmembrane passage despite high affinity binding (Tsien et al., 1987). Convincing evidence for a multi-ion pore with such ion-ion repulsions can be obtained by presenting a channel with mixtures of two permeant ions. If the channel is a multi-ion pore, the unitary conductance will not increase monotonically with an increasing mole fraction of the more permeant ion species. Instead it goes through a minimum and then increases. This phenomenon is called the anomalous mole fraction effect (Hille, 1984). The two permeant ions used to test for an anomalous mole fraction effect on the SA K^+ channel were K^+ and Rb^+. The chord conductance of 100 % symmetrical K^+ measured from -100 to 120 mV was 79 ± 1.7 pS. Although SA K^+ channel unitary chord conductance for 100 % Rb^+ as measured from -100 to 120 mV was small (16 ± 0.1 pS), when a solution containing a mixture of 25 % K^+ and 75 % Rb^+ was used, it decreased even further (~40 %) to a minimum of 9.5 ± 0.2 pS (Fig. 7.2).

Permeability of SA K^+ Channel Based on Reversal Potentials Under Biionic Conditions

I investigated the ability of SA K^+ channels to discriminate among various monovalent cations by estimating their permeability relative to K^+. Permeability ratios are determined by measuring the reversal potential when equimolar concentrations of K^+ and a test cation are placed on either side of the membrane. The relative permeability of a test cation is operationally defined by the relationship obtained from Nernst-Planck

electrodiffusion, $P_A/P_K = ([K]_i/[A]_o)*e^{(FV_{rev}/RT)}$, where A is the test cation on the outside, V_{rev} is the reversal potential and F, R, and T have their usual meanings (Goldman, 1943; Hodgkin & Katz, 1949). Using excised inside-out patches, with 50 mM K^+ on the inside, and either 50 mM K^+ or the test cation outside, the reversal potential of SA K^+ channel responses to voltage ramps was measured and permeability ratios were obtained for Rb^+, NH_4^+, Na^+, Li^+, and Cs^+ (Fig. 7.3.). Although the reversal potential with Tl^+ was contaminated due to the Tl·Ac interaction with the silver-silver chloride electrodes, making it inadvisable to use this as a measure of selectivity, inward Tl^+ currents were observed which were 60 % smaller than inward K^+ currents but still 3.5 times larger in amplitude than inward Rb^+ currents (Fig. 7.3). Inward currents were observed for Rb^+ and NH_4^+ as well but not for Na^+, Li^+, or Cs^+. Although no inward Cs^+ currents were observed, the reversal potential (-1.5 ± 1.3 mV) yields a relative permeability of 1.1 ± 0.05 suggesting that Cs^+ interacts with an external site(s) of the pore with higher affinity than does K^+. The selectivity sequence based on reversal potential measurements was $Cs^+ > K^+ > Rb^+ > NH_4^+ > Na^+ > Li^+$ (Table 1; column 2). The fact that a site in the channel is more selective for Cs^+ than K^+ and yet no discernable inward Cs^+ currents were observed suggests that Cs^+ binding to that site would block the channel. The shape of the I-Vs was sublinear at extreme depolarizations only for K^+ and to a small degree, for NH_4^+ whereas the I-V shape for Cs^+ and Tl^+ was linear and for Rb^+, Na^+, and Li^+, supralinear.

Permeability of SA K^+ Channel Based on Relative Conductance in Symmetrical Solutions

Reversal potentials reveal the relative affinity of a site(s) for a range of cations. This issue of binding is one aspect of selectivity. Conductance provides information about

Figure. 7.2. Anomalous mole fraction effect with Rb^+. Excised inside-out patches with symmetrical solutions on both sides of the membrane. Total cation concentration is 50 mM. *A*, Examples of SA K^+ channel responses to 2 s voltage ramps from -100 to 120 mV (V_m). Mixtures of K^+ and Rb^+ are as indicated at left of each trace. Scale 5 pA; 25 mV; 225 ms. *B*, Plot of SA K^+ channel unitary chord conductance from -100 to 120 mV (V_m) against fraction of K^+ concentration. Means (symbols) and s.e.m. (mostly within symbols) are shown of 5, 4, 6, 5, and 7 patches for 0, 25, 50, 75 and 100 % K^+, respectively. Line is fit by eye to symbols. Dotted horizontal line represents conductance with 0 % K^+ and 100 % Rb^+.

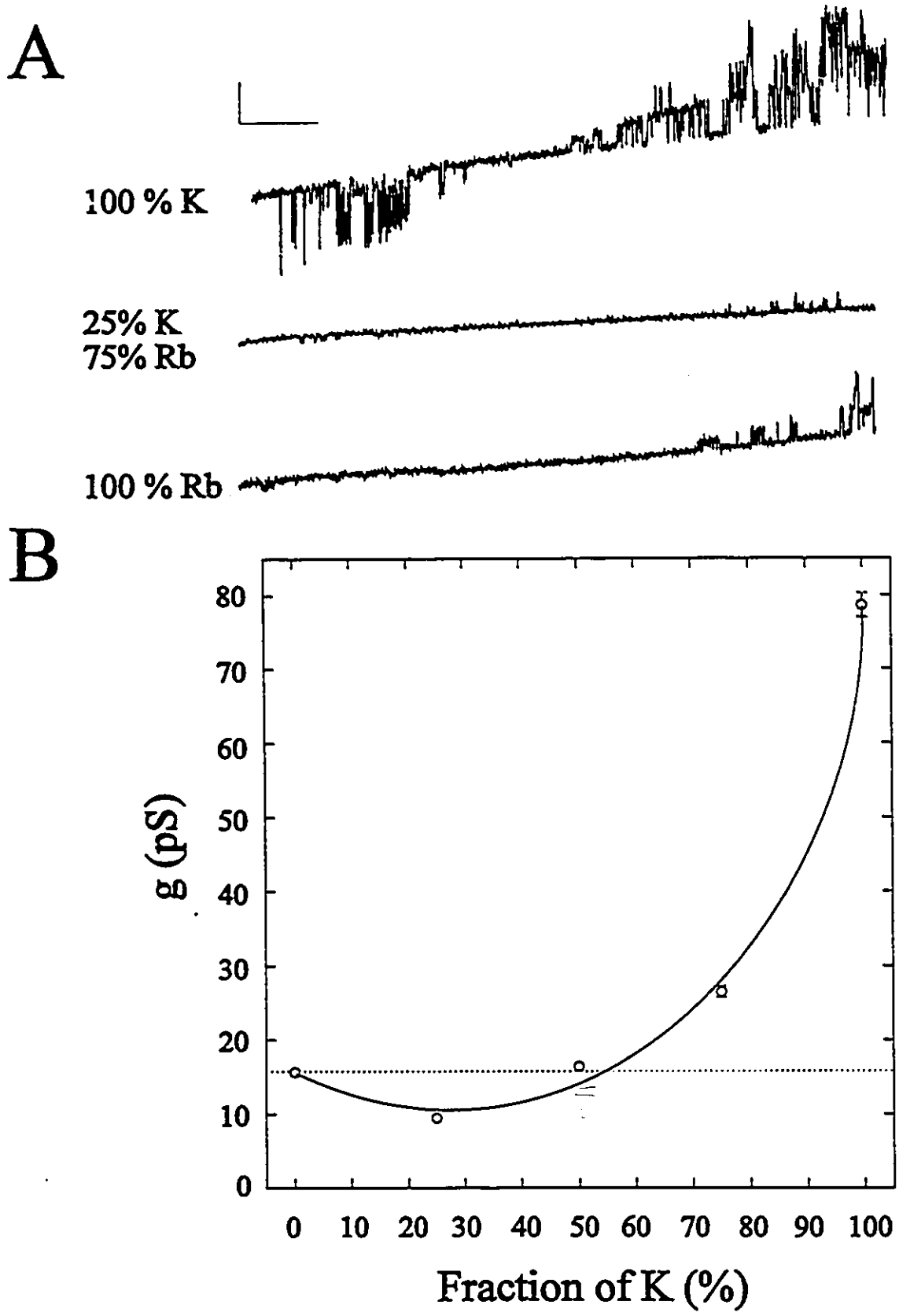
A
100 % K
25% K
75% Rb
100 % Rb
B
g (pS)
0
10
20
30
40
50
60
70
80
0
10
20
30
40
50
60
70
80
90
100
Fraction of K (%)

Figure. 7.3. Permeability of SA K^+ channel using reversal potentials under biionic conditions. Excised inside-out patches with 50 mM K^+ in the bath and 50 mM K^+ or the indicated test cation in the pipette. I-Vs obtained as described in Methods. Means (symbols) and s.e.m. (mostly within symbols) for currents and for zero current potentials (except for Tl which was arbitrarily set at 0 mV) are shown of 7, 9, 5, 8, 7, 8 and 6 patches for K^+, Rb^+, Tl^+, Na^+, Li^+, Cs^+ and NH_4^+, respectively. Insets are examples of SA K^+ channel responses to 2 s voltage ramps from -100 to 120 mV (V_m). Tl^+ current response inset is truncated at -50 and 50 mV (V_m). Scale 10 pA.

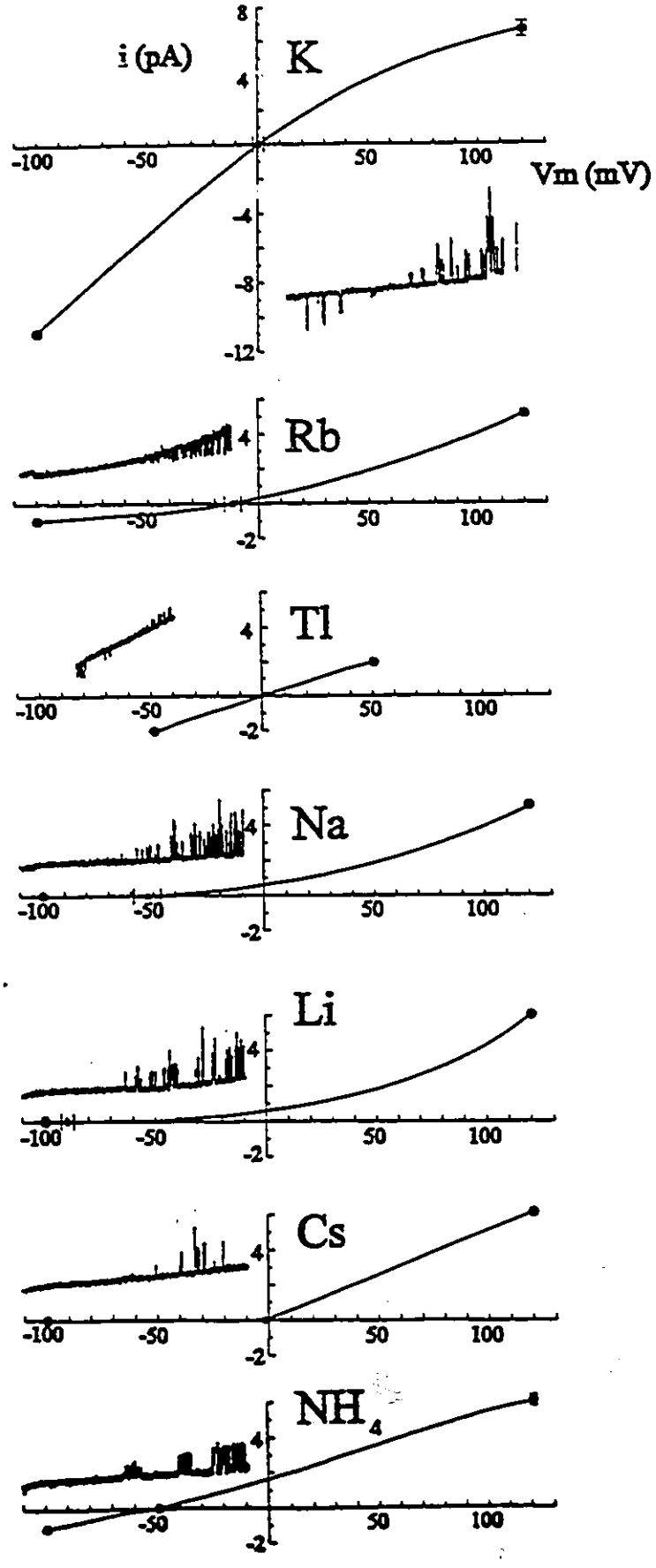
i (pA)
K
Vm (mV)
Rb
Tl
Na
Li
Cs
NH4

another aspect, the rate of net movement through the channel (Hille, 1984; Tsien et al., 1987). The selectivity of a channel as determined by conductance ratios is different from that determined by relative permeability. Single SA K^+channel I-V responses were obtained with 2 s voltage ramps from -100 to 120 mV (V_m) in symmetrical solutions of K^+, Rb^+, Tl^+, NH_4^+, Na^+, Li^+, and Cs^+ (Fig. 7.4.). There were no detectable inward or outward currents with Na^+, Li^+, or Cs^+. An upper limit for conductance of these three monovalents was obtained by assuming the amplitude of events was less than the noise level. Values of conductance for K^+, Rb^+, and NH_4^+ were obtained by measuring the chord conductances from -100 to 120 mV. Values of conductance for Tl were obtained by measuring the chord conductances from -50 to 50 mV. Large inward and outward Tl currents were observed and both appeared flickery. Rb^+ and NH_4^+ currents were small in amplitude. The selectivity sequence from these measurements is $Tl^+ = K^+ > Rb^+ > NH_4^+ >> Na^+ = Li^+ = Cs^+$ (Table 1; column 3).

Table 7.1. SA K^+ channel relative and absolute permeabilities.

Ion (X)	P_X/P_K	g_X/g_K
Tl^+	—	1.00 ± 0.03
K^+	1.0	1.0
Rb^+	0.63 ± 0.03	0.20 ± 0.01
NH_4^+	0.15 ± 0.01	0.18 ± 0.01
Na^+	0.13 ± 0.01	< 0.06
Li^+	0.03 ± 0.002	< 0.06
Cs^+	1.10 ± 0.05	< 0.06

Figure. 7.4. Permeability of SA K^+ channel based on relative conductances in symmetrical solutions. Excised inside-out patches with 50 mM symmetrical KCl or test cation as indicated. I-Vs were obtained as described in Methods. For Tl^+ I-Vs, current measurements were carried out at 50 mV either side of the reversal potential. Means (symbols) and s.e.m. (mostly within symbols) are shown of 7, 5, 5, and 6 patches for K^+, Rb^+, Tl^+, and NH_4^+, respectively. Insets are examples of SA K^+ channel responses to 2 s voltage ramps from -100 to 120 mV (V_m). Scale 10 pA.

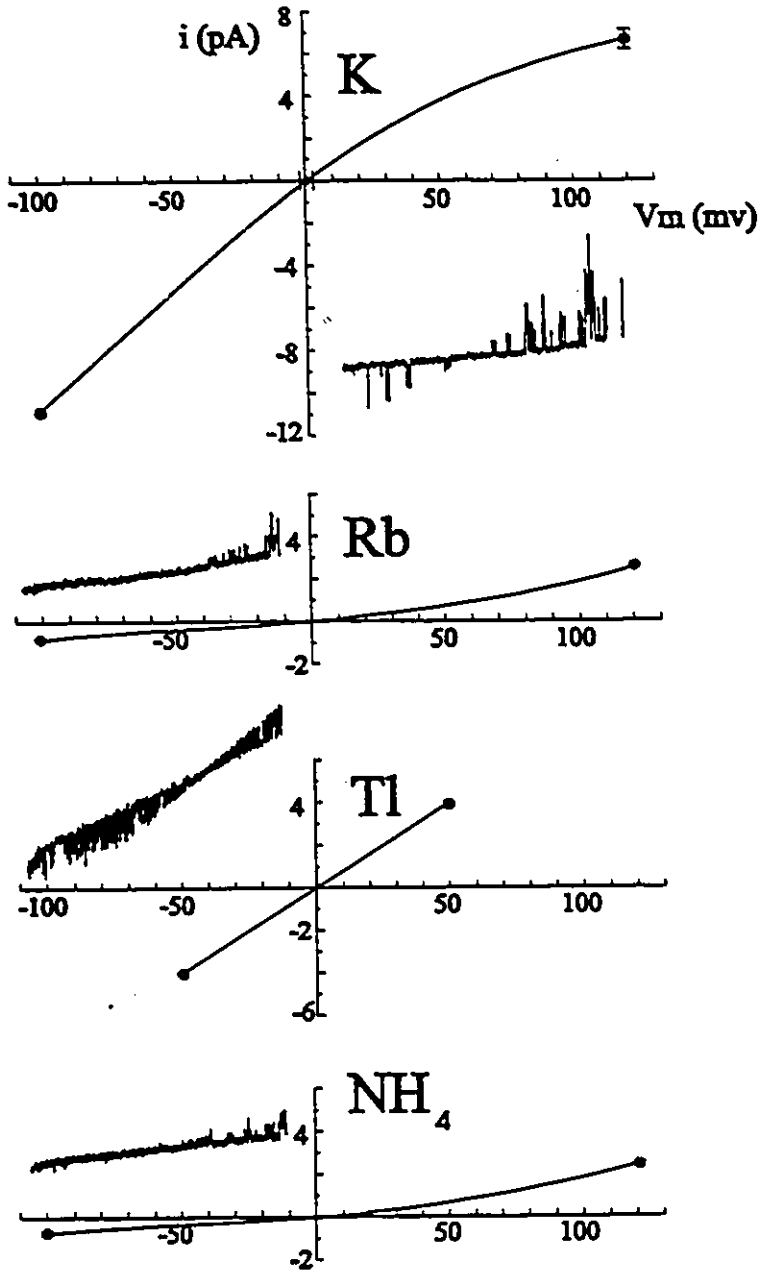
i (pA)
8
4
K
-100
-50
50
100
Vm (mv)
-4
-8
-12
4
Rb
-50
50
100
-2
4
Tl
-100
-50
50
100
-2
-6
NH4
4
-50
50
100
-2

Effect of pH Extremes on SA K^+ Channel

Because some channels are pH sensitive, I sought to determine whether proton or hydroxide ion concentrations had any substantial effect on SA K^+ channel unitary conductance. I used KOH and HCl to obtain desired pH values for the recording pipette solutions (Fig. 7.5.). I chose pH values as far from pH 7.6 (normal) as would permit seal formation. Solutions with pH values beyond these hindered seal formation presumably through membrane destabilizing effects. Surprisingly, pH extremes had no detectable effects on SA K^+ channel responses to voltage steps or ramps in cell-attached patches (Fig. 7.5.). Neither SA K^+ channel kinetics, as judged by the appearance of single channel events, nor unitary current amplitude was affected.

Mg^{2+} Block of SA K^+ Channel

I noted that for a given pipette [K^+], the inward K^+ currents in cell-attached experiments (Fig. 7.5.) were smaller (~40%) than in excised inside-out patches (Fig. 7.1). Either a cytoplasmic component not included in the bath of excised patches or a component of the recording pipette of cell-attached patches not present in excised patch pipettes (i.e. 2 mM Mg^{2+}, 3.5 mM Ca^{2+}, 5 mM HEPES) could be responsible. Large inward K^+ currents were observed in cell attached patches in pipettes containing 1 mM Ca^{2+} and 5 mM HEPES but no Mg^{2+} (Sigurdson and Morris, 1989) suggesting that the reduced current amplitude in our excised patches was caused by Ca^{2+} or HEPES. However, with just 50 mM K^+ and 1 mM TEA in the pipette (cell-attached configuration), (i.e. identical to excised patches), inward K^+ currents were not different (not shown), from

Figure. 7.5. Effect of pH extremes on SA K^+ channel conductance. Cell-attached patches with "high" K^+ normal pipette recording solution and NS in the bath. I-Vs were obtained as described in Methods. Means (symbols) and s.e.m. (mostly within symbols) are shown of 5 patches for *A-C*. Insets are examples of SA K^+ channel responses to 2 s voltage ramps from -100 to 120 mV (V_m). Scale 10 pA.

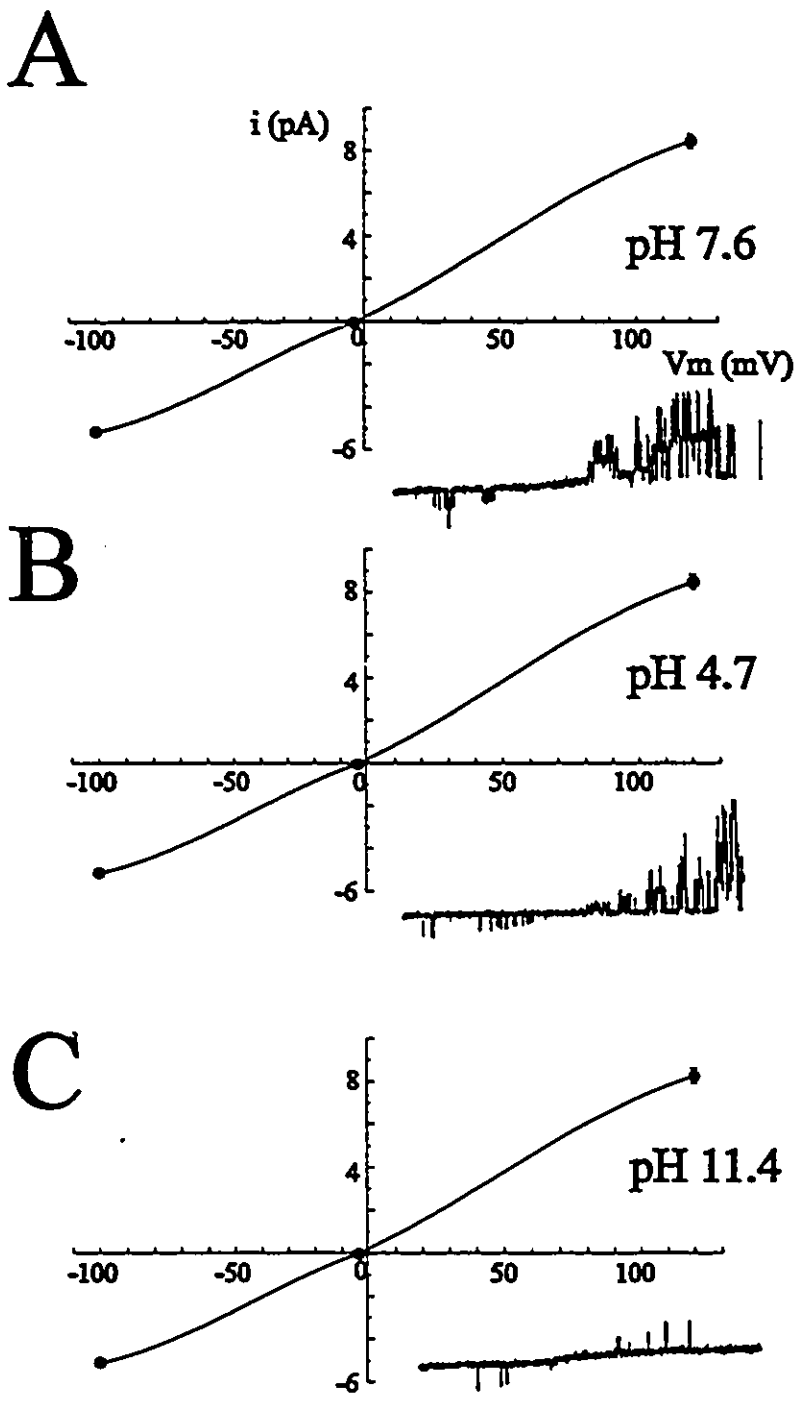
A
i (pA)
8
4
pH 7.6
-100
-50
0
50
100
Vm (mV)
-6
B
8
4
pH 4.7
-100
-50
0
50
100
-6
C
8
4
pH 11.4
-100
-50
0
50
100
-6

of excised inside-out patches, suggesting that the extracellular Mg^{2+} acts as a fast blocker of inward K^+ current.

Ba^{2+} Block of SA K^+ Channel

Another divalent which has been shown to block monovalent cationic channels is Ba^{2+}. Ba^{2+}, whose ionic radius is 1.35 Å (K^+ is 1.33 Å; Hille, 1984), blocks several K^+ channels from both the inside and outside but generally acts from inside with much greater affinity (micromolar as opposed to tens to hundreds of millimolar; Armstrong et al., 1982; Eaton and Brodwick, 1980; Vergara and Latorre, 1983). Internal Ba^{2+} produces a slow block of *Aplysia* S-channels (Shuster & Siegelbaum, 1987). I characterized the internal Ba^{2+} block of *Lymnaea* SA K^+ channels. Channel P_{open} was elevated to maximal levels and maintained with -20 mm Hg throughout the experiment to ensure that the channel remained in the open configuration. 50 mM extracellular Ba^{2+} did not block outward K^+ currents of *Lymnaea* SA K^+ channels (Sigurdson, 1990) but intracellular Ba^{2+} (5 mM) results in a complete block of SA K^+ channels (Fig. 7.6A). The concentration dependence of the intracellular Ba^{2+} block of SA K^+ channels (Fig. 7.6B) yields an IC_{50} of 0.14 ± 0.08 mM. The kinetics of Ba^{2+} block were analysed in 3 patches held at 40 mV. 10 s records were made into events lists with Fetchan and then used to construct dwell time histograms which were fit with a double exponential curve to obtain fast and slow open and closed time constants (Control: τ_{open1}= 0.71 ± 0.01, τ_{open2}= 4.7 ± 0.80, $\tau_{closed1}$= 0.72 ± 0.08, $\tau_{closed2}$= 13 ± 5.2; 1 mM internal Ba^{2+}: τ_{open1}= 0.48 ± 0.13, τ_{open2}= 2.8 ± 0.95; $\tau_{closed1}$= 0.49 ± 0.12, $\tau_{closed2}$= 110 ± 23; values are means ± s.e.m.). The slow closed time constant was

Figure. 7.6. Slow Ba^{2+} block of SA K^+ channels. *A*, SA K^+ channel responses to -20 mm Hg applied to an excised inside-out patches in the presence (below) and absence (above) of 5 mM intracellular Ba^{2+}. *B*, Concentration response curve. P_{opcn} was determined from 40 s records of SA K^+ channels in 3 excised patches held at -40 mV (V_m). Each patch was exposed to all 4 concentrations of intracellular Ba^{2+}. Symbols are means with s.e.m.. IC_{50} mean, ●, was obtained by fitting data from each patch. Line is reconstructed using mean parameters a, b, c and d from fits to data using the 4-parameter logistic equation; $y = (a-d)/(1+(x/c)^b)+d$, where a is the asymptotic maximum, b is the slope parameter, c is the inflexion point, d is the asymptotic minimum (fixed to zero), x is the Ba^{2+} concentration and y is the decrease in P_{opcn} as a % of the control response. *C*, SA K^+ channel responses to 2 s voltage steps to 120 mV (V_m) in the presence of 2 mM Ba^{2+}.

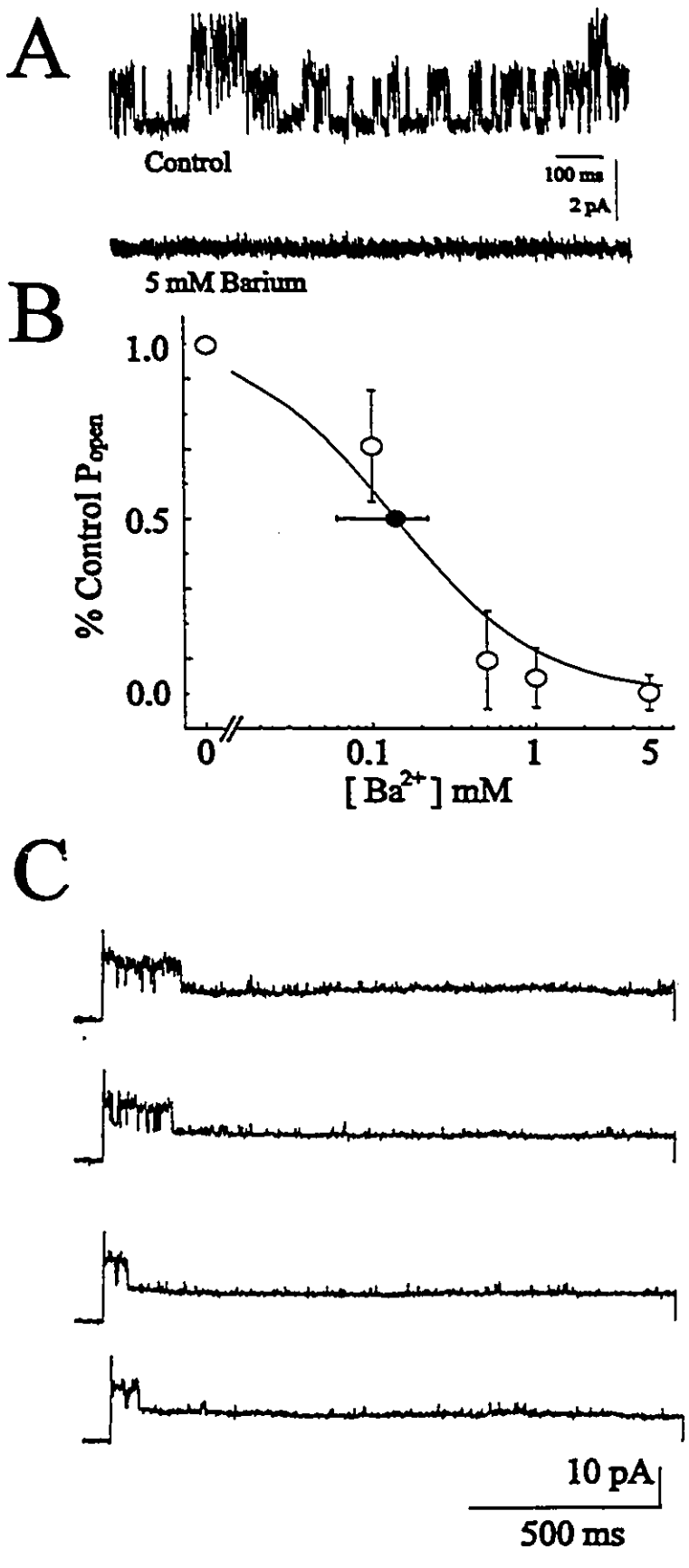
A
Control
100 ms
2 pA
5 mM Barium
B
1.0
0.5
0.0
% Control P open
0
0.1
1
5
[Ba2+] mM
C
10 pA
500 ms

significantly increased more than 800% with 1 mM Ba^{2+}. A question not answered in the study of Ba^{2+} block of *Aplysia* S-channels (Shuster & Siegelbaum, 1987), was whether Ba^{2+} could block a closed channel or whether the channel had to be in the open conformation to be blocked. When excised patches were stepped from 0 mV to strong depolarizing potentials [120 mV (V_m)] under conditions in which SA K^+ channel P_{open} was near maximal (SA K^+ channels do not inactivate) and the intracellular Ba^{2+} concentration was sufficient to ensure channel block (2 mM), the channel began in the open state but was blocked after a delay (mean ± s.e.m. of 10 steps of one patch = 280 ± 93 ms; four example traces are shown in Fig. 7.6C). This suggests that SA K^+ channels are needed to be open before they can be blocked by internal Ba^{2+}.

On one patch I was able to obtain enough data to test whether the unblocking rate of Ba^{2+} is voltage-dependent. The on rate of a ligand to a site should be dependent on the ligand concentration whereas the off rate should be independent of ligand concentration. Therefore, the voltage dependence of Ba^{2+} interactions with the channel should not be complicated by the concentration dependence of Ba^{2+} block when only off rates are measured. With 2 mM intracellular Ba^{2+}, (likelihood of block greater than 90%), an excised patch was stepped from 70 mV (this depolarized potential favoured the blocked state) to increasingly hyperpolarizing potentials which would unblock the channel and the delay to unblock was measured (Fig. 7.7A). The delay to unblock plotted in Fig. 7.7. C and D illustrates the voltage dependence of the unblock; the decreasing delay to unblock with more hyperpolarizing steps suggesting that Ba^{2+} is electrostatically repelled by increasing electropositivity at the external face.

Figure. 7.7. Voltage-dependence of Ba^{2+} unblock of SA K^+ channels. *A*, SA K^+ channel responses (below) to voltage steps (above) illustrating periods of open block at depolarized potentials (a), hyperpolarizing potentials (b) and unblock at hyperpolarizing potentials (c). Shown is an excised inside-out patch. Scale 10 pA; 20 ms. *B*, Cartoon illustrating configuration of patch and solution compositions as well as the proposed mechanism of Ba^{2+} block corresponding to *A*. *C*, Means and s.e.m. of ten responses to each hyperpolarizing step (hollow bar) are plotted after being summed with the percentage of 10 responses which failed to unblock before the end of the step (solid bar).

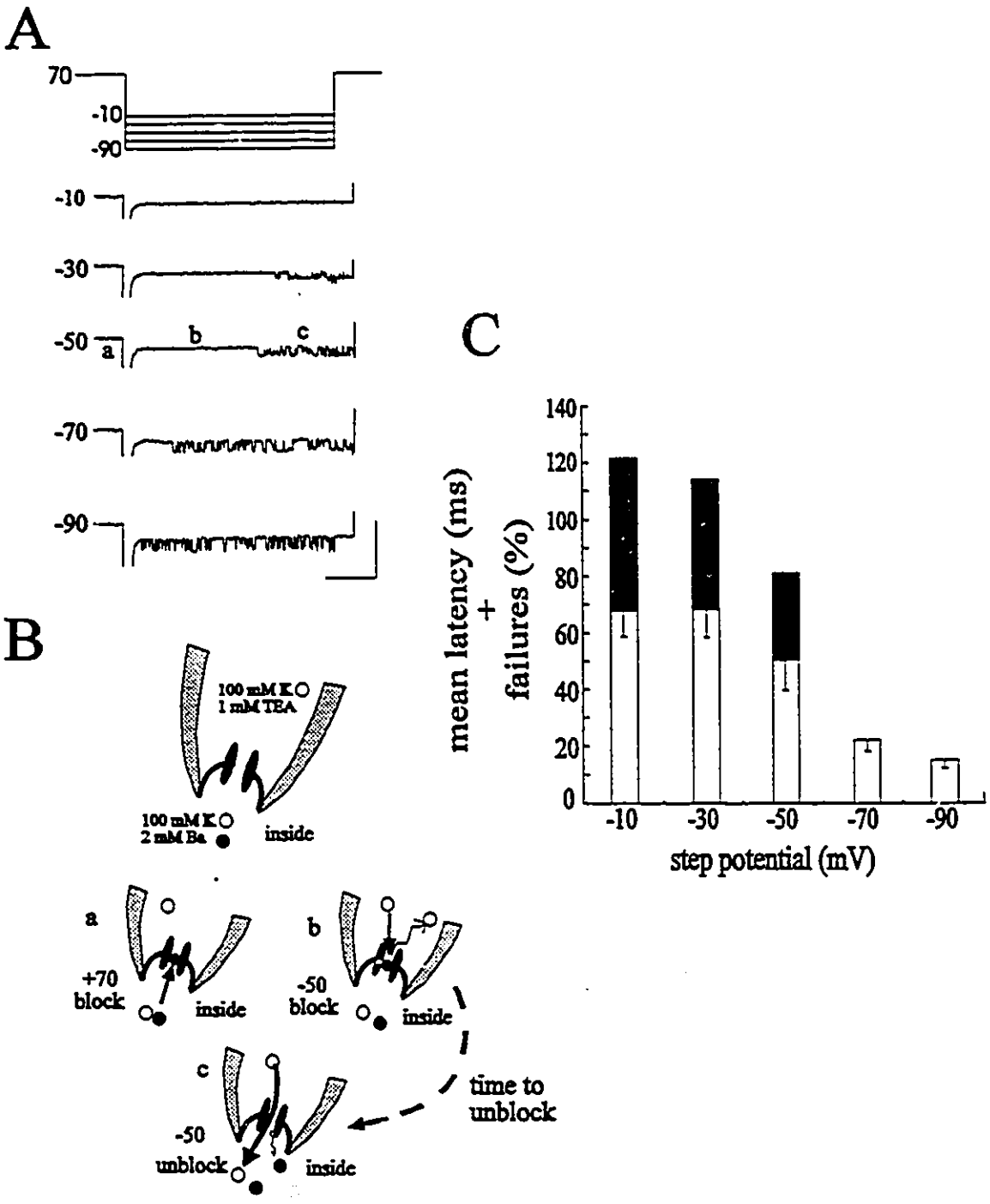
A
70
-10
-90
-10
-30
-50
a
b
c
-70
-90
B
100 mM K
1 mM TEA
100 mM K
2 mM Ba
inside
a
+70
block
inside
b
-50
block
inside
c
-50
unblock
inside
time to
unblock
C
mean latency (ms)
+
failures (%)
140
120
100
80
60
40
20
0
-10
-30
-50
-70
-90
step potential (mV)

4. Discussion

Effect of Symmetrical K^+ Concentration on Single SA K^+ Channel Conduction

SA K^+ channel conductance saturates at high K^+ concentrations similar to that described in other K^+ channels (Coronado et al., 1980; Eisenman et al., 1986) consistent with the idea that there is at least one binding site in the conduction pathway. The affinity of the SA K^+ channel for K^+, based on the Michealis Menton constant (Fig. 7.1.), is much greater (K_m = 35.0 ± 7.8 mM), than the *Shaker* K^+ channel (~300 mM; Heginbotham & MacKinnon, 1993). The affinity of the *Shaker* K^+ channel for K^+ is similar to that of a high conductance Ca^{2+}-activated K^+ channel (Eisenman et al., 1986). Single channel permeability coefficient , P_K (cm/s) was estimated using the "limiting conductance" (I_K/V) for symmetrical [K^+]. Ideally, I_K(V)/V= limiting g = a constant. In practice, even with symmetrical solutions some rectification occurred (Fig. 7.1), so limiting g (110 ± 1.5 pS (n=7)) was taken from the steepest linear region (inward current), yielding P_K = 5.8 x 10^{-13} cm· s^{-1} (50 mM K). The P_K value obtained for *Aplysia* S-channels (1.5 x 10^{-13} cm· s^{-1}) (Shuster et al., 1991) (360 mM K) suggests that its affinity for K^+ is similar to SA K^+ channels in fish embryos (1.3 x 10^{-13} cm· s^{-1}) (Medina and Bregestovski, 1988) (140 mM K), *Shaker* K^+ channels (~4 x 10^{-13} cm· s^{-1}) (140 mM K), *Cepaea* SA K^+ channels (3.4 x 10^{-13} cm· s^{-1}, Bedard and Morris, 1992) (70 mM K) and *Lymnaea* SA K^+ channels. Given the abundance of K^+ ions in the normal physiological environment of S-channels (*Aplysia* is a marine snail ~360 mM cytoplasmic K^+) compared to the dearth of K^+ ions normally bathing *Lymnaea* SA K^+ channels (freshwater snail ~50 mM cytoplasmic K^+), it is not at all surprising that the freshwater form has a somewhat higher K^+ affinity (Vandorpe &

Morris, 1992). The fact that I obtained different affinity constants for inward and outward currents suggests that there are at least two binding sites for K^+ and that SA K^+ channels are multi-ion pores.

Anomalous Mole Fraction Effect With Mixtures of Rb^+ and K^+

The most convincing evidence for a channel possessing a multi-ion pore, short of unidirectional flux studies with radiotracers (Hille and Schwarz, 1978; Hodgkin and Keynes, 1955), is to test the channel for anomalous mole fraction effects. Using Rb^+ as a companion permeant ion species to K^+, I observed the key feature of anomalous mole fraction behaviour, a conductance minimum. Most K^+ channels exhibit this behaviour (for review see Pallotta & Wagoner, 1992). Two cloned K^+ channels, *Shaker* (Heginbotham and MacKinnon, 1993), and a high conductance Ca^{2+}-activated K^+ channel (Neyton and Miller, 1988), have proven to be multi-ion pores and the affinities of the individual binding sites within the pore have been determined for the Ca^{2+}-activated K^+ channel (Neyton and Miller, 1988).

Permeability of SA K^+ Channel

The selectivity sequence determined using reversal potentials under biionic conditions was $Cs^+>K^+>Rb^+>NH_4^+>Na^+>Li^+$ whereas the selectivity sequence determined using relative conductance in symmetrical solutions was $Tl^+=K^+>Rb^+>NH_4^+>Na^+=Li^+=Cs^+$. The apparent high selectivity of the SA K^+ channel for Cs^+ using biionic reversal potentials suggests that there was a fast non-permeant block (Yellen, 1987), of the SA K^+

channel lumen by Cs^+ at an external site. There is a block by Na^+ ions at an internal site of *Cepaea* neuron SA K^+ channels (Bedard and Morris, 1992) which is similar to the one I observed for Cs^+ (reduction in current but no change in reversal potential). The selectivity for Rb^+ by SA K^+ channels determined using reversal potentials (0.63 ± 0.03) is very different from the selectivity determined using relative conductances (0.20 ± 0.01). This is not surprising considering that 0.63 represents the potential energy barriers (relative to K^+) faced by Rb^+ as it permeates the channel whereas 0.20 represents the affinity of the binding sites (relative to K^+) that Rb^+ interacts with as it permeates the channel. Comparable differences are observed in a large conductance Ca^{2+}-activated K^+ channel (BK) (relative biionic permeability of 0.7 ,(Yellen, 1984), and relative conductance permeability of 0.07, (Blatz & Magleby, 1984) . This suggests that the potential energy barriers facing Rb^+ as it permeates K^+ channels is similar (~63% in the case of SA K^+ channels) to K^+ but that there is a binding site within the channel which has a much greater affinity (~80% in the case of SA K^+ channels) for Rb^+ than K^+. Given that bi-ionic selectivity, but not conductance is similar in BK^+ and *Shaker* channels, these characteristics - energy barriers and binding sites - are thought to be discrete channel features, with corresponding structures associated with each (Heginbotham & MacKinnon, 1993).

Effect of pH Extremes on SA K^+ Channel

The effects of pH on ion channels are not trivial especially in light of a recently cloned K^+-selective channel which is activated by protons (Suzuki et al., 1994). It has a unique structure and is voltage-independent and the pH range over which activation

occurs is 6.8 to 7.6. Acid pH depresses the Na^+ conductance of nerve (Woodhull, 1973) and the outer segment of isolated retinal rods of frog, (Mueller and Pugh, 1983). Extracellular protons decrease L-type Ca^{2+} channel conductance (Prod'hom et al., 1989; Pietrobon et al., 1989). Nevertheless, the conductance of two different mechanosensitive channels, a SA K^+ channel found in rat heart, (Kim, 1992), and a SA Cat channel in chick skeletal muscle, (Guharay and Sachs, 1985), is unaffected by pH even though, in both cases, there is evidence of specific pH effects on channel kinetics. It is clear that *Lymnaea* SA K^+ channel conductance too, is quite insensitive to extreme extracellular pH variations.

Mg^{2+} Block of SA K^+ Channel

For inwardly rectifying K^+ channels, Mg^{2+} blocks from the inside (Rudy, 1988). The Mg^{2+} block of SA K^+ channels was from the outside. Extracellular Mg^{2+} has also been reported to block a SA K^+-selective channel (Hisada et al., 1991) in amphibian gastric smooth muscle. 2 mM extracellular Mg^{2+} decreased the conductance of SA K^+ channels from 110 pS to 62.5 pS (~43 % decrease), which is nearly identical to the decrease in SA K^+ channel conductance with 2 mM extracellular Mg^{2+} that I obtained. Although this is a feature unlike most other K^+-selective channels, the fact that these two SA K^+-selective channels exhibit this characteristic may prove useful in differentiating SA K^+ channels from other K^+ channels. It is also worth noting that cyclic nucleotide-gated channels which are cation selective are blocked by extracellular Mg^{2+} and that the cyclic nucleotide-gated channel's cation selectivity can be transferred to K^+-selective *Shaker* channels with the

elimination of two amino acids from the pore region (Heginbotham et al., 1992).

Ba^{2+} Block of SA K^+ Channel

Several K^+ channels are blocked from both sides of the membrane by Ba^{2+} but with much greater affinity from the inside (Rudy, 1988). SA K^+ channels in *Aplysia* mechanosensory neurons (Shuster & Siegelbaum, 1987) and *Lymnaea* neurons (Vandorpe & Morris, 1992) are blocked by Ba^{2+} from the inside, similar to the delayed rectifier K^+ channel in squid axons (Armstrong et al., 1982). Although each of these three K^+ channels have very different affinities for internal Ba^{2+}, [K_ds for internal Ba^{2+} block in *Aplysia* (Shuster & Siegelbaum, 1987), squid (Armstrong et al., 1982) and *Lymnaea* are 20 μM, 0.1 μM, 140 ± 80 μM, respectively], the block for squid and *Lymnaea* by internal Ba^{2+} is voltage dependent. It is not known whether the block of *Aplysia* S-channels by internal Ba^{2+} is voltage dependent. Other SA K^+ channels exhibit an internal Ba^{2+} sensitivity. Mechanosensititive K^+ channels similar to *Aplysia* S-channels which are responsible for I_M (named for the fact that muscarinic receptors decrease a persistent K^+ current responsible for modulating membrane excitability; for review see Rudy, 1988) in bullfrog sympathetic neurons, are completely blocked by 4-8 mM internal Ba^{2+} (Hara & Kuba, 1993). SA K^+ channels in rat atrial myocytes are completely blocked by 1 mM internal Ba^{2+} (Kim, 1992) and SA K^+ channels in *Drosophila* body wall muscle are completely blocked by 100 μM internal Ba^{2+} (Gorczyca & Wu, 1988).

The internal Ba^{2+} block of K^+ channels is usually characterized by the following: slow channel block (i.e. decreased P_{open} with no change in single channel conductance),

voltage-dependence (i.e. increased blocking efficacy at depolarized potentials), effective at concentrations in the high micromolar range and only able to access the channel when it is in the open state (Armstrong & Taylor, 1980; Rudy, 1988). My results here are consistent with this picture: internal Ba^{2+} blocked open SA K^+ channels, it decreased the long closed time (i.e. slow channel block), and the rate of unblock was voltage dependent. The fact that all SA K^+ channels are blocked by intracellular Ba^{2+}, a characteristic shared by several other non-mechanosensitive K^+ selective channels suggests that SA K^+ channels belong to some larger family of K^+ channels.

In summary, SA K^+ channels are multi-ion pores with high affinity for K^+ and highly selective for K^+ over other monovalent ions suggesting that SA K^+ channels are very much "K-selective" channels. They exhibit a sensitivity to intracellular Ba^{2+}, extracellular Mg^{2+} and an insensitivity to extreme fluctuations in extracellular pH.

CHAPTER VIII General discussion and conclusions

i) S-Channel is a SA K^+ channel

The S-channel of *Aplysia* mechanosensory neurons which modulates cellular excitability by regulating resting K^+ selective conductances is a stretch-activated K^+ channel (Vandorpe and Morris, 1992; Vandorpe et al., 1994). The kinetic analysis I did on multi-channel patches helped confirm this view; I tested whether channels in a given patch activated by FMRF-amide and then by stretch were "identical". The fact that molluscan SA K^+ channels are present throughout the nervous system, as well as in other cell types suggests that these channels are not specialized mechanotransducers (such specialization would not be ubiquitous). Consistent with this hypothesis, macroscopic mechanosensitive K^+ currents are either absent or several orders of magnitude smaller than anticipated based on single channel measurements (Morris and Horn, 1991). What do SA K^+ channels in molluscan neurons do if they are not special mechanotransducers?

ii) Are all molluscan SA K^+ channels S-like?

SA K^+ channels might be activated by neurotransmitters via second messengers resulting in changes in the channel's state of phosphorylation. Stretch-activation of SA K channels might be through a manipulation of cytoskeletal elements which normally interact with and regulate kinases and phosphatases which are also modulated by second messengers. This prediction is consistent with observations presented in Chapter IV. Patch-clamp studies of an *Aplysia* voltage-gated channel in neurons have demonstrated

that a tyrosine phosphatase endogenous to excised patches determines both the gating mode and the response of the channel to protein kinase A (Wilson and Kaczmarek, 1994). Morecver, there is considerable cross-talk between phosphatases, kinases and cytoskeletal elements, (Luna and Hitt, 1992), with an end result of complex regulation of channels whose behaviour is modulated in this way. There is even some recent evidence, (Bockholt, and Burridge, 1993) suggesting that some tyrosine kinases/phosphatases are mechanosensitive enzymes and that they too are modulated by neurotransmitters [e.g. Bombesin regulation of tyrosine kinase (Sinnett-Smith et al., 1993)]. The possibility that SA K channels are modulated by a mechanosensitive tyrosine kinase or phosphatase should be investigated.

The reasonable hypothesis that molluscan SA K^+ channels are, in a broad sense, S-like (in that they are modulated by neurotransmitters via second messengers) has not been adequately tested, therefore the role of SA K^+ channels remains unclear.

This unanswered question along with the interest in the basis of mechanosensitivity (physiologically or not) has motivated efforts to clone SA channels. Further characterization of these channels, both biophysical and pharmacological, would facilitate these efforts.

iii) Attempts to Clone SA Channels

The only MS channel cloned to date, appears to be a totally unique type of channel (Sukharev, et al., 1994). It is a non-selective SA channel from *E. coli* with no sequence similarities shared by any other eukaryotic channel, mechanosensitive or otherwise. Not

only is this channel's sequence unusual but it has a single channel conductance (~600 pS). Furthermore, SA Cat channels have pore properties which would suggest that they are rather discriminating with regard to permeation and selectivity. *Xenopus* oocyte SA Cat channel pore diameter is estimated at ~4 Å (Yang and Sachs, 1990), which is much smaller than most ligand gated channels. This small size is closer to most K-selective channels and some small cationic channels like CNG channels which are close relatives to K channels (Heginbotham and MacKinnon, 1993). This is consistent with the idea that SA Cat channels are "related" to SA K channels. This was, in part, the motivation for trying to clone SA Cat channels in *Xenopus* oocytes using K-channel like clones as probes. Evidently, the nucleic acid sequence for SA Cat channels is not similar enough to the K-channel probes we used to yield successful cross-hybridization.

iv) Dynamic Behaviour of SA Channels

SA Cat channels in *Xenopus* oocytes display intriguing dynamic properties which are fragile and dependent on patch integrity (Hamill and McBride, 1992). SA Cat channels respond to square suction steps with rapid onset and almost as quickly, adapt to the stimuli. In spite of the fact that this phenomenon only occurs at hyperpolarizing potentials Hamill and McBride, (1992), suggested that this adaptation might explain both physiological adaptation in mechanotransducers and the failure to elicit macroscopic SA K^+ currents.

SA K^+ channels in molluscan neurons, however, differ vastly in their dynamic behaviour from SA Cat channels in frog eggs. SA K channels respond with a marked

delay (seconds) to rapidly applied suction steps with indifference to membrane potential. A delay would not account for adaptation of physiological mechanotransducers and it is unlikely to account for any difficulties in obtaining large macroscopic SA K^+ currents in molluscan neurons. The only similarity to SA Cat dynamics is the fragile nature of the responses; both are lost with mechanical disruption or repeated stimuli. Cells left longer in culture are more resistant to mechanical disruption of this behaviour. Disruption of membrane cytoskeleton with cytochalasins increases SA K channel stretch-sensitivity and significantly decreases time to onset of a response to suction. This observation is consistent with the idea that SA K channels normally do not feel membrane tension. Instead they seem to be protected from small changes in membrane tension through some connection to the membrane cytoskeleton.

v) SA K Channel Mechanosensitivity and the Cytoskeleton

Several channels and membrane transporters have "relationships" with membrane cytoskeletal proteins as judged by their physical associations with these components. Red blood cell anion exchangers, (Bennett and Stenbuck, 1980), and voltage-gated sodium channels, (Srinivasan et al., 1988), are found associated with the cytoskeletal protein ankyrin. This protein is believed responsible for anchoring these channels to the membrane in places where they are required at high densities. It is essential for saltatory conduction and action potential propagation along an axon that many Na^+ channels remain at the nodes of Ranvier and not under the myelin sheath along internodal spaces. In spite of the physical association of cytoskeletal proteins with these membrane transporters and

channels, there does not seem to be a functional relationship other than to anchor the proteins in place unless we stop to consider the case of the red blood cell anion exchanger. It continues to function normally in the face of what must be tremendous forces tugging and pulling on them as a red blood cell is squashed while passing through tiny capillaries. In addition to anchoring these membrane proteins in place, they presumably dissipate mechanical energy, thereby protecting the exchangers from disruptive membrane-skeleton tension. This may be the case for SA K channels, except they must not be as well protected as red blood cell anion exchanger. Perhaps for true mechanosensitive channels, the cytoskeletal linkages are such that mechanical energy is transferred with great efficiency rather than dissipated. Under special circumstances where the membrane is jeopardized by disruptive mechanical forces, SA channel mechanosensitivity may be adaptive and actually useful or alternatively, detrimental, resulting in further damage. Ectopic discharges from demyelinated rat spinal roots are thought to be due to depolarization via a persistent inward leak of cations through a stretch-activated ion channel, (Baker and Bostock, 1992). Mechanosensitivity has been observed in other demyelinated lesions associated with spontaneous ectopic activity (Smith and McDonald, 1980; Calvin et al., 1982), as well as multiple sclerosis (Nordin et al., 1984). The mechanosensitivity of demyelinated axons may be due to easy activation of stretch-activated channels and spontaneous activity may be due to depolarization by these channels, activated by mechanical stresses from within the root or fibre due to non-uniform loss of myelin.

In spite of knowing that actin decoupling renders SA K channels more

mechanosensitive, the nature of SA K channel interaction with the cytoskeleton is unknown. An understanding of this channel/cytoskeleton interaction could establish whether SA K channel mechanosensitivity is adventitious, detrimental or an asset to cells which express SA K channels. "Gentle seals" permit assays of the integrity of a cell's membrane cytoskeleton and allow for measurements of naive SA K channel behaviour (not previously exposed to mechanical stimuli). Therefore, "gentle seals" provide an opportunity to ask how SA K channels interact with membrane cytoskeletal proteins.

vi) Pharmacology

The pharmacology of *Lymnaea* neuron SA K channels is unique. Even SA K channels in neurons of another species of mollusc, *Aplysia californica*, have a different pharmacological profile. Intracellular TEA blocks *Aplysia* SA K channels and does not affect *Lymnaea* SA K channels. Even extracellular TEA has a slightly different blocking efficacy in the two molluscs. There are pharmacological characteristics which SA K channels share with other channels which warrant more than passing curiosity. *Lymnaea* neuron SA K channels, SA Cat channels in *Xenopus* oocytes, and mechanosensitive currents in hair cells are all blocked by amiloride whereas there is no report yet of a K-selective channel which is blocked by amiloride. On the other hand, SA K channels are not blocked by Gd^{3+} an agent which blocks many SA Cat channels. Also, SA K channels are blocked by K-selective channel blockers TEA and quinidine. This suggests to me that SA K channels may be close relatives to other K-selective channels and not some totally unique type of channel unlike most voltage-gated channels.

vii) Pore Properties of SA K^+ Channels

Lymnaea neuron SA K^+ channels are multi-ion pores with a high affinity for K^+ (28 mM for inward and 92 mM for outward currents), and are highly selective for K^+ over other monovalent ions suggesting that these SA channels are very much "K-selective" channels. High micromolar concentrations of intracellular barium block SA K^+ channels in both *Lymnaea* and *Aplysia*, (Shuster and Seigelbaum, 1987), neurons; this is similar to the block of calcium-activated K^+ channels, (Neyton and Miller, 1988). Extreme pH variations have no apparent effect on SA K^+ channel conductance; this is similar to other SA K^+, (Kim, 1992), and Cat, (Guharay and Sachs, 1985), channels. By contrast, acid pH decreases Na channel conductance in isolated retinal rods of frog, (Mueller and Pugh, 1985).

Given that *Lymnaea* SA K^+ channels are K-selective, not strongly activated by voltage, insensitive to calcium, and are persistently active but with a low probability of being open, these channels are likely involved in establishing a variable resting K conductance, analagous with the S-channel, a SA K^+ channel that modulates cellular excitability.

Until a clone is obtained, knowledge of SA K^+ channels' role in modulating cellular excitability and of the mechanism underlying SA K^+ channel mechanosensitivity, will be limited so I have characterized *Lymnaea* neurons SA K^+ channels to facilitate cloning SA K^+ channels. The following is the current picture of *Lymnaea* neuron SA K^+ channels:

Table 8.1 **Current Picture of *Lymnaea* Neuron SA K^+Channels**

Gating

-- Relatively insensitive to voltage-- increase P_{open} e fold/70 mV. (Small and Morris, 1994a)

-- Insensitive to intracellular calcium. (Sigurdson and Morris, 1989)

-- Stretch activated (sensitivity varies with "state" of membrane cytoskeleton). (Small and Morris, 1994a)

Dynamic Properties

-- Delayed response to rapid onset stimuli (Small and Morris, 1994a)

-- Delay decreases with suction steps of increasing magnitude (Small and Morris, 1994a)

-- Delay is lost with repeated stimuli or non-gentle seal formation (Small and Morris, 1994a)

-- Cells left longer in culture respond with longer delays (Small and Morris, 1994a)

-- Cytochalasin D increases the sensitivity of SA K channels and decreases the delay (Small and Morris, 1994a)

Pharmacology

-- Blocked by amiloride (IC_{50} ~2 mM), quinidine (IC_{50} ~0.8 mM), and TEA (IC_{50} ~50 mM) applied to the outside but not blocked when these agents are applied to the inside at concentrations as high as 10 mM, 10 mM and 200 mM, respectively (Small and Morris, 1994b).

-- Not blocked by extracellular diltiazem (10 mM) or gadolinium (10 mM) and unaffected by ethanol (3%) (Small and Morris, 1994b).

-- Ethanol (3%) decreases the efficacy of extracellular quinidine block (Small and Morris, 1994b).

Pore Properties

-- Channel pore exhibits affinity for inward and outward K^+ currents of ~30 mM and ~90 mM, respectively.

-- Channel exhibits an anomalous mole fraction effect with mixtures of Rb^+ and K^+, indicative of a multi-ion pore.

-- Selectivity based on reversal potentials under biionic conditions is $Cs^+ > K^+ > Rb^+ > NH_4^+ > Na^+ > Li^+$.

-- Selectivity based on relative conductances in symmetrical solutions is $Tl^+ = K^+ > Rb^+ > NH_4^+ >> Na^+ = Li^+ = Cs^+$.

-- Extreme variations in external pH had no effect on single SA K^+ channel conductance.

-- External Mg^{2+} (2 mM) blocked inward K^+ currents.

-- Internal Ba^{2+} (IC_{50} ~0.14 mM) produces a long block of open SA K^+ channels which is stronger at more depolarized potentials.

References

Armstrong, C.M., & Bezanilla, F. (1977) Inactivation of the sodium channel. II Gating current experiments. *J. Gen. Physiol.* 70:567-590.

Armstrong, C.M., Swenson, R.P., & Taylor, S.R. (1982). Block of squid axon K channels by internally and externally applied barium ions. *J. Gen. Physiol.* 80:663-682.

Armstrong, C. M. & Taylor, S. R. (1980). Interaction of barium ions with potassium channels in squid giant axons. *Biophys. J.* 30, 473-488.

Armstrong, D.L.,, Rossier, M.F., Shcherbatko, A.D., & White, R.E. (1991) Enzymatic gating of voltage-activated calcium channels. *Ann. NY Acad. Sci.* 635:26-34.

Assad, J.A., Shepherd, G.M.G., & Corey, D.P. (1991) Tip-link integrity and mechanical transduction in vertebrate hair cells. *Neuron* 7:985-994.

Baker, M. & Bostock, H. (1992). Ectopic activity in demylinated spinal root axons of the rat. *J. Physiol.* 451:539-552.

Baud, C., Kado, R.T., & Marcher, K. (1982) Sodium channels induced by depolarization of the *Xenopus laevis* oocyte. *Proc Natl. Acad. Sci. U.S.A.* 79:3188-3192.

Baxter, D.A. & Byrne, J.H. (1990) Differential effects of cAMP and serotonin on membrane current, action potential duration, and excitability in somata of pleural sensory neurons of *Aplysia. J. Neurophysiol.* 64:978-990.

Bear, C.E. (1990) A nonselective cation channel in rat liver cells is activated by membrane stretch. *Am. J. Physiol.* 258C:421-428.

Bedard, E., & Morris, C.E. (1992) Channels activated by stretch in neurons of the helix snail. *Can. J. Physiol. Pharmacol.* 70:207-213.

Belardetti, F., Campbell, W.B., Falck, J.R., Demontis, G., & Rosolowsky, M. (1989) Products of heme-catalyzed transformation of the arachidonic derivative 12-HPETE open S-type K^+ channels in *Apysia. Neuron* 3:497-505.

Belardetti, F., Kandel, E.R., & Siegelbaum, S.A. (1987) Neuronal inhibition by the peptide FMRF-amide involves opening of S K channels. *Nature* 325:153-156.

Belardetti, F., Schacher, S., Kandel, E.R., & Siegelbaum, S.A. (1986) The growth cone of *Aplysia* sensory neurons: Modulation by serotonin of action potential duration and

single potassium channel currents. *Proc. Natl. Acad. Sci. USA* 83:7094-7098.

Bennett, V., & Stenbuck, P.J. (1980). Association between ankyrin and cytoplasmic domain of band 3 isolated from the human erythrocyte membrane. *J. Biol. Chem.* 255:6426-6432.

Blatz, A. & Magleby, K. (1984). Ion conductance and selectivity of sing'e calcium-activated potassium channels in cultured rat muscle. *J. Gen. Physiol.* 84, 1-23.

Bockholt, S.M. & Burridge, K. (1993). Cell spreading on extracellular matrix proteins induces tyrosine phosphorylation of tensin. *J. Biol. Chem.* 268:14565-14567.

Bokvist, K., Rorsman, P., Smith, P.A. (1990) Block of ATP-regulated and Ca^{2+}-activated K^+ channels in mouse pancreatic beta-cells by external tetraethylammonium and quinidine. *J. Physiol.*, 423:327-342.

Brezden, B.L., Benjamin, P.R., & Gardner, D.R. (1991) The peptide FMRF-amide activates a divalent cation-conducting channel in heart muscle cells of the snail *Lymnaea stagnalis*. *J. Physiol.* 443:727-738.

Brezden, B.L., & Gardner, D.R. (1983) The effect of the molluscicide frescon on smooth and cross-striated muscles of *Lymnaea stagnalis* and *Helix aspersa*. *Pestic. Biochem. Physiol.* 20:259-268.

Brezden, B.L., Gardner, D.R., and Morris, C.E. (1986) A potassium-selective channel in isolated *Lymnaea stagnalis* heart muscle cells. *J. Exp. Biol.* 123:175-189.

Brown, H.M., Ottoson, D., & Rydqvist, B. (1978) Crayfish stretch receptor: an investigation with voltage-clamp and ion selective electrodes. *J. Physiol.* 284:155-179.

Buckett, K.J., Dockray, G.J., Osborne, N.N., & Benjamin, P.R. (1990) Pharmacology of the myogenic heart of the pond snail *Lymnaea stagnalis*. *J. Neurophysiol.* 63:1413-1425.

Budavari, S. (1989) The Merck Index 11th Ed. pp. 3182. Rahway, N.J. U.S.A.: Merck & Co. Inc.

Buttner, N, Siegelbaum, S.A., & Volterra, A. (1989) Direct modulation of *Aplysia* S-K^+ channels by a 12-lipoxygenase metabolite of arachidonic acid. *Nature* 342:553-555.

Calvin, W.H., Devor, M., & Howe, J.F. (1982). Can neuralgias arise from minor demylination? Spontaneous firing, mechanosensitivity and after discharges from conducting axons. *Exp. Neurol.* 75:755-763.

Canessa, C.M., Schild, L., Buell, G., Thorens, B., Gautschi, I., Horisberger, J. D., & Rossier, B.C. (1994) Amiloride-sensitive epithelial Na^+ channel is made of three homologous subunits. *Nature* **367**:463-467.

Carl, A., Kenyon, J.L., Uemura, D., Fusetani, N., & Sanders, K.M. (1991) Regulation of Ca^{2+}-activated K^+ channels by protein kinase A and phophatase inhibitors. *Am. J. Physiol.* **261C**:387-392.

Chen, T.Y., Peng, Y.W., Dhallan, R.S., Ahamed, B., Reed, R.R., & Yau, K.W. (1993) A new subunit of the cyclic nucleotide-gated cation channel in retinal rods. *Nature*, **362**:764-767.

Choi, K.L., Aldrich, R.W., & Yellen, G. (1991) Tetraethylammonium blockade distinguishes two inactivation mechanisms in voltage-activated K^+ channels. *Proc. Natl. Acad. Sci. USA* **88**:5092-5095.

Chung, S., Reinhart, P.H., Martin, B.L., Brautigan, D., & Levitan, I.B. (1991) Protein kinase activity closely associated with a reconstituted calcium-activated potassium channel. *Science* **253**:560-562.

Colquhoun, D. & Sigworth. F.J. (1983) Fitting and statistical analysis of single channel records. *In* Single Channel Recording, Ed.s B. Sakmann and E. Neher, p. 217. Plenum Press. New York.

Coronado, R., Rosenberg, R. L. & Miller, C. (1980). Ionic selectivity, saturation and block in a K^+-selective channel from sarcoplasmic reticulum. *J. Gen. Physiol.* **76**, 425-453.

Dabrowski, A.R., McDonald, D., & Rosler, U. (1990) Renewal theory properties of ion channels. *Ann. Statistics* **18**:1091-1202.

Dabrowski, A.R. & McDonald, D. (1992) Statistical analysis of multiple ion channel data. *Ann. Statistics* **20**:1180-1202.

Davis, M.J., Donovitz, J.A., & Hood, J.D. (1992) Stretch-activated single-channel and whole cell currents in vascular smooth muscle. *Am. J. Physiol.* **262C**:1083-1088.

Dilger, J.P., Liu, Y., Roper, J.F., & Bradley, R.J. (1994) Effects of ethanol on ACh receptor channels. *Biophys. J.*, **66**:A9.

Doroshenko, P., & Neher, E. (1992). Volume sensitive chloride conductance in bovine chromaffin cell membrane. *J. Physiol.* **499**:197-218.

Dubois, J.M. (1981) Evidence for the existence of three types of potassium channels in the

frog Ranvier node membrane. *J. Physiol.*, **318**:297-316.

Eaton, D.C. & Brodwick, M.S. (1980). Effect of barium on the potassium conductance of squid axon. *J. Gen. Physiol.* 75:727-750.

Edwards, C., Ottoson, D., Rydqvist, B., & Swerup, C. (1981) The permeability of the transducer membrane of the crayfish stretch receptor to calcium and other divalent cations. *Neurosci.* **6**:1455-1460.

Eisenmann, G., Latorre, R. & Miller, C. (1986). Multi-ion conduction in high-conductance Ca^{2+}-activated K^+ channel from skeletal muscle. *Biophys. J.* 50, 1025-1034.

Endo, S., Ichinose, M., Critz, S.D., Eskin, A., Byrne, J.H., & Shenolikar, S. (1991) Protein phosphatases and their role in control of membrane currents in *Aplysia* neurons. *Adv. Prot. Phosph.* **6**:411-432.

Erxleben, C. (1989) Stretch-activated current through single ion channels in the abdominal stretch receptor organ of the crayfish. *J. Gen. Physiol.* **94**:1071-1083.

Evans, P.D., Swales, L.S., & Whim, M.D. (1988) Second messenger systems in insects: and introduction. *In* Neurotox'88: Molecular Basis of Drug & Pesticide Action. pp. 225-234. Eds. G.G. Lunt. Exerpta Medica, Amsterdam.

Finn, A.R., Gaido, M.L., Dillard, M., & Brautigan, D.L. (1992) Regulation of an epithelial chloride channel by direct phosphorylation and dephosphorylation. *Am. J. Physiol.* **263C**:172-175.

Flock, A., Flock, B., & Murray, E. (1977) Studies on the sensory hairs of receptor cells in the inner ear. *Acta Otolaryngol.* **83**:85-91.

French, A. (1992). Mechanotransduction. *Ann. Rev. Physiol.* 54:135-152.

Franco, A. & Lansman, J.B. (1990). Calcium entry through stretch-inactivated ion channels in *mdx* myotubes. *Nature* **344**:670-673.

Frost, D. (1989) Dissociated cell culture. *In* The Zebrafish Book. pp. 5.1-5.2 Ed. M. Westerfield, University of Oregon Press, Oregon.

Gardner, D.R., & Brezden, B.L. (1990) Ion channels in *Lymnaea stagnalis* heart ventricle cells. *Comp. Biochem. Physiol.* **96A**:79-85.

Goldin, A.L. (1992) Maintenance of *Xenopus laevis* and oocyte injection. *Meth. Enzymol.* **107**:266-278.

Goldman, D. E. (1943). Potential, impedance, and rectification in membranes. *J. Gen. Physiol.* 27, 37-60.

Goldstein, D.B. (1986) Effect of alcohol on cellular membranes. *Ann. Emerg. Med.*, 15:1013-1018.

Gorczyca, M.G., & Wu. C-F. (1991) Single-channel K^+ currents in *Drosophila* muscle and their pharmacological block. *J. Memb. Biol.* 121:685-701.

Guharay, F., & Sachs, F. (1984) Stretch-activated single ion channel currents in tissue-cultured embryonic chick skeletal muscle. *J. Physiol.* 352:685-701.

Guharay, F., & Sachs, F. (1985) Mechanotransducer ion channels in chick skeletal muscle: the effects of extracellular pH. *J. Physiol.* 363:119-134.

Gustin, M.C. (1992) Mechanosensitive ion channels in yeast. Mechanisms of activation and adaptation. *In* Advances in comparative and Envrionmental Physiology, Vol.10. Spriger-Verlag. Berlin.

Gustin, M.C., Martinac, B., Siami, Y., Culbertson, M.R., & Kung, C. (1986) Ion channels in yeast. *Science* 233:1195-1197.

Gustin, M.C., Sachs, F., Sigurdson, W.J., Ruknudin, A., Bowman, C. Morris, C.E., & Horn, R. (1991) Technical comments. Single-channel mechanosensitive currents. *Science* 253:800-802.

Gustin, M.C., Zhou, X.L., Martinac, B., & Kung, C. (1988) A mechanosensitive ion channel in the yeast plasma membrane. *Science* 242:762-766.

Hamill, O.P., Lane, J.W., & McBride, D.W.Jr. (1992) Amiloride: a molecular probe for mechanosensitive channels. *Trends Pharmacol. Sci.*, 13: 373-376.

Hamill, O.P., Marty, A., Neher, E., Sakmann, B., and Sigworth, F.J. (1981) Improved patch-clamp techniques for high-resolution current recording from cells and cell-free membrane patches. *Pfluegers Arch.* 391:85-100.

Hamill, O.P. and McBride, D.W. (1992) Rapid adaptation of single mechanosensitive channels in *Xenopus* oocytes. *Proc. Natl. Acad. Sci. U.S.A.* 89:7462-7466.

Hara, S. & Kuba, K. (1993). Mechanical modulation of a voltage-dependent non-inactivating K^+ current in cultured bullfrog sympathetic neurons. *Pflügers Arch.* 422, 305-315.

Hartmann, H.A., Kirsch, G.E., Drewe, J.A., Taglialatela, M., Joho, R.H., & Brown, A.M.

(1991) Exchange of conduction pathways between two related K^+ channels. *Science* **251**:942-944.

Heginbotham, L., Abramson, T. & MacKinnon, R. (1992) A functional connection between the pores of distantly related ion channels as revealed by mutant K^+ channels. *Science*, **258**:1152-1154.

Heginbotham, L. & MacKinnon, R. (1993). Conduction properties of the cloned *Shaker* K^+ channel. *Biophys. J.* **65**, 2089-2096

Hille, B. (1984). Ionic Channels of Excitable Membranes. Sinauer Associates Inc. Sunderland, Mass. pp. 263.

Hille, B. & Schwarz, W. (1978). Potassium chanels as multi-ion single-file pores. *J. Gen. Physiol.* 72, 409-442.

Hodgkin, A. L. & Katz, B. (1949). The effect of Na ions on the electrical activity of the giant axon of the squid. *J. Physiol.* **108**, 37-77.

Hodgkin, A. L. & Keynes, R. D. (1955). The potassium permeability of a giant nerve fibre. *J. Physiol.* **128**, 61-88.

Hong, K. & Driscoll, M. (1994) A transmembrane domain of the putative channel subunit MEC-4 influences mechanotransduction and neurodegeneration in *C. elegans. Nature* **367**:470-473.

Howard, J., Roberts, W.M., & Hudspeth, A.J. (1988) Mechanoelectrical transduction by hair cells. *Ann. Rev. Biophys. Biophys. Chem.* **17**:99-124.

Huang, M. & Chalfie, M. (1994) Gene interactions affecting mechanosensory transduction in *Caenorhabditis elegans. Nature* **367**:467-470.

Hudson, R.L., & Schultz, S.G. (1988) Sodium-coupled glycine uptake by Ehrlich ascites tumor cells results in an increase in cell volume and plasma membrane channel activities. *Proc. Natl. Acad. Sci. USA* **85**:279-283.

Hudspeth, A.J. (1989) How the ear's works work. *Nature* **341**:397-404.

Hudspeth, A.J., & Jacobs, R.A. (1979) Stereocilia mediate transduction in vertebrate hair cells. *Proc. Natl. Acad. Sci. USA* **76**:1506-1509.

Ichinose, M., & Byrne, J.H. (1991) Role of protein phosphatases in the modulation of neuronal membrane currents. *Brain Res.* **549**:146-150.

Iverson, L.E., & Rudy, B. (1990) The role of divergent amino acid and carboxyl domains on the inactivation properties of potassium channels derived from the *Shaker* gene of *Drosophila*. *J. Neurosci.* **10**:2903-2916.

Jacobs, R.A., & Hudspeth, A.J. (1990) Ultrastructure correlates of mechanoelectric transduction in hair cells of the bullfrog's inner ear. *Cold Spring Harbor Symp. Quant. Biol.* **55**:547-561.

Jennings, H.S. (1906) Behavior of the Lower Organisms, *Columbia University Press*, New York.

Jones, H.D., (1983) The circulatory systems of gastropods and bivalves. *In* The Mollusca 5, pp. 189-238. Eds. A.S.M Saeuddin & K.M. Wilbur. Academic Press, New York.

Jorgensen, F. & Ohmori, H. (1988) Amiloride blocks the mechano-electrical transduction channel of hair cells of the chick. *J. Physiol.*, **403**:577-578.

Kaang, B.K., Pfaffinger, P.J., Grant, S.G., Kandel, E.R., & Furukawa, Y. (1992). Over expression of an *Aplysia shaker* K^+ channel gene modifies the electrical properties and synaptic efficacy of identified *Aplysia* neurons. *Proc. Natl. Acad. Sci.* **89**:1133-1137.

Kandel, E.R., & Hawkins, R.D. (1992) The biological basis of learning and individuality. *Sci. Am.* **267**:79-86.

Kim, D. (1992). A mechanosensitive K^+ channel in heart cells. Activation by arachidonic acid. *J. Gen. Physiol.* **100**, 1021-1040.

Kim, D., & Duff, R.A. (1990) Regulation of K^+ channels in cardiac myocytes by free fatty acids. *Circ. Res.* **67**:1040-1046.

Kirber, M.T., Ordway, R.W., Clapp, L.H., Walsh, J.V., & Singer, J.J. (1990) Both membrane stretch and fatty acids directly activate large conductance, Ca^{2+}-activated K^+ channels in vascular smooth muscle cells. *FEBS Lett.* **297**:24-28.

Kirber, M.T., Walsh, J.V.Jr., & Singer, J.J. (1988) Stretch-activated ion channels in smooth muscle: a mechanism for the initiation of stretch-induced contraction. *Pflugers Arch.*, **412**:339-345.

Kubo, M. & Okada, Y. (1992) Volume-regulated Cl^- channel currents in cultured human epithelial cells. *J. Physiol.* **456**:351-371.

Kuffler, S.W., Nicholls, J.G., & Martin, A.R. (1984) How sensory signals arise and their centrifugal control. *In* From Neuron to Brain: A Cellular Approach to the Function

of the Nervous System. 2nd Ed. pp. 379-407. Sinauer Associates Inc., Sunderland.

Kullberg, R. (1987). Stretch-activated ion channels in bacteria and animal cell membranes. *Trends Neurosci.* **10**:387-388.

Lane, J.W., McBride, D.W., & Hamill, O.P. (1993) Ionic effects on amiloride block of the mechanosensitive channel in *Xenopus* oocytes. *Br. J. Pharmacol.*, **108**:116-119.

Lane, J.W., McBride, D.W., & Hamill, O.P. (1992) Structure-activity relations of amiloride and its analogues in blocking the mechanosensitive channel in *Xenopus* oocytes. *Br. J. Pharmacol.*, **106**:283-286.

Lane, J.W., McBride, D.W., & Hamill, O.P. (1991) Amiloride block of the mechanosensitive cation channel in *Xenopus* oocytes. *J. Physiol.*, **441**:347-366.

Lamoureux, P., Buxbaum, R.E., & Heidemann, S.R. (1989) Direct evidence that growth cones pull. *Nature* **340**:159-162.

Loewenstein, W.R. (1971). Mechanoelectrical transduction in the Pacinian corpuscle. Initiation of sensory impulses in mechanoreceptors. *In* Handbook of Sensory Physiology, ed. W. R. Loewenstein, I:269-290. Berlin: Springer-Verlag.

Ludwig, J., Terlau, H., Bruggemann, A., Weseloh, R., Wunder, F., Martinez, A., Stuhmer, W., & Pongs, O. (1994) Cloning and functional expression of a rat homologue of the voltage gated *eag* ion channel. *Biophys. J.*, **66**:A426.

Luna, E.J. & Hitt, A.L. (1992). Cytoskeleton-plasma membrane interactions. *Science* **258**:955-964.

McBride, D.W. and Hamill, O.P. (1992) Pressure-clamp: a method for rapid step perturbation of mechanosensitive channels. *Pfiigers Arch.* **421**:606-612.

McBride, D.W. and Hamill, O.P. (1993) A pressure-clamp technique for measuring the dynamic properties of mechanosensitive channels. *Axobits* **12**:16-18.

McCormack, K., Tanouye, M.A., Iverson, L.E., Lin, J.W., Ramaswami, M., McCormack, T., Campanelli, J.T., Mathew, M.K., & Rudy, B. (1991) A role for hydrophobic residues in the voltage-dependent gating of Shaker K^+ channels. *Proc. Natl. Acad. Sci. USA* **88**:2931-2935.

McCormack, T., Vega-Sandez De Miera, E.C., & Rudy, B. (1990) Molecular cloning of a member of a third class of *Shaker* family K^+ channel genes in mammals. *Proc. Natl. Acad. Sci. USA*, **87**:5227-5231.

Maricq, A.V., Peterson, A.S., Brake, A.J., Myers, R.M., & Julius, D. (1991) Primary structure and functional expression of the 5-HT_3 receptor a serotonin-gated ion channel. *Science* **254**:432-437.

Martinac, B., Adler, J., & Kung, C. (1990) Mechanosensitive ion channels of *E. coli* activated by amphipaths. *Nature* **348**:261-263.

Matthews, P.B.C. (1981). Evolving views on the internal operation and functional role of the muscle spindle. *J. Physiol.* **320**:1-30.

Medina, I.R., & Bregestovski, P.D. (1988) Stretch-activated ion channels modulate the resting membrane potential during early embryogenesis. *Proc. R. Soc. London B* **235**:95-102.

Medina, I.R., & Bregestovski, P.D. (1991) Sensitivity of stretch-activated K^+ channels changes during cell-cleavage cycle and may be regulated by cAMP-dependent protein kinase. *Proc. R. Soc. London B* **245**:159-164.

Mercer, A.R., Emptage, N.J., & Carew, T.J. (1991) Pharmacological dissociation of serotonin in *Aplysia* sensory neurons. *Science* **254**:1811-1813.

Methfessel, C., Witzeman, V., Takahashi, T., Mishina, M., Numa, S., & Sakmann, B. (1986) Patch-clamp measurements on *Xenopus laevis* oocytes: currents through endogenous channels and implanted acetylcholine receptor and sodium channels. *Pflügers Arch.* **407**:572-578.

Meuller, P. & Pugh, Jr. E.N. (1983). Protons block the dark current of isolated retinal rods. *Proc. Natl. Acad. Sci. USA.* **80**,1892-1896.

Mills, J.W., Schwiebert, E.K., & Stanton, B.A. (1994). Evidence for the role of actin filaments in regulating cell swelling. *J. Exp. Zool.* **268**:111-120.

Mitchell, D.C. & Litman, B.J. (1994) Effect of ethanol on receptor conformation change: phospholipid acyl chain unsaturation augments ability of ethanol to enhance both meta II formation and acyl chain packing free volume. *Biophys. J.*, **66**:A48.

Moczydlowski, E. (1992) Analysis of drug action at single-channel level. *Meth. Enzymol.*, **207**:791-806.

Moody, W.J., & Bosma, M.M. (1989) A non-selective cation channel activated by membrane deformation in oocytes of the Ascidian *Boltenia villosa. J. Memb. Biol.* **107**: 179-188.

Morris, C.E. (1992) Are stretch-sensitive channels in molluscan cells and elsewhere physiological transducers? *Experientia* **48**:852-858.

Morris, C.E. (1990) Mechanosensitive ion channels *J. Memb. Biol.* **113**:93-107.

Morris, C.E., & Horn, R. (1991) Failure to elicit neuronal macroscopic mechanosensitive currents anticipated by single-channel studies. *Science* **251**:1246-1249.

Morris, C.E. & Lecar, H. (1993) Biophysics of mechanotransduction. *In* Mechanoreception by the Vascular Wall. Ed G.M. Rubanyi. Futura Publishing Co. Inc., Mount Krisco, N.Y.

Morris, C.E., & Moore, D. (1992) Efflux of $^{86}Rb^{+}$ from *Lymnaea* heart: Effects of osmotic stress, depolarization, quinidine and 5-hydroxytryptamine. *Comp. Physiol.* **11**: 192-198.

Morris, C.E., & Sigurdson, W.J. (1989) Stretch-inactivated ion channels coexist with stretch-activated ion channels. *Science* **243**:807-809.

Naitoh, Y. (1974) Bioelectric basis of behavior in protozoa. *Amer. Zool.* **14**:883-893.

Naitoh, Y. (1984) Mechanosensory transduction in protozoa. *In* Membranes and Sensory Transduction. pp. 113-135. Eds. C. Giuliano & L. Francesco. Plenum Press, New York.

Nakajima, S. & Onodera, K. (1969). Membrane properties of the stretch receptor neurons of crayfish with particular reference to mechanisms of sensory adaptation. *J. Physiol.* **200**:161-185.

Neher, E. & Sakmann, B. (1976). Single channel currents recorded from membrane of denervated frog muscle fibres. *Nature* **260**:799-802.

Neyton, J. & Miller, C. (1988). Potassium blocks barium permeation through a calcium-activated potassium channel. *J. Gen. Physiol.* **92**:549-567.

Nguyen, A.N., Grissmer, S., Hanson, D.C., Mather, R.J., Gutman, G.A., Karmilowicz, M.J., Auperin, D.D., & Chandy, K.G. (1994) Pharmacological characterization of five cloned voltage-gated K^{+} channels, Kv1.1, Kv1.2, Kv1.3, Kv1.5, and Kv3.1, stably expressed in mammalian cell lines. *Biophys. J.*, **66**:A106.

Nordin, M., Nystrom, B., Wallin, U., & Hagbarth, K.E. (1984). Ectopic sensory discharges and paresthesiae in patients with disorders of peripheral nerves, dorsal roots and sorsal columns. *Pain* **20**:231-245.

Ohmori, H. (1985) Mechano-electrical transduction currents in isolated vestibular hair cells of the chick. *J. Physiol.* **359**:189-217.

Okada, Y., Hazama, A., Hashimoto, A., Maruyama, Y., & Kubo, M. (1992) Exocytosis upon osmotic swelling in human epithelial cells. *Biochim. Biophys. Acta.* **1107**:201-205.

Olesen, S.P., Clapham, D., & Davies, P.F. (1988) Haemodynamic shear stress activates a K^+ current in vascular endotheliai cells. *Nature* **331**:168-170.

Oliet, S. H. R. & Bourque, C.W. (1993a). Mechanosensitive channels transduce osmosensitivity in supraoptic neurons. *Nature* **364**:341-343.

Oliet, S. H. R. & Bourque, C.W. (1993b). Steady-state osmotic modulation of cationic conductance in neurons of rat supraoptic nucleus. *Am. J. Physiol.* **265**:R1475-1479.

Pallotta, B. S. & Wagoner, P. K. (1992). Voltage-dependent potassium channels since Hodgkin and Huxley. *Physiol. Rev.* 72, S49-S67.

Pelligrino, M., Pelligrini, M., Simoni, A., & Gargini, C. (1990) Stretch-activated channels with large unitary conductance in leech central neurons. *Brain Res.*, 525, 322-326.

Peroutka, S. (1990) 5-Hydroxytryptamine receptor subtypes. *Pharmacol. Toxicol.* **67**:373-383.

Pickles, O.J., Comis, S.D., & Osborne, M.P. (1984) Cross-links between stereocilia in the guinea-pig Organ of Corti, and their possible relation to sensory transduction. *Hear. Res.* **15**:103-112.

Piomelli, D. (1991) Metabolism of arachidonic acid in nervous system of marine mollusc *Aplysia californica. Am. J. Physiol.* **260R**:844-848.

Piomelli, D., Feinmark, S.J., Shapiro, E., & Schwartz, J.H. (1988) Formation and biological activity of 12-ketoeicosatetraenoic acid in the nervous system of *Aplysia. J. Biol. Chem.* **263**:16591-16596.

Piomelli, D., Shapiro, E., Feinmark, S.J., & Schwartz, J.H. (1987a) Metabolites of arachidonic acid in the nervous system of *Aplysia:* Possible mediators of synaptic modulation. *J. Neurosci.* 7:3675-3686.

Piomelli, D., Shapiro, E., Zipkin, R., Schwartz, J.H., & Feinmark, S.J. (1989) Formation and action of 8-hydroxy-11,12-epoxy-5,9,14-icosatrienoic acid in *Aplysia*: A possible second messenger. *Proc. Natl. Acad. Sci. USA* **86**:1721-1725.

Piomelli, D., Volterra, A., Dale, N., Siegelbaum, S.A., Kandel, E.R., Schwartz, J.H., & Belardetti, F. (1987b) Lipoxygenase metabolites of arachidonic acid as second messengers for presynaptic inhibition of *Aplysia* sensory cells. *Nature* **328**:38-43.

Pongs, O. (1992) Molecular biology of voltage-dependent potassium channels. *Physiol. Rev.*, **72**: S69-S88.

Prudhom, B., Pietrobon, D., & Hess, P. (1989). Interactionsof protons with single open L-type calcium channels. Location of protonation site and dependence of proton-induced current fluctuations on concentration and species of permeant ion. *J. Gen. Physiol.* **94**:23-42.

Raynauld, J. P. (1994). The silver-silver chloride electrode: A possible generator of offset voltages and currents. *Axobits* **14**, 10-12.

Rehder, V., & Kater, S.B. (1992) Regulation of neuronal growth cone filopodia by intracellular calcium. *J. Neurosci.* **12**:3175-3186.

Reinhart, P.H., Chung, S., Martin, B.I., Brautigan, D.L., & Levitan, I.B. (1991) Modulation of calcium-activated potassium channels from rat brain by protein kinase A and phosphatase 2A. *J. Neurosci.* **11**:1627-1635.

Rettig, J., Wunder, F., Stocker, M., Lichtinghagen, R., Mastiaux, F., Beckh, S., Kues, W., Pedarzani, P., Schroter, K.H., Ruppersberg, J.P., Veh, R., & Pongs, O. (1992) Characterization of a Shaw-related potassium channel family in rat brain. *EMBO J.*, **11**:2473-2486.

Rich, T.C., Mays, D.J., Tamkun, M.M., & Snyders, D.J. (1994a) Quinidine block of the human cardiac hKv1.5 channel in inside-out patches. *Biophys. J.*, **66**, A209.

Rich, T.C., Yeola, S.N., Blair, I.A., Yeola, S.W., & Snyders, D.J. (1994b) Quaternary quinidine derivatives as a tool to study block of human potassium channels. *Biophys. J.*, **66**:A143.

Ross, R.E., Garber, S.S., & Calahan, M.D. (1994) Membrane chloride conductance and capacitance in Jurkat T lymphocytes during osmotic swelling. *Biophys. J.* **66**:169-178.

Ruknudin, A., Sachs, F. & Bustamante, J.O. (1993) Stretch-activated ion channels in tissue-cultured chick heart. *Am. J. Physiol.*, **264**:H960-H972.

Rudy, B. (1988) Diversity and ubiquity of K channels. *J. Neurosci.* **25**:729-749.

Sachs, F. (1986) *In* Ionic Channels in Cells and Model Systems. pp. 181-193. Ed. R. Latorre

Plenum, New York.

Sachs, F. (1987) Baroreceptor mechanisms at the cellular level. *Fed. Proc.* 46:12-16.

Sachs, F. (1990) Stretch-sensitive ion channels. *Sem. Neurosci.* 2:49-57.

Sachs, F. & Lecar, H. (1991) Stochastic models for mechanical transduction. *Biophys. J.* 59:1143-1145.

Sackin, H. (1989) A stretch-activated K^+ channel sensitive to cell volume. *Proc. Natl. Acad. Sci. USA* 86:1731-1735.

Sawada, M., Ichinose, M., Ito, I., Maeno, T., & M°Adoo, D.J. (1984) Effects of 5-hydroxytryptamine on membrane potential, contractility, accumulation of cyclic AMP, and Ca^{2+} movements in anterior aorta and ventricle of *Aplysia*. *J. Neurophysiol.* 51:361-374.

Schacher, S. & Proshansky, E. (1983) Neurite regeneration by *Aplysia* neurons in dissociated cell culture: modulation by *Aplysia* hemolymph and the presence of initial axonal segment. *J. Neurosci.* 3:2403-2413.

Schachtman, D.P., Schroeder, J.I., Lucas, W.J., Anderson, J.A., & Gaber, R.F. (1992) Expression of an inward-rectifying potassium channel by the *Arabidopsis* KAT1 cDNA. *Science*, 258:1654-1658.

Schwiebert, E.M., Mills, J.W., & Stanton, B.A. (1994). Actin-based cytoskeleton regulates a chloride channel and cell volume in a renal cortical collecting duct cell line. *J. Biol. Chem.* 269:7081-7089.

Shotwell, S.L., Jacobs, R., & Hudspeth, A.J. (1981) Directional sensitivity of individual veretbrate hair cells to controlled deflection of their hair bundles. *Ann. NY Acad. Sci.* 374:1-10.

Shuster, M.J., Camarado, J.S., & Siegelbaum, S.A. (1991) Comparison of the serotonin-sensitive and Ca^{2+}-activated K^+ channels in *Aplysia* sensory neurons. *J. Physiol.* 440:601-621.

Shuster, M.J., Camarado, J.S., Siegelbaum, S.A., & Kandel, E.R. (1985) Cyclic AMP-dependent protein kinase closes the serotonin-sensitive K^+ channels of *Aplysia* sensory neurons in cell-free membrane patches. *Nature* 313:392-395.

Shuster, M.J., & Siegelbaum, S.A. (1987) Pharmacological characterization of the serotonin-sensitive potassium channel of *Aplysia* sensory neurons. *J. Gen. Physiol.* 90:587-608.

Siegelbaum, S.A., Camarado, J.S., & Kandel, E.R. (1982) Serotonin and cyclic AMP close single channel K channels in *Aplysia* sensory neurons. *Nature* **299**:413-417.

Sigurdson, W.J. (1990). Mechanosensitive ion channels in the freshwater snail *Lymnaea stagnalis*. Ph.D. Thesis, University of Ottawa.

Sigurdson, W.J., & Morris, C.E. (1989) Stretch-activated ion channels in growth cones of snail neurons. *J. Neurosci.* **9**:2801-2808.

Sigurdson, W.J., Morris, C.E., Brezden, B.L., & Gardner, D.R. (1987) Stretch-activation of a K channel in molluscan heart cells. *J. Exp. Biol.* **127**:191-209.

Sigurdson, W.J., Ruknudin, A., & Sachs, F. (1992) Calcium imaging of mechanically induced fluxes in tissue-cultured chick heart: role of stretch-activated ion channels. *Am. J. Physiol.* **262H**:1110-1115.

Sigworth, F.J. & Sine, S.M. (1987) Data transformation for improved display and fitting of single-channel dwell time histograms. *Biophys. J.* **52**:1047-1054.

Silberman, S., McGarvey, T.W., Comrie, E., & Persky, B. (1990) The influence of ethanol on cell membrane fluidity, migration, and invasion of murine melanoma cells. *Exp. Cell Res.*, **189**:64-68.

Sinnett-Smith, J., Zachary, I., Valverde, A.M., & Rozengurt E. (1993). Bombesin stimulation of p125 focal adhesion kinase tyrosine phosphorylation. *J. Biol. Chem.* **268**:14261-14268.

Slade, C.T., Mills, J., & Winlow, W. (1981) Neuronal organisation of the paired pedal ganglia of *Lymnaea stagnalis*. *Comp. Biochem. Physiol.* **69A**:798-803.

Small, D.L. & Morris, C.E. (1994a). Delayed activation of single mechanosensitive channels in *Lymnaea* neurons. *Am. J. Physiol.* **In Press.**

Small, D.L. & Morris, C.E. (1994b). Pharmacology of stretch-activated K^+ channels in *Lymnaea* neurons. *Br. J. Pharmacol.* **In Press.**

Small, D.L., Wan, X., & Morris, C.E. (1993). Modulation of SA K channels by neurotransmitters via 2nd messengers? *Biophys. J.* **64**:A313.

Smith, K.J. & McDonald, W.I. (1980). Spontaneous and mechanically evoked activity due to a central demylinating lesion. *Nature* **286**:154-156.

Sokabe, M., & Sachs, F. (1990) The structure and dynamics of patch-clamped membranes:

a study using differential interference contrast light microscopy. *J. Cell Biol.* **111**:599-606.

Sokabe, M., Sachs, F., & Jing, Z. (1991) Quantitative video microscopy of patch clamped membranes stress, strain, capacitance, and stretch channel activation. *Biophys. J.* **59**:722-728.

Srinivasan, Y. Elmer, L., Davis, J., Bennett, V., & Angelides, K. (1988). Ankyrin and spectrin associate with voltage-dependent sodium channels in brain. *Nature* **333**:177-180.

Steffensen, I., Bates, W.R., & Morris, C.E. (1991) Embryogenesis in the presence of blockers of mechanosensitive ion channels. *Dev. Growth Differ.* **33**:437-442.

Stockbridge, L.L. & French, A.S. (1988) Stretch-activated cation channels in human fibroblasts. *Biophy. J.* **54**:187-190.

Sukharev, S.I., Blount, P., Martinac, B., Blattner, F.R., & Kung, C. (1994) A large-conductance mechanosensitive channel in *E. coli* encoded by *mscL* alone. *Nature*, **368**:265-268.

Surprenant, A., Horstman, D.A., Akbarali, H., & Limbird, L.E. (1992) A point mutation of the α_2-adrenoceptor that blocks coupling to potassium but not calcium currents. *Science* **257**:977-980.

Suzuki, M., Takahashi, K., Ikeda, M., Hayakawa, H., Ogawa, A., Kawaguchi, Y. & Sakai, O. (1994). Cloning of a pH-sensitive K^+ channel possessing two transmembrane segments. *Nature* **367**, 642-645.

Sweatt, J.D., Volterra, A., Edmonds, B., Karl, K.A., Siegelbaum, S.A., & Kandel, E.R. (1989) FMRF-amide reverses protein phosphorylation produced by 5-HT and cAMP in *Aplysia* sensory neurons. *Nature* **342**:275-278.

Tabcharani, J.A., Chang, X.B., Riordan, J.R., & Hanrahan, J.W. (1991) Phosphorylation-regulated Cl^- channel in CHO cells stably expressing the cystic fibrosis gene. *Nature* **352**:628-631.

Tasaki, I. & Hagiwara, S. (1957) Demonstration of two stable potential states in the squid giant axon under tetraethylammonium chloride. *J. Gen. Physiol.*, **40**:859-885.

Tsien, R. W., Hess, P., McCleskey, E. W. & Rosenberg, R. L. (1987). Calcium channels: Mechanisms of selectivity, permeation, and block. *Ann. Rev. Biophys. Biophys. Chem.* **16**, 265-290.

Ubl, J., Murer, H., & Kolb, H-A. (1988) Ion channels activated by osmotic and mechanical stress in membranes of opossum kidney cells. *J. Memb. Biol.* **104**:223-232.

Vale, R.D., Banker, G., & Hall, Z.W. (1992) The neuronal cytoskeleton. *In* An Introduction to Molecular Neurobiology. Ed. Z.W. Hall. 247-280, Sinauer Associates, Inc. Mass.

Vandorpe, D.H., & Morris, C.E. (1992) Stretch-activation of the *Aplysia* S-channel. *J. Memb. Biol.* **127**:205-214.

Vandorpe, D.H., Small, D.L., Dabrowski, A.R., & Morris, C.E. (1994) FMRF-amide and membrane stretch as activators of the *Aplysia* S-channel. *Biophys. J.* **66**:46-58.

Vergara, C. & Latorre, R. (1983). Kinetics of Ca^{2+}-activated K^+ channels from rabbit muscle incorporated into planar bilayers. *J. Gen. Physiol.* **82**:543-568.

Volterra, A., & Siegelbaum, S.A. (1988) Role of two different guanine nucleotide binding G-proteins in the antagonistic modulation of S-K^+ channel activity by cyclic AMP and arachidonic acid metabolites. *Proc. Natl. Acad. Sci. USA* **85**:7810-7814.

Walters, E.T., Byrne, J.H., Carew, T.J., & Kandel, E.R. (1983) Mechanoafferent neurons innervating tail of *Aplysia*. I Response properties and synaptic connections. *J. Neurophysiol.* **50**:1522-1542.

Wan, X., Harris, J.A., & Morris, C.E. (1994). Responses of neurons to extreme osmomechanical stress. *J. Membr. Biol.* **In Press.**

Witte, O. W., Speckmann, E. J. & Walden, J. (1985). Acetylcholine responses of identified neurons in *Helix pomatia*. II. Pharmacological properties of acetylcholine responses. *Comp. Biochem. Physiol.* **80**, C25-35.

Wong, B.S. & Adler, M. (1986) Tetraethylammonium blockade of calcium-activated potassium channels in clonal anterior pituitary cells. *Pflügers Arch.* **407**:279-284.

Woodhull, A.M. (1973). Ionic blockage of sodium channels in nerve. *J. Gen. Physiol.* **61**, 687-708.

Yang, X.C. & Sachs, F. (1990) Characterization of stretch-activated ion channels in *Xenopus* oocytes. *J. Physiol.*, **431**:103-122.

Yang, X-C. & Sachs, F. (1989) Block of stretch-activated ion channels in *Xenopus* oocytes by gadolinium and calcium ions. *Science*, **243**:1068-1071.

Yellen, G. (1984a) Ion permeation and blockade in Ca^{2+}-activated K^+ channels of bovine

chromaffin cells. *J. Gen. Physiol.* **84**:157-186.

Yellen, G. (1984b). Relief of Na^+ block of Ca^{2+}-activated K^+ channels by external cations. *J. Gen.Physiol.* **84**, 187-199.

Zagotta, W.N., Brainard, M.S., & Aldrich, R.W. (1988) Single channel analysis of four distinct classes of potassium channels in *Drosophila* muscle. *J. Neurosci.* **8**:4765-4779.

Zhou, X-L., Stumpf, M.A., Hoch, H.C., & Kung, C. (1991) A mechanosensitive channel in whole cell and membrane patches of the fungus *Uromyces*. *Science* **253**:1415-1417.

Zubay, G. (1984) Biochemistry. p.12. addison-Wesley Publishing Co., Don Mills, Ontario.

APPENDIX A Cloning Strategy

Two main approaches to cloning an SA channel are considered here: probing a cDNA library and expression cloning. Both approaches require access to a preparation which express SA channels in abundance and which shows little expression of other channels. Ideally, the preparation would express no other channel types. Either for probing an appropriate cDNA library or for preparing cRNA for expression cloning, the presence of several other types of channel or a "dilute" source of SA channels would be a hindrance. There might be cross hybridization of a nucleic acid probe to another channel type in the first strategy or with expression cloning there might be diffuculties differentiating SA channels from other channel types. I spent 3 months on this, but it would have required a "lucky strike" which we did not get. The strategies outlined here are being followed up in the lab however.

Strategy #1. Probing cDNA Library

The first approach involves probing a cDNA library constructed from a preparation rich in SA channels. I chose to use a cDNA library constructed from *Xenopus* oocytes (I obtained a well characterized library from Doug Melton). *Xenopus* oocytes abundantly express SA Cat channels which have been well characterized, (Taglietti and Toselli, 1988; Yang and Sachs, 1990), and are similar in many respects to SA K channels of *Lymnaea* neurons (Small and Morris, 1994b). There are few other channel types expressed in *Xenopus* oocytes and none similar to SA K channels.

I chose nucleic acid probes which code for discrete functional domains of channels predicted to be homologous to nucleic acid coding for similar functional domains of SA channels based on characterizations and comparisons of the channels. An example of such a probe is the

nucleic acid coding for an extended H5 pore region with flanking S4 and S5 regions of a *Shaker* mutant. Cathy Morris and Robert Greenberg had tried a 17-mer coding for the H5 pore region of *Shaker* but it did not hybridize well (even at low stringency) on a *Drosophila* cDNA library [*Drosophila* muscle expresses SA K^+ channels (Zagotta et al., 1988)]. Upon obtaining a clone of the SA Cat channel from *Xenopus* oocytes I planned to express it in snail neurons which have SA K channels using a vector (pNEX), [this vector has been used to successfully express other K channels in snail neurons (Kaang et al., 1992)]. The two SA channels, in their native environments, are sufficiently different from one another that I could clearly distinguish expressed SA Cat channels from native SA K channels. Another advantage of this approach is that because snail neurons express SA K channels, snail neurons are likely to have everything needed to successfully express another type of SA channel.

Stategy #1. Results

Peter Juranka (a research associate in Cathy Morris's lab) and I have tried this first approach with probes for mutant (no inactivation ball) *Shaker* channels, the pore region of *Shaker* channels with S4-S5 flanking regions, and cyclic nucleotide-gated channels. We probed the *Xenpopus* oocyte cDNA library. It would have been encouraging if we had obtained several positives which necessitated further screening but, unfortunately we did not obtain a positive suggesting none of the probes possessed enough homology to recognize the endogenous nucleic acid coding for oocyte SA cat channels.

Medina and Bregestovski, (1988; 1991) showed that SA K channels were present in abundance in weather loach (*Fossilus misgurnis*) embryos and that these channels played an

active role during development of these organisms. Since we had available a cDNA library for the gastrula stage of developing zebra fish (*Brachydanio rerio*) embryos and since it seemed likely that zebra fish would have these channels in abundance as well, I made patch-clamp recordings of developing zebra fish embryos and of cultured cells dissociated from the gastrula stage of the embryos (see general methods). Unfortunately I did not see SA K channels.

Stategy #2. Expression Cloning from Lymnaea Neurons

An alternate appoach involves expression cloning. I have been involved in some of the earlier controls. Since I know more about SA K channels from *Lymnaea* neurons than from any other source it seemed reasonable to attempt to purify mRNA from *Lymnaea* neurons and express it in *Xenopus* oocytes. I know that *Lymnaea* neurons have SA K channels in abundance (1 per μm^{-2}) but, unfortunately, this is a much lower abundance than, for example AChRs in *Torpedo* electroplax organs and we cannot be sure that the assay will be adequate. Due to this problem, expression cloning was not our first approach. I would need a very high level of expression because SA K channels do not exhibit macroscopic currents so I would have to make single channel recordings. To increase the sampling area when making single channel recordings, I would record from macropatches 10 to 20 μm in diameter. *Xenopus* oocytes possess SA cat channels and no K-selective channels. When checking *Xenopus* oocytes for *Lymnaea* SA K channel expression Gd^{3+} can be used to block SA cat channels without affecting SA K channels (Small and Morris, 1994b). Other K channels can be eliminated from the electrophysiological records by using TEA which affects SA K channels only at very high concentrations (Small and Morris, 1994b). An added advantage of this approach is that by using *Xenopus* oocytes as an

expression system it is likely that if any auxillary membrane proteins or associated cytoskeletal proteins are necessary for normal SA K channel behaviour, the oocyte should have them as they presumably would also be necessary for normal behaviour of endogenous SA Cat channels.

APPENDIX B

2. Solutions and Chemicals (units in mM)

(i) Aplysia

ACM	ARS
400 NaCl	460 NaCl
10 KCl	10 KCl
11 $CaCl_2$	55 $MgCl_2$
27 $MgCl_2$	11 $CaCl_2$
27 $MgSO_4$	10 HEPES- NaOH pH 7.6
2 $NaHCO_3$	
2% (w/v) glucose	
10 HEPES- NaOH pH 7.4	
100 U/ml streptomycin	

(ii) Lymnaea

LCM	LPM	LNS
55 NaCl	55 NaCl	55 NaCl
1.6 KCl	1.6 KCl	1.6 KCl
2 $MgCl_2$	2 $MgCl_2$	2 $MgCl_2$
0.5 $CaCl_2$	3.5 $CaCl_2$	3.5 $CaCl_2$
5 Glucose	5 Glucose	5 HEPES-NaOH pH 7.6
0.1 mg/ml gentamicin	0.1 mg/ml gentamicin	
5 HEPES-NaOH pH 7.6	5 HEPES-NaOH pH 7.6	

(iii) Xenopus

OR2	ND96	FNS	HYPER
82.5 NaCl	96 NaCl	115 NaCl	200 K-aspartate
2 KCl	2 KCl	2.5 KCl	20 KCl
1 $MgCl_2$	1.8 $CaCl_2$	1.8 $CaCl_2$	1 $MgCl_2$
5 HEPES	1 $MgCl_2$	10 HEPES	5 EGTA
NaOH pH 7.5	5 HEPES-NaOH pH 7.5	NaOH pH 7.2	10 HEPES-KOH pH 7.4

(iv) Zebrafish

Hank's Saline	ZNS
137 NaCl	116 NaCl
5.4 KCl	2.9 KCl
1.3 CaCl2	1.8 CaCl2
1 MgSO4	5 HEPES-NaOH pH 7.2
0.44 KH2PO4	
0.25 Na2HPO4	
4.2 NaHCO3	

APPENDIX C

Notation comparisons for ADaM: I used a notation appropriate to the channel literature rather than one appropriate to the biostatistics literature. The following list equates our terms to those used by Dabrowski and colleagues in ADaM and in the full mathematical treatment of renewal theory and channel kinetics (Dabrowski, McDonald & Rosler, 1990; Dabrowski & McDonald, 1992).

$N = c$; $P_{open} = p$

$F = F$; $G = G$; $\tau_o = \mu_F$; $\tau_c = \mu_G$

Nomenclature for F (and G) functions: the true open (closed) time distribution for the channel under consideration is unknown. ^F is the estimator in the one state case. The other renewal theoretic estimator used in ADaM is the function referred to as the estimated F. Figure 3.10 shows estimates (the estimated ^F and the estimated F) obtained from applying each of these estimators to data.

Total current at time t = X(t)

Chunk length = u

Levels:

Occupation of current level s during chunk j = M_{sj}

occupation density vector (Figure 1) = M_j = [INT(*j*-1)to*j*]X(t)dt

and in ADaM, occ(s) = 1/n Σ(j=1 to n)M_{sj} (= mean occupation vector)

Downsteps

Number of downsteps from level s to s-1 during chunk j = N_{sj}

downstep vector (Figure 1) = $N_j = N(j)-N(j-1)$

and in ADaM, $dwn(s) = 1/n \Sigma(j=1 \text{ to } n)N_{sj}$ (= mean downstep vector)

Covariance Matrix = T_n

Saw-toothed nature of the plot for 1-F(t): Both F and G are, by definition, monotonic functions of t, yet their estimates are saw-toothed (as in 1-F(t) plots in Figure 3.10). The explanation is that the estimates are computed by the ratio of two numeric integrals - integrals which change values (as functions of t). Because one of these integrals varies smoothly in time, and the other in discrete jumps, the ratio of the two exhibits a saw-toothed pattern. There is no a priori reason to pick the upper or lower envelope of this saw-tooth as the estimate of F (or G). The size of the saw-tooth is determined by the amount of data for a particular duration.

Appendix. D Single letter assignments, abbreviations, and chemical structure of side chains of essential 20 amino acids (Zubay, 1983).

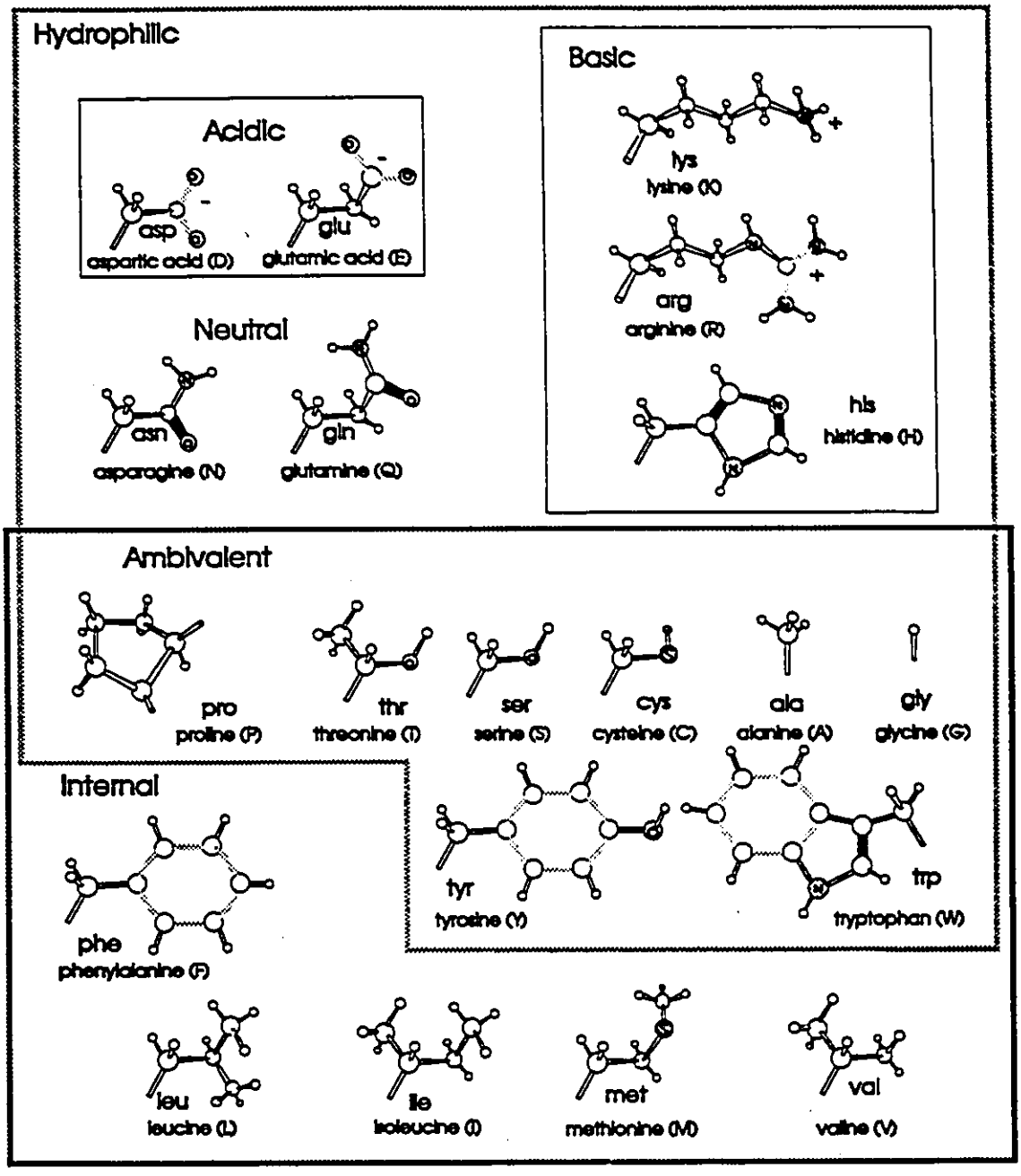

GLOSSARY

Hill Plot:

A **Hill plot** is a linear transformation of a sigmoidally shaped concentration curve. The x-y coordinates are obtained by mathematically transforming the horizontal y values with log(y/(maximum response-y)) and using the same horizontal x values. The horizontal intercept of this linear function is the IC_{50} (Operational definition: concentration of the inhibitor which inhibits 50% of the maximum response) and the slope of the line represents the number of binding sites of on the receptor site for the ligand.

Markov Process:

A finite state-space **Markov process** for modelling ion channel gating is one in which the complex trajectory of a channel through its protein conformational space is modelled as a series of jumps between a finite number of states within which the conductance is relatively constant. Each state is therefore either open or closed and the rate of transition between states, when the system is stationary, is constant (time-independent) and the distribution of the lifetimes in a single state is always exponential. The rate at which the channel leaves its present state is dependent on that state and not on any previously occupied state.

Renewal Theory:

A **Renewal Process** is one in which the assumption is made that the sojourn times